Fuzzy Logic Based Efficiency Optimization of IPM Synchronous Motor Drive

By

Jamshid Khastoo

Submitted in partial fulfilment of the requirements for the

Degree of Master of Science in Electrical Engineering

At

Lakehead University

Thunder Bay, Ontario

May 2011

Abstract

Interior permanent magnet synchronous motor (IPMSM) is highly appreciated by researchers in variable speed drive applications due to some of its advantageous features such as small size, high power density, simple maintenance, high output torque, high power factor, low noise and robustness as compared to the conventional IM and other ac motors. Although these motor drives are well known for their relatively high efficiency, improvement margins still exist in their operating efficiency. Particularly, the reduction of power loss for IPMSM still remains a challenge for researchers. Improvement of motor drives efficiency is important not only from the viewpoints of energy loss and hence cost saving, but also from the perspective of environmental pollution. The thesis presents development of a fuzzy logic based efficiency and speed control system of an IPMSM drive. In order to maximize the efficiency in steady state operation while meeting the speed and load torque demands a search based fuzzy efficiency controller is designed to minimize the drive power losses to achieve higher efficiency by reducing the flux. The air gap flux level can be reduced by controlling the d-axis armature current as it is supplied by rotor permanent magnet. In order for the drive to track the reference speed in transient operation another fuzzy logic based controller is designed to increase the flux depending on the speed error and its derivative. The torque component of stator current (q-axis component of stator current) is generated by fuzzy logic based speed controller for different dynamic operation depending on speed error and its derivative. In this work a torque compensation algorithm is also introduced to reduce the torque and speed fluctuations.

In order to verify the effectiveness of the proposed IPMSM drive, at first simulation model is developed using Matlab/Simulink. Then the complete IPMSM drive incorporating the novel search based efficiency optimization algorithm has been successfully implemented using digital signal processor (DSP) controller board-DS1104 for a laboratory VSI-Inverter-fed 5 hp motor. The effectiveness of the proposed drive is verified both in simulation and experiment at different operating conditions. The results show efficiency improvement, less torque ripples and robustness of the proposed FLC based as compared to the traditional FLC based drive.

Acknowledgements

First of all I would like to express my deepest gratitude and appreciation to my thesis supervisor Dr. M. Nasir Uddin for his invaluable suggestions and continuous encouragement. This work would not have been possible without his support. I acknowledge the support from all faculty and staff members especially Dr. Carlos Christoffersen for his useful guidance throughout the program. I wish to thank my thesis examiners Dr. Dimiter Alexandrov and Dr. Xiaoping Liu for their useful suggestions. I also appreciate my fellow graduate students Mr.Muhammad Hafeez and Mr. Ronald Shourav Rebeiro for providing a healthy research environment and assisting me in the experimental demonstration of the thesis. I also wish to thank faculty members of Amirkabir University of Technology who taught me in undergraduate study and motivated me to pursue greater achievements.

Finally, I express my sincere appreciation to my parents Dr. Bahman Khastoo and Golandam Sareh, without their support and encouragement I would never have been able to achieve so much. I especially wish to express my love for Fereshteh Ghashghaee who only knows the real price of this dissertation as we suffered and paid it together. I thank for her endless love, patience and understanding.

Contents

List of Symbols

V_{DC}	DC link voltage
I_{DC}	DC link current
P_{in}	Input drive power
P_{out}	Output drive power
P_{Loss}	Drive's total power loss
ΔP_{Loss}	Change of drive's total power loss
ω_s	Stator angular frequency
ω_r	rotor speed
ω_r^*	motor command speed
Δe	Change of speed error
$\Delta\omega_r$	Speed error
V_a	Maximum phase voltage amplitude
I_a	Maximum line current amplitude
v_a, v_b, v_c	a, b and c phase voltages
v_a^*, v_b^*, v_c^*	command a, b and c phase voltages
i_a, i_b, i_c	a, b and c phase currents
$v_{d,}$ v_d^r	d-axis voltage
$v_{q,}$ v_q^r	q-axis voltage

$i_{d,}\ i_d^r$	d-axis current
$i_{q,}\ i_q^r$	q-axis current
i_q*	q-axis command current
R	stator resistance per phase
L_d	d-axis inductance
L_q	q-axis inductance
L_l	Leakage inductance
L_{md}	d-axis magnetizing inductance
L_{mq}	q-axis magnetizing inductance
Θ_r	rotor position
p	differential operator *d/dt*
P	number of pole pairs
T_e	developed electromagnetic torque
T_L	load torque
J	rotor inertia constant
B_m	friction damping coefficient
ψ	magnetic flux linkage

List of Abbreviations

ANN	Artificial neural network
AOC	Analog to digital converter
BJT	Bipolar junction transistor
BLDC	Brushless DC
FLC	Fuzzy logic controller
FW	Flux weakening
HPD	High Performance Drive
HPVSD	High performance variable speed drive
IGBT	Inverted gate bipolar transistor
IM	Induction motor
IPMSM	Interior Permanent Magnet Synchronous Motor
LCR	Linguistic control rule
LMA	Loss minimization algorithm
MIMO	Multi-input-multi-output
MOSFET	Metal-oxide-semiconductor field-effect transistor
MTPA	Maximum torque per ampere
NNC	Neural network controller
NFC	Neuro-fuzzy logic controller

PI	Proportional Integral
PID	Proportional Integral Derivative
PM	Permanent Magnet
PMSM	Permanent Magnet Synchronous Motor
PWM	Pulse Width Modulation
RTI	Real-time Interface
VSI	Voltage Source Inverter

Chapter 1

Introduction

1.1 Electric Motors

An electric motor in its simplest term is a converter of electrical energy to useful mechanical energy. Electric motors have played a leading role in the high productivity of modern industry. The beginnings of the electric motor are shrouded in mystery, but this much seems clear that the basic principles of electromagnetic induction were discovered in the early 1800's by Oersted, Gauss and Faraday, and this combination of Scandinavian, German and English thought gave us the fundamentals for the electric motor. In the late 1800's the actual invention of the alternating current motor was made by Nikola Tesla, a Serb who had migrated to the United States. One measure of Tesla's genius is that he was granted more than 900 patents in the electrical field. Before Tesla's time, direct current motors had been produced in small quantities, but it was his development of the versatile and rugged alternating current motor that opened a new age of automation and industrial productivity.

An electric motor's principle of operation is based on the fact that a current-carrying conductor, when placed in a magnetic field, will have a force exerted on the conductor

proportional to the current flowing in the conductor and to the strength of the magnetic field. In alternating current motors, the windings placed in the laminated stator core produce the magnetic field. The aluminum bars in the laminated rotor core are the current carrying conductors upon which the force acts. The resultant action is the rotary motion of the rotor and shaft, which can then be coupled to various devices to be driven and produce the output [1].

Electric motors are found in applications as diverse as industrial fans, blowers and pumps, machine tools, household appliances, power tools and disk drives. They may be powered by direct current (e.g., a battery powered portable device or motor vehicle) or by alternating current from a central electrical distribution grid. The smallest motors may be found in electric wristwatches. Medium-size motors of highly standardized dimensions and characteristics provide convenient mechanical power for industrial uses. The very largest electric motors are used for propulsion of ships, pipeline compressors, and water pumps with ratings in the millions of watts. Electric motors may be classified by the source of electric power, by their internal construction, by their application, or by the type of motion they give [2].

1.2 Classification of Electric Motors

Electric motors are broadly classified into two different categories: DC (Direct Current) and AC (Alternating Current). Within these categories there are numerous types, each offering unique abilities that suit them well for specific applications.

1.2.1 DC Motors:

The name dc motor comes from the dc electric power used to supply the motor. The dc motor was in wide spread use in street railways, mining and industrial applications by the year 1900.The concept of controlled delivery of energy from a dc power source to a motor in order to meet the specific demands of an application is emerged around the same year. The same technique is used today in the majority of high performance control systems. However, the disadvantage of dc motors such as excessive wear in the electro-mechanical commutator, low efficiency, fire hazards due to sparking, limited speed and the extra room requirement to house the commutator, high cost of maintenance, became evident and leads to further investigation in order to overcome these dc motor disadvantages[3-5].

Michael Faraday's discovery of the electromagnetic induction concept paved the way towards the invention of induction motors. After careful study of this electromagnetic theory Nikola Tesla invented the first alternating current, brushless, induction motor .By the year 1900 the principles of operation of synchronous and induction motors were well known, but they were not widely used at that time due to the fact that ac power was not yet commercially available. The ac power is easier to produce, distribute, and utilize, as compared to dc power. This flexibility of ac power led to its initial commercial success even if dc power still cost less at that time. Even though, the decoupled nature of the field and armature magneto motive force (MMF) makes dc motor very easy to control its torque and speed in a very precise manner, it has many disadvantages such as high cost, frequent need of maintenance, power loss in the field circuit, lack of overload capability, lack of ruggedness, high weight to power ratio, low torque density and narrow speed

range [6]. As a result the fierce competition between ac and dc power was finally resolved in favour of the ac power in 1890.The ac motor has no commutator therefore there is no need for frequent maintenance, no need for housing the commutator, it has rugged construction and it's speed is only limited by the physical constraints of the motor and the supply frequency. Wide spread utilization of ac motors in motion control applications was caused by these flexibilities [7].

1.2.2 AC Motors:

Ac Motors are driven by alternating current. It commonly consists of two basic parts, an outside stationary stator having coils supplied with alternating current to produce a rotating magnetic field and an inside rotor attached to the output shaft that is given a torque by the rotating field [8]. There are two main types of ac motors depending on the type of rotor used. The first type is the induction motor, which only runs slightly slower or faster than the supply frequency. The magnetic field on the rotor of this motor is created by an induced current. The second type is the synchronous motor, which does not rely on induction and as a result, can rotate exactly at the supply frequency or a sub-multiple of the supply frequency. The magnetic field on the rotor is either generated by current delivered through slip rings or by a permanent magnet.

(a) Induction Motors: In an induction motor the current flow in the rotor is not caused by any direct connection of the conductors to a voltage source, but rather by the influence of the rotor conductors cutting across the lines of flux produced by the stator magnetic fields. The induction motor is a rotating electric machine designed to operate from a three-phase source of alternating voltage. The stator is a classic three phase stator with the winding displaced by 120° from each other. The most common type of induction

motor has a squirrel cage rotor in which aluminum conductors or bars are shorted together at both ends of the rotor by cast aluminum end rings. When three currents flow through the three symmetrically placed stator windings, a sinusoidal distributed air gap flux generating rotor current is produced. The interaction of the rotating and sinusoidal distributed stator air gap flux and the flux generated by induced rotor currents produces a rotation. The rotor is connected to the motor shaft, so the shaft will also rotate and drive the load. The mechanical angular velocity of the rotor is always lower than the angular velocity of the flux wave by the so called slip velocity [9, 10].

The main advantages of induction motors are lower cost, maintenance free operation and greater reliability especially in harsh industrial environments. However, they have some limitations associated with their use in high performance variable speed drive (HPVSD) applications. One of the limitations of induction motor is that it always operates at lagging power factor as the rotor induced current is supplied from the stator side. Another problem is that it always runs at a speed lower than the synchronous speed and rotor quantities depend on slip speed. Thus the control of this motor is very complex. Furthermore, the real-time implementation of the induction motor drive depends on sophisticated modeling and estimation of machine parameters with complex control circuitry. Some other disadvantages are low torque density and the required inverter over sizing and finally induction motors require very complex control scheme because of their nonlinear relationship between the torque generating and magnetizing currents [8, 9]. In today world, most of the electric energy in the world is consumed by electric machines therefore the need for more energy efficient high performance motor drive becomes the key factor in the advancement of electric machines. Recent developments in power

electronics and microprocessors led to a revolutionary advancement in the design and control technique of electric machines. As a result, new machines such as synchronous motor emerged very recently.

(b) Synchronous Motors: Synchronous motors utilize the same type of stator winding structure as induction motors and which is either a wound dc field or permanent magnet rotor. Synchronous motors run and generate torque at the synchronous speed which is the same as the source frequency. On the other hand, induction motors run and generate torque in a wide range of speed including zero speed. Therefore, prior to 1950 the speed of synchronous motors has to be increased to synchronous speed initially by means of an auxiliary motor before the motor can be used [10]. In 1950 as an alternative to the auxiliary motor, a line-start permanent magnet synchronous motor which has a rotor made up of permanent magnet embedded inside a squirrel-cage winding is introduced. A line start permanent magnet synchronous motor starts as an induction motor and when the rotor speed reaches the synchronous speed it gets synchronized and rotate at synchronous speed. However, the advancement of power electronics and the introduction of high performance motor drives have rendered the line start permanent magnet synchronous motor almost obsolete because electronic converters can deliver appropriate power to synchronous motors so that they can start from zero speed by themselves as of induction motor [11].

1.3 Permanent Magnet Synchronous Motors

In permanent magnet synchronous motor (PMSM), extra power supply, slip ring brush and the power loss due to excitation are eliminated because the field excitation is

provided by permanent magnets contained in the rotor. PMSM gives more torque density than the induction motor and the inverter size is also greatly reduced within the constant torque and power speed range [12]. The permanent magnet machine can be suitable for field weakening if it is properly designed. The PMSM has advantages of high torque to current ratio, large power to weight ratio, high efficiency, high power factor, low noise and robustness etc. The properties of the permanent magnet material will affect directly the performance of the motor and proper knowledge is required for the selection of the materials and for understanding PM motors. The earliest manufactured magnet materials were hardened steel. Magnets made from steel were easily magnetized. However, they could hold very low energy and it was easy to demagnetize. In recent years other magnet materials such as Aluminum Nickel and Cobalt alloys (AlNiCo), Strontium Ferrite or Barium Ferrite (Ferrite), Samarium Cobalt (First generation rare earth magnet) (Sm2Co5) and Neodymium Iron-Boron (Second generation rare earth magnet) (NdFeB) have been developed and used for making permanent magnets. The rare earth magnets are categorized into two classes: Samarium Cobalt (Sm2Co5) magnets and Neodymium Iron Boride (NdFeB) magnets. Sm2Co5 magnets have higher flux density levels but they are very expensive. NdFeB magnets are the most common rare earth magnets used in motors these days.

1.4 Classification of PMSM

Permanent magnet (PM) motors are classified by the manner in which the magnets are positioned. Two primary classifications of PM motors with regard to magnet location and orientation are surface mounted permanent magnet synchronous motor (SPMSM)

and interior permanent magnet synchronous motor (IPMSM), shown in Fig 1.1. The SPMSM design consists of magnets that are mounted on the surface of the rotor, while the IPMSM design has magnets contained within the rotor. Therefore, the mechanical integrity of the IPMSM is superior to SPMSM since it is easier to secure the magnets, which are subject to centrifugal forces from rotation as well as intensive transients due to magnetic forces. This mechanical security is especially important in high speed applications.

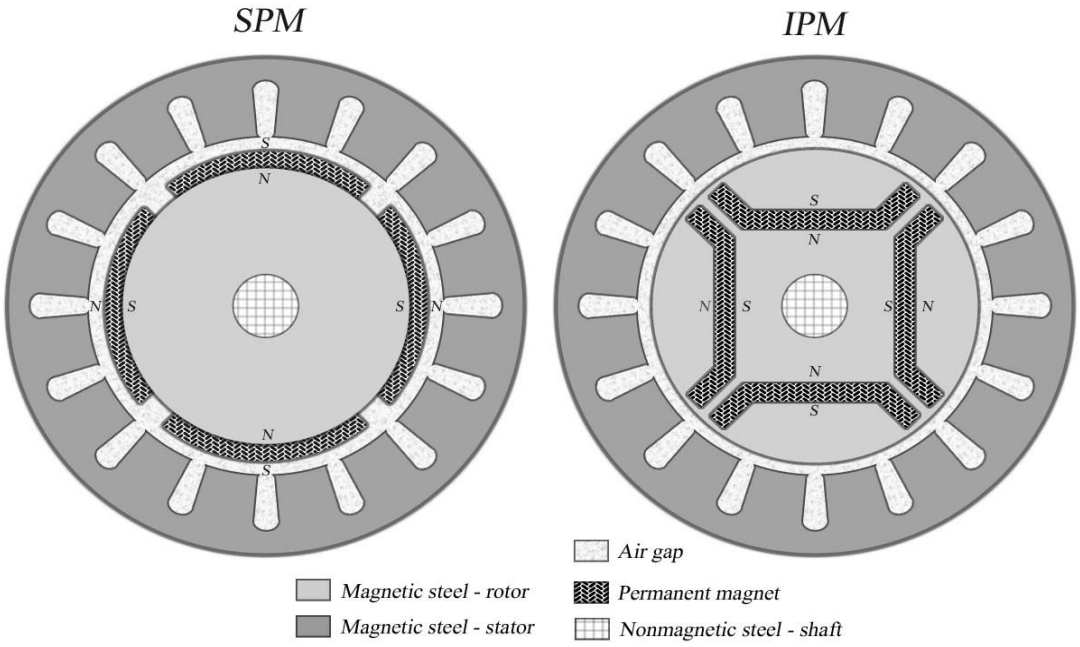

Fig 1.1 Cross section of surface mounted and interior type PM motor.

SPMSM is typically non-salient, meaning that the permeance of rotor does not vary significantly around the circumference. In an SPMSM flux generated by current in the stator windings must pass through the air gap, PM and steel rotor to complete the magnetic circuit as shown in Figure 1.2 When compared to magnetic materials such as iron or steel, the permeability of the PM material is very small and is about the same as

that of air. Consequently, the permeance of the rotor is substantially limited by the air gap and magnet material. The permeance varies in IPMSM since flux paths that do not include the PM are available at some angles, as shown in Fig 1.2. Therefore, IPMSM is referred as salient, which means its q-axis inductance (Lq) is larger than the d-axis inductance (Ld). This saliency gives the provision of utilizing reluctance torque, and applying flux weakening operation and thereby enabling the motor operation above rated speed in constant power region.

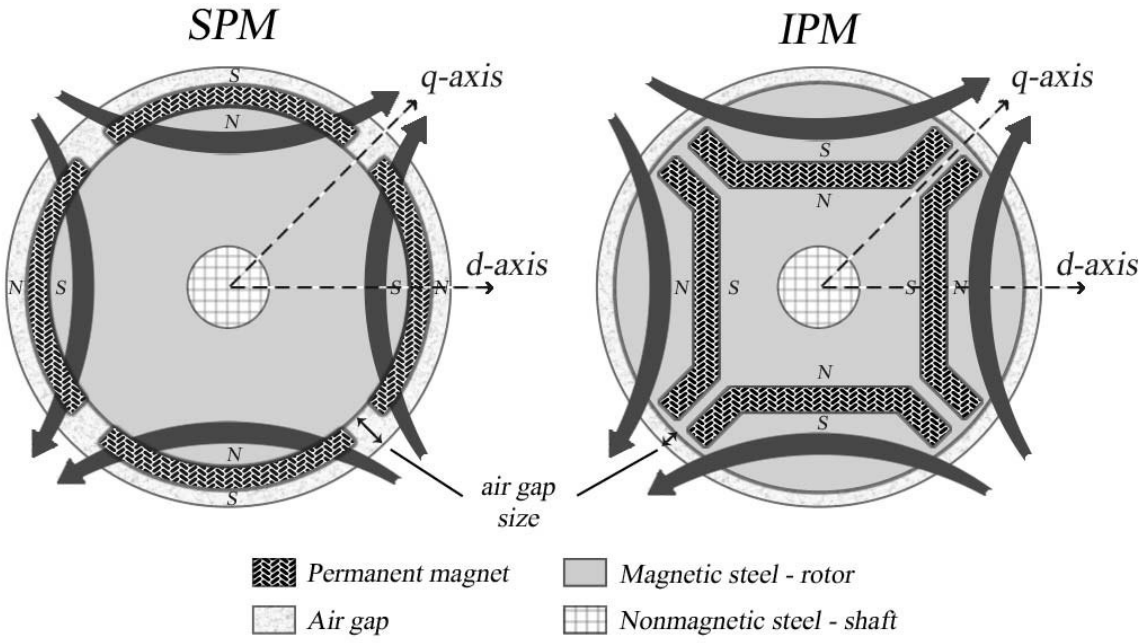

Fig 1.2 Comparison of air gap size and saliency between SPM and IPM

Interior permanent magnet type is the most recently developed method of mounting the magnet. Interior magnet designs offer q-axis inductance larger than the d-axis inductance. The saliency makes possible a degree of flux weakening, enabling operation above nominal speed at constant voltage and should also help to reduce the harmonic

losses in the motor. This kind of PM motor has the advantages of mechanical robustness and a smaller magnetic air gap. Therefore the interior magnet design is better suited to applications where operation in the voltage limited high speed region is desired. Because of its smooth rotor surface and narrower air gap, the noise level of IPMSM is much lower than SPMSM [13]. By applying closed loop vector control for IPMSM drive and using Park's transformation method. it is possible to decouple the flux and torque controlling components of IPMSM quantities. Thus, the motor behaves like a separately excited dc motor while maintaining general advantages of ac motor over dc motor.

1.5 Literature Review

IPMSM can offer significant efficiency advantages over induction machines when employed in adjustable-speed drives. This motor operates at synchronous speed and therefore does not have the slip losses inherent in induction motor operation. In addition, since much of the excitation in the PM motor is provided by the magnets, the PM motor will have smaller losses associated with the magnetizing component of stator current; these factors make the IPMSM an attractive alternative to the induction machine in drives where overall efficiency is critical, notably in pump, compressor, or fan drives. Although these motor drives are well known for their relatively high efficiency, improvement margins still exist in their operating efficiency. Particularly, the reduction of power loss for IPMSM still remains a challenge for researchers. Improvement of motor drives efficiency is important not only from the viewpoints of energy loss and hence cost saving, but also from the perspective of environmental pollution. Several efficiency

optimization methods for IPMSM drives have been introduced by researchers [14-29] Most of them are divided to following 4 main strategies:

(a) Optimum Rotor Structure Design Approach

In this approach a conventional IPMSM with a single-layer rotor design can be split into several layers, creating a multilayer rotor structure. It has been shown that the multilayer rotor design can reduce flux leakage and improve the rotor saliency. Hence, the IPMSM with a multilayer rotor design has many performance advantages over the single-layer rotor design, such as enhancing efficiency, extending a high-speed constant power operating range, and improving the power factor. From the analysis of torque characteristics and high-efficiency performance, the magnet torque and reluctance torque can serve as the objective functions to search an optimum efficiency. However, it is difficult to calculate the torque component separately. On the other hand, it is well known that back electromotive force and rotor saliency relate to the magnet torque and reluctance torque closely and can be calculated easily. Therefore, the objective functions are chosen as back electromotive force and rotor saliency ratio at main operation speed point in the optimization analysis [14-16]. In a similar approach to reduce the reluctance torque in IPMSM, rotor is designed in such a way to have unequal air gap [17]. It shows good performance but control characteristic is not considered. In addition, verification of mechanical stress on the rotor under motoring is needed to find out that whether the rotor can withstand mechanical stress or not.

(b) Power Factor Control Approach

In this method, the power factor is calculated from a variation of DC-link current at the inverter main circuit. This calculated power factor controls the applied voltage of the

motor and the unity power factor is obtained [18]. The strategy is when the power factor is lagging PI control decreases the voltage and when the power factor is leading PI control increases the voltage. However although the real to apparent power ratio (kW/kVA) of IPMSM is maximized, power losses are not minimized in this method.

(c) Loss Model Based Control Strategy

This method employs a loss model of the IPMSM and regulates the controlled quantities (voltages and currents) to minimize the estimated loss. In this method, the loss minimization algorithm (LMA) is developed based on motor model and operating conditions. The d-axis armature current is utilized to minimize the losses of the IPMSM in a closed loop vector control environment. However because of dependency on motor parameter and complexity of calculations, application of this strategy is limited.

This approach can be used to good advantage where the losses in the machine can easily be modeled in terms of the controlled quantities. For example, in a motor with no core loss a drive that operates at maximum torque per ampere will be optimally efficient. It has been shown that an IPMSM operating at a fixed speed and torque has a unique optimum voltage that will minimize the total electrical loss. The existence of core loss will cause this optimum value to deviate from the maximum torque per ampere condition, especially for high-speed operation [19-22].

(d) Search Based Control Strategy

The search based approach to optimal efficiency control is to measure the power delivered to the drive and use a search algorithm to adjust a control variable until it detects a minimum value in the power. The optimizing controller has the advantage that it does not depend on a loss model of the machine and therefore is insensitive to variations

in the motor parameters, such as the temperature change in resistance, and does not require accurate modeling of complicated phenomena such as core loss. This method has previously been used in an optimum efficiency control of a field-oriented induction motor drive [23,24] in which the magnetizing component of current was used as the control variable. Implementation of the optimizing control on an IPMSM motor drive is simpler than with an induction motor drive because the control variable does not affect the motor speed as it does with the induction machine, and so the slip calculations of the field-oriented induction motor drive are not needed in the IPMSM drive. For the optimizing control to work, it is necessary that the losses are related to the control variable by a function. This control method is implemented in the thesis.

In this thesis closed loop vector control method is utilized, which uses feedback from the motor to maintain a desired speed or torque output. The principle of vector control is to eliminate the coupling between the direct (d) and quadrature (q) axes components of voltage and current. For vector control, a-b-c quantities can be transformed into the d-q quantities using Park's transformation. In vector control, the q-axis current (i_q) is responsible to control the torque and d-axis current (i_d) is responsible for control of the flux in such a way to achieve optimum efficiency. Thus the IPMSM can be controlled like a separately excited dc motor while keeping the advantages of ac over dc motors. Once the system determines the rotor-flux angle, a vector control algorithm determines the optimum timing and magnitude of the voltages to apply to the stator-phase windings. Thus the vector control provides significantly better performance and reduces torque ripple and current spikes.

Despite many advantageous features of interior permanent magnet synchronous

motor (IPMSM), the precise speed control of an IPMSM drive is a complex issue due to nonlinear coupling among its winding currents and the rotor speed as well as the nonlinearity present in the electromagnetic developed torque due to magnetic saturation of the rotor core [25]. To solve this issue intelligent controllers are applied because their designs do not need the exact mathematical model of the system and theoretically they are capable of handling any nonlinearity. Over the last decade researchers have done extensive research for application of fuzzy logic controller (FLC), artificial neural network (ANN) and neuro-fuzzy (NF) controllers for HPVSD systems [26-40]. Simplicity and less intensive mathematical design requirements are the main features of intelligent controllers, which are suitable to deal with nonlinearities and uncertainties of electric motors. Therefore, the intelligent controllers demand particular attention for high performance nonlinear IPMSM drive systems. Among the intelligent controller FLC is the simplest for speed control of high performance IPMSM drive.

1.6 Thesis motivation

Traditionally, the IPMSM has been controlled by keeping the d-axis component of the stator current, $i_d = 0$ in order to make the control task easier. However, with $i_d = 0$ control it is not possible to control the air gap flux and hence the efficiency of the motor cannot be optimized. Moreover, with $i_d = 0$ control of reluctance torque of IPMSM cannot be utilized, which is an advantageous feature of IPMSM as compared to a surface mounted permanent magnet synchronous motor . Especially, at light load condition the motor flux become excessive for the developed torque resulting in higher iron loss and

poor efficiency of the motor so if i_d remains zero the efficiency can not be optimized . Thus this thesis present a novel efficiency and speed control of the IPMSM using fuzzy logic. In this work efficiency optimization criterion is the online minimization of the drive losses instead of the motor power losses. An optimum flux search algorithm is used, and the drive power consumption is measured. The drive power losses are sampled and calculated. The drive power loss value is then compared with the previous value. A change in dc link current value is determined from this comparison, since the dc voltage is essentially constant. A stator flux value is calculated based on the change in dc link current value. Finally, the flux component of the stator current i_d is generated by a search based fuzzy logic controller depending on the stator flux value. The torque component of the stator current i_q is generated by the vector control strategy using fuzzy logic. In recent years, some efforts have been made on the use of fuzzy algorithms for system modeling and control application [28-38]. In a fuzzy logic controller (FLC), the system control parameters are adjusted by a fuzzy rule based system, which is a logical model of the human behaviour for process control.

1.7 Thesis organization

The remaining chapter of the thesis is organized as follows. Chapter 2 describes the derivation of the mathematical model of the IPMSM. Here it is shown that the vector control technique greatly simplifies the control of the motor. Next, Chapter 3 shows the IPMSM drive's power loss modeling, proposes loss minimization strategy and complete drive incorporating the search based efficiency optimization. At the end of the Chapter 3

the model development and the simulation results of the complete drive system are given. Chapter 4 describes the real-time implementation of the complete drive system using dSPACE DSP and the detailed experimental results. Finally, a summary of the thesis and suggestions for future works are highlighted in Chapter 5. After that, all pertinent references and appendices are listed.

Chapter 2

Modeling of IPMSM

2.1 Park's Transformation

In order to simplify the mathematical model of the motor and make the equations independent on rotor position the model will be expressed in terms of the synchronously rotating reference frame .This transformation is also known as Park's Transformation . This transformation has two steps. In the first step, the machine equations are changed from the stationary a-b-c frame into the stationary d-q frame and in second step from the stationary d-q frame to the synchronously rotating d^r-q^r frame. The phase variables in terms of d-q-0 variables can be written in matrix form as:

$$\begin{bmatrix} x_q \\ x_d \\ x_0 \end{bmatrix} = \frac{2}{3} \begin{bmatrix} \cos\theta_r & \cos(\theta_r - \frac{2\pi}{3}) & \cos(\theta_r + \frac{2\pi}{3}) \\ \sin\theta_r & \sin(\theta_r - \frac{2\pi}{3}) & \sin(\theta_r + \frac{2\pi}{3}) \\ \frac{1}{2} & \frac{1}{2} & \frac{1}{2} \end{bmatrix} \begin{bmatrix} x_a \\ x_b \\ x_c \end{bmatrix} \tag{2.1}$$

The corresponding inverse relation can be written as:

$$\begin{bmatrix} x_a \\ x_b \\ x_c \end{bmatrix} = \begin{bmatrix} \cos\theta_r & \sin\theta_r & 1 \\ \cos(\theta_r - \frac{2\pi}{3}) & \sin(\theta_r - \frac{2\pi}{3}) & 1 \\ \cos(\theta_r + \frac{2\pi}{3}) & \sin(\theta_r + \frac{2\pi}{3}) & 1 \end{bmatrix} \begin{bmatrix} x_q \\ x_d \\ x_0 \end{bmatrix} \tag{2.2}$$

The rotor location or rotor position angle is defined as:

$$\theta_r = \int_0^t \omega_r(\tau) d\tau + \theta_r(0) \tag{2.3}$$

For balanced three phase, '0' sequence component (x_0) does not exist, and it is convenient to set initial rotor position $\theta_r(0) = 0$ so that the q axis coincides with a-phase. Under these condition the above equations can be written as,

$$\begin{bmatrix} x_a \\ x_b \\ x_c \end{bmatrix} = \begin{bmatrix} 1 & 0 \\ -\frac{1}{2} & -\frac{\sqrt{3}}{2} \\ -\frac{1}{2} & \frac{\sqrt{3}}{2} \end{bmatrix} \begin{bmatrix} x_q \\ x_d \end{bmatrix} \tag{2.4}$$

and

$$\begin{bmatrix} x_q \\ x_d \end{bmatrix} = \begin{bmatrix} \frac{2}{3} & -\frac{1}{3} & -\frac{1}{3} \\ 0 & -\frac{1}{\sqrt{3}} & \frac{1}{\sqrt{3}} \end{bmatrix} \begin{bmatrix} x_a \\ x_b \\ x_c \end{bmatrix} \tag{2.5}$$

The relative positions of the stationary and rotating d-q axes are shown in Fig 2.1.

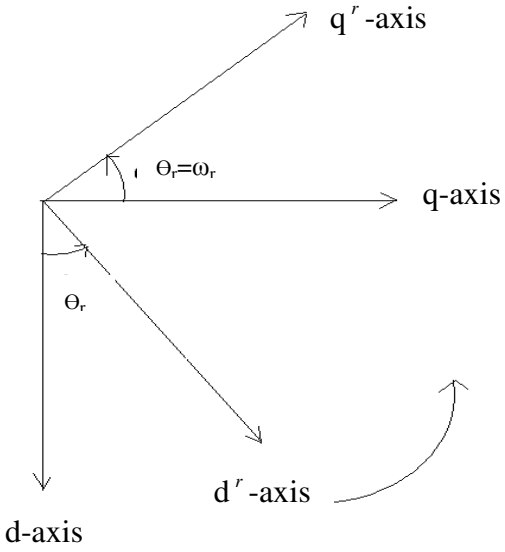

Fig 2.1 Relative positions of stationary and rotating d-q axes

Now the quantities in the stationary d-q frame can be converted to synchronously rotating d^r-q^r frame with the help of Fig 2.1 as:

$$\begin{bmatrix} x_q^r \\ x_d^r \end{bmatrix} = \begin{bmatrix} \cos\theta_r & -\sin\theta_r \\ \sin\theta_r & \cos\theta_r \end{bmatrix} \begin{bmatrix} x_q \\ x_d \end{bmatrix} \tag{2.6}$$

And inverse relation:

$$\begin{bmatrix} x_q \\ x_d \end{bmatrix} = \begin{bmatrix} \cos\theta_r & \sin\theta_r \\ -\sin\theta_r & \cos\theta_r \end{bmatrix} \begin{bmatrix} x_q^r \\ x_d^r \end{bmatrix} \tag{2.7}$$

In order to drive the d^r-q^r axis model of IPMSM drive, the following assumptions are made:

- The eddy current and hysteresis losses are negligible
- The induced Emf is sinusoidal
- The saturation is neglected
- The stator resistance of the three phases are balanced

2.2 Derivation of the Mathematical Model of IPMSM

IPMSM is similar to the conventional wire-wound synchronous motor except the rotor excitation is provided by permanent magnets instead of wire-wound dc rotor field. Therefore, the *d- q* axis model of the IPMSM can be derived from the standard model for synchronous motors by removing the equation related to the field current and associated dynamics.If ψ is the constant flux linkage provided by the permanent magnets, then the flux linkages in the three phase stator winding due to PM of the rotor can be given as:

$$\begin{bmatrix} \psi_{am} \\ \psi_{bm} \\ \psi_{cm} \end{bmatrix} = \psi \begin{bmatrix} \sin\theta_r \\ \sin(\theta_r - \frac{2\pi}{3}) \\ \sin(\theta_r + \frac{2\pi}{3}) \end{bmatrix} \tag{2.8}$$

Where $\psi_{am}, \psi_{bm}, \psi_{cm}$ are the a, b, c, flux linkages due to permanent magnet of the rotor and θ_r is the rotor position. So total air gap flux linkage for three phases are the summation of the flux linkage for the corresponding phase current, mutual flux linkage for the currents in other phases and the flux linkages in the three phase stator winding due to PM of the rotor. The equations for the air gap flux linkage for three phases are given as:

$$\begin{bmatrix} \psi_a \\ \psi_b \\ \psi_c \end{bmatrix} = \begin{bmatrix} L_{aa} & M_{ab} & M_{ac} \\ M_{ba} & L_{bb} & M_{bc} \\ M_{ca} & M_{cb} & L_{cc} \end{bmatrix} \begin{bmatrix} i_a \\ i_b \\ i_c \end{bmatrix} + \psi \begin{bmatrix} \sin\theta_r \\ \sin(\theta_r - \frac{2\pi}{3}) \\ \sin(\theta_r + \frac{2\pi}{3}) \end{bmatrix} \tag{2.9}$$

Where ψ_a , ψ_a , ψ_a are the air gap flux linkage for the phase a, b, c, respectively; $L_{aa,}$ $L_{bb,}$ L_{cc} are the self inductances and $M_{ab,}$ M_{bc}, M_{ca} are the mutual inductances. Now the voltage equations of the three phases of the IPMSM can be defined as:

$$v_a = r_a i_a + \frac{d\psi_a}{dt} \tag{2.10}$$

$$v_b = r_b i_b + \frac{d\psi_b}{dt} \tag{2.11}$$

$$v_c = r_c i_c + \frac{d\psi_c}{dt} \tag{2.12}$$

Where v_a, v_b , v_c are the three phase voltages, i_a, i_b, i_c are the three phase currents and r_a, r_b, r_c are the three phase stator resistances. Now, using equations (2.10)-(2.12), the

transformation equations (2.1) and (2.6) the model of the IPMSM can be written in the synchronously rotating d-q frame as:

$$v_q^r = Ri_q^r + \frac{d\psi_q^r}{dt} + \omega_s \psi_d^r \tag{2.13}$$

$$v_d^r = Ri_d^r + \frac{d\psi_d^r}{dt} - \omega_s \psi_q^r \tag{2.14}$$

Where v_d^r, v_q^r are d,q axis voltages and i_d^r, i_q^r are d,q axis currents, ψ_d^r, ψ_q^r are d,q axis flux linkages and R is the stator resistance per phase and ω_s is the stator frequency. ψ_d^r and ψ_q^r can be written as,

$$\psi_q^r = L_q i_q^r \tag{2.15}$$

$$\psi_d^r = L_d i_d^r + \psi \tag{2.16}$$

Where,

$$L_q = L_l + L_{mq} \tag{2.17}$$

$$L_d = L_l + L_{md} \tag{2.18}$$

L_d and L_q are d-q axis inductances, L_{md}, L_{mq} are d-q axis magnetizing inductances and L_l is the leakage inductance per phase. The stator frequency related to rotor frequency as:

$$\omega_s = P\omega_r \tag{2.19}$$

Using equations (2.13)-(2.16), the motor equations can be written as:

$$v_q^r = L_q i_q^r + Ri_q^r + P\omega_r L_d i_d^r + P\omega_r \psi \tag{2.20}$$

$$v_d^r = L_d i_d^r + Ri_d^r - P\omega_r L_q i_q^r \tag{2.21}$$

In these equations all the stator voltages and currents are in rotor reference frame According to Equation (2.15), (2.16), (2.20) and (2.21) the motor can be represented by the equivalent circuit diagrams shown in Fig 2.2.

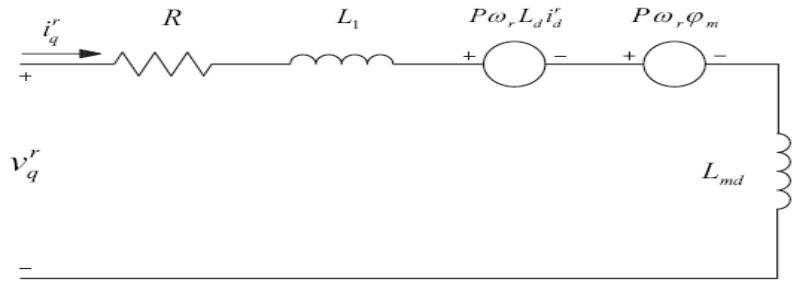

(a) d-axis equivalent circuit

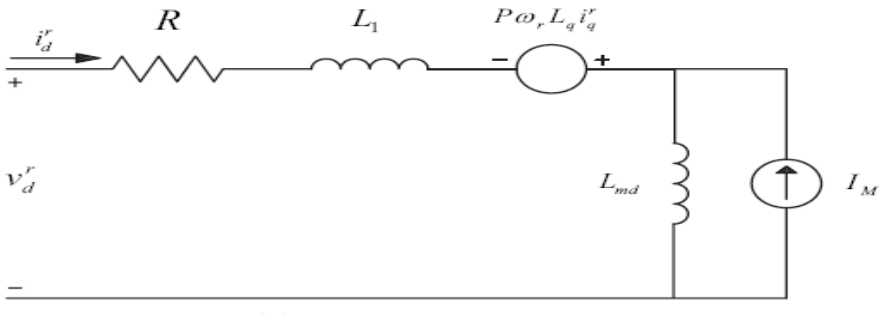

(b) q-axis equivalent circuit

Fig 2.2 Equivalent circuits model of the IPMSM

The torque developed by the machine is obtained by considering the power entering the two sources in the circuit diagram. The total average power entering the sources per phase is given by:

$$P_{phase} = \frac{1}{2}(-P\omega_r L_q i_q^r i_d^r + P\omega_r L_d i_q^r i_d^r + P\omega_r \psi i_q^r) \tag{2.22}$$

Therefore, the total power developed by the machine is:

$$P_{mech} = \frac{3P\omega_r}{2}\{\psi i_q^r + (L_d - L_q) i_q^r i_d^r\} \tag{2.23}$$

Now the developed electromagnetic torque is given by

$$T_e = \frac{P_{mech}}{\omega_r} = \frac{3P}{2}\{\psi i_q^r + (L_d - L_q) i_q^r i_d^r\} \tag{2.24}$$

The motor dynamic can be represented by the following equation:

$$T_e = T_L + B_m \omega_r + J \dot{\omega}_r \tag{2.25}$$

Where T_L is the load torque in Nm, B_m is the friction damping coefficient in Nm/rad/sec and J is rotor inertia constant in kg-m^2.

2.3 Vector Control Strategy for IPMSM Drive

As discussed previously, the vector control technique is an effective technique for use with ac motors in high performance drives. The IPMSM can be vector controlled when the machine equations are transformed from the abc frame to the synchronously rotating d-q frame. The complexity of control of the IPMSM drive arises due to the nonlinear nature of the torque in equation (2.24). One way of simplifying this is to set $i_d = 0$. The torque equation then becomes:

$$T_e = \frac{3P}{2} \psi i_q = K_t i_q \tag{2.26}$$

This is linear and similar to the torque equation of a dc motor. Using phasor notation and taking the *d* axis as the reference phasor, the steady state phase voltage *Va* and current can be derived from equation (2.20) as:

$$\begin{aligned} V_a &= v_d^r + j v_q^r \\ &= R I_a - \omega_s L_q i_q^r + j \omega_s L_d i_d^r + j \omega_s \psi \end{aligned} \tag{2.27}$$

$$I_a = i_d^r + j i_q^r \tag{2.28}$$

Based on equation (2.27) and (2.28) the basic vector diagram of the IPMSM is shown in Fig 2.3.

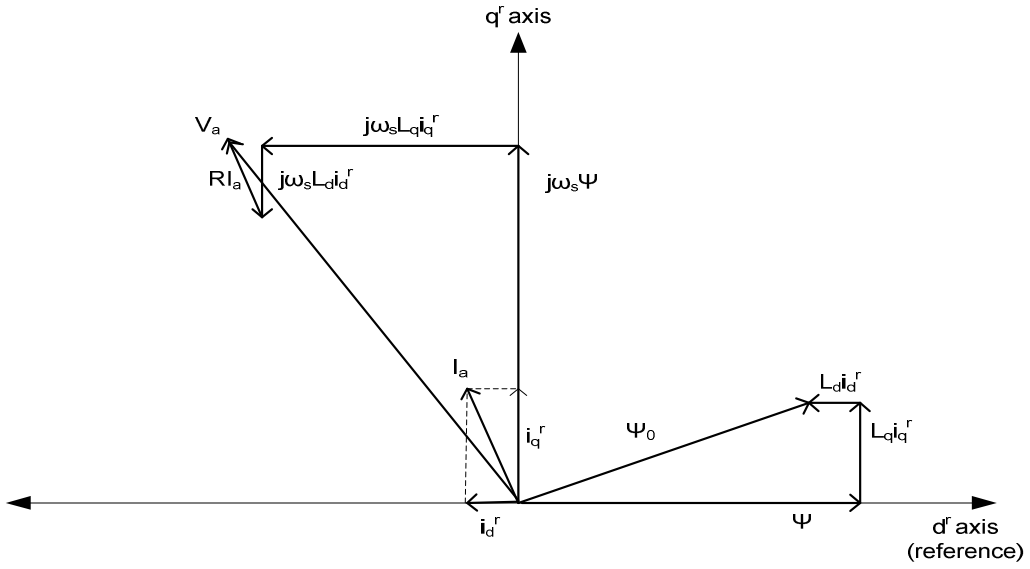

Fig.2.3 Vector diagram of IPMSM

The stator current can be controlled by controlling the individual d-q current components. When i_d is set to zero, the torque is a function of only the q-axis current component, and hence the torque can be controlled by controlling i_q. Constant torque can be obtained by ensuring that i_q is kept constant. In the case of IPM motor, the d^r axis current is negative and it demagnetizes the main flux provided by the permanent magnets. Thus in order to take the absolute value of i_d^r, we can rewrite the equation as:

$$V_a = RI_a - \omega_s L_q i_q^r - j\omega_s L_d i_d^r + j\omega_s \psi \tag{2.29}$$

The stator current vector can be controlled by controlling the individual d-q current components. The proposed control algorithm presented in this work, this technique is used to control the motor up to its rated speed. In order to control the motor beyond its rated speed, the flux weakening technique must be incorporated.

Chapter 3

Development of Fuzzy Logic Based Efficiency and Speed Control Scheme of an IPMSM

3.1 Power Loss Modeling and Proposed Loss Minimization Strategy

The IPMSM drive's total power losses are calculated as the difference between input and output drive power:

$$P_{Loss} = P_{in} - P_{out} = V_{DC} I_{DC} - \omega_r T_e \tag{3.1}$$

Where P_{in}, P_{out} are the drive input and output power, V_{DC} and I_{DC} are voltage and current in the dc link, ω_r and T_e are motor speed and electromagnetic torque, respectively. These are known variable in a drive so we are able to calculate the total drive power losses without the need of knowledge of the motor parameters and independently of the parameter changes (due to saturation and heating). The minimization of P_{Loss} implies into the minimization of P_{in} which is the minimization of the dc link current I_{DC}, since the dc link voltage V_{DC} is virtually constant. The change of P_{Loss} or ΔP_{Loss} represents at each instance the difference between the current and a previous value over a constant time interval. A negative value of ΔP_{Loss} indicates a power input efficiency improvement. The Power "Loss Processing Unit" is incorporated into the proposed fuzzy efficiency system in order to calculate the drive's power losses, during steady states, by (3.1). The proposed

search based control technique uses online power searching algorithms to adjust flux component of stator current (motor's d-axis current) to obtain the minimum input power on condition of keeping output power constant. This control method is independent on motor parameters. The principle of efficiency optimization by flux programming at a steady-state torque and speed condition is shown in Fig 3.1.

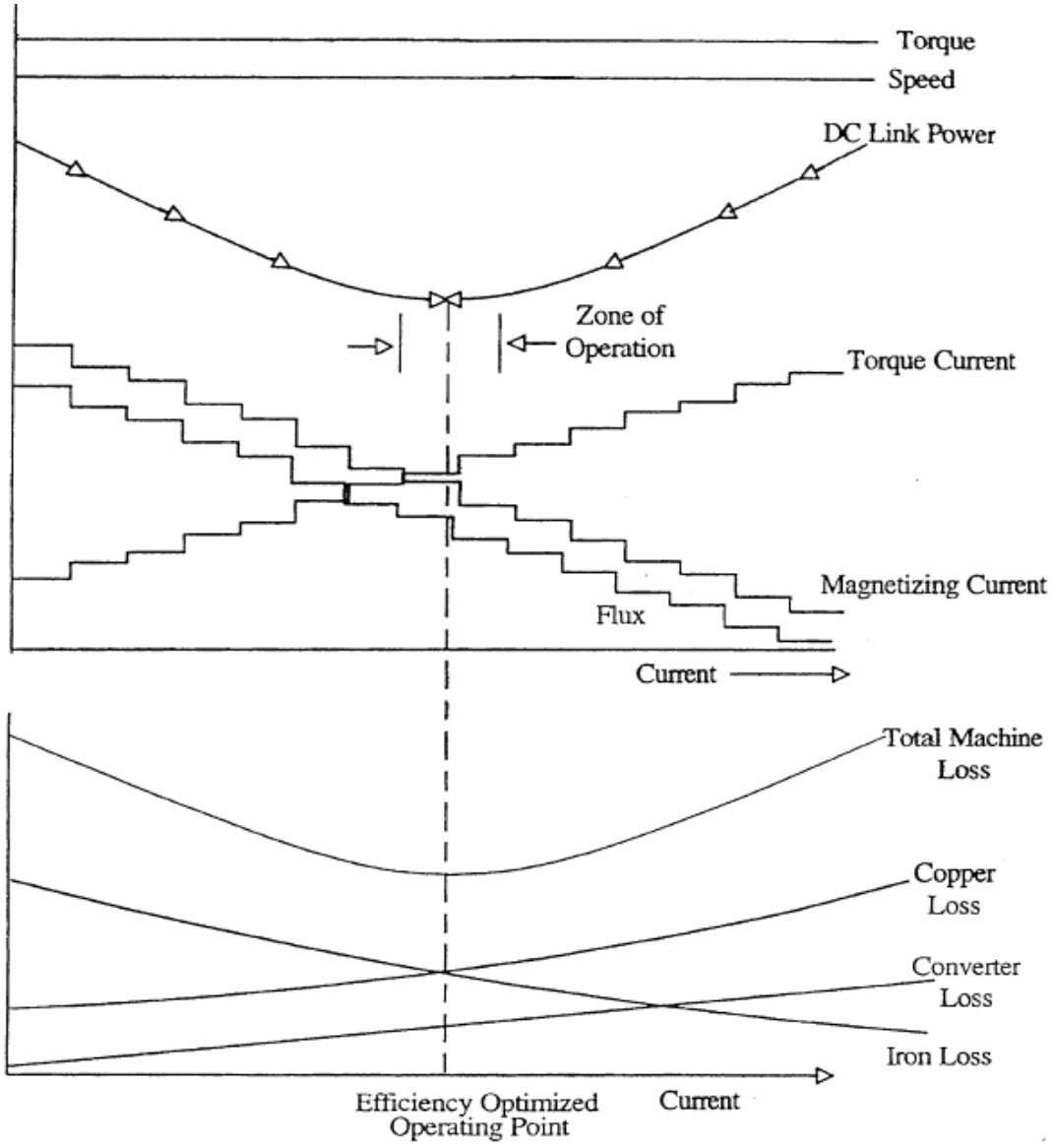

Fig 3.1 Principle of efficiency optimization by flux programming

As it is shown in Fig 3.1 to achieve efficiency optimized operating point the motor's d-axis current and the air gap flux are reduced in order to produce the lowest possible input power. The rotor air gap flux is decreased by reducing the magnetizing component of the stator current. This ultimately results in a corresponding increase in the torque component of the stator current by the action of the speed controller so that the developed torque and speed remain constant at the desired values. As the air gap flux is decreased in steps, the iron core loss decreases as well. However, due to the rise in the torque component of the stator current, the copper (resistive) loss increases. At the operating point where the core loss decrease is offset by the copper loss increase, the minimum input power level is reached. Any excursion past this point will cause the controller to return to the previous point. In efficiency optimization the d-axis current is adjusted in order to achieve minimum measured input power to the IPMSM drive. A minimum input power can be related to a minimum controllable electrical loss only when the motor output power (developed torque times speed) and motor load are assumed to be constant. In that case the changes in i_d vary the torque, and therefore the output power, unless it is modified accordingly to compensate for the torque variations.

In recent years, some efforts have been made on the use of fuzzy algorithms for system modeling and control application. In a fuzzy logic controller (FLC), the system control parameters are adjusted by a fuzzy rule based system, which is a logical model of the human behaviour for process control. The advantages of FLC over the conventional controllers are: (1) the design of FLC does not need the exact mathematical model of the system; (2) the FLC is more robust than the conventional controllers; (3) it can handle

nonlinear functions of any arbitrary complexity; (4) it is based on the linguistic control rules (LCR) which is also the basis of human logic [41].

This thesis presents a novel efficiency and speed control of the IPMSM using fuzzy logic. In this work efficiency optimization criterion is the online minimization of the drive losses instead of the motor power losses. An optimum flux search algorithm is used, and the drive power consumption is measured. The drive power loss value is then compared with the previous value. A change in dc link current value is determined from this comparison, since the dc voltage is essentially constant. A stator flux value is calculated based on the change in dc link current value. Finally, the flux component of the stator current i_d is generated by a search based fuzzy logic controller depending on the stator flux value. The torque component of the stator current i_q is generated by the vector control strategy using fuzzy logic. Obviously, this approach does not require the knowledge of motor parameters. In this work, advantages of using a fuzzy logic based search controller to optimize the efficiency at steady state are described. For transients, a fuzzy logic based controller, actuating as a supervisor, is proposed to let the drive track the reference depending on the speed error and its derivative.

Among the various intelligent controllers, FLC is the simplest for speed control of high performance IPMSM drive. The FLC is better than the conventional controllers in terms of insensitivity to parameter and load variations, response time, settling time and robustness. So far none of the reported works considers the design of FLC incorporating flux control to achieve optimum efficiency for IPMSM drive.

3.2 Fundamentals of fuzzy logic controller

A fuzzy control system is a control system based on fuzzy logic which is a mathematical system that analyzes analog input values in terms of logical variables that take on continuous values between 0 and 1, in contrast to classical or digital logic, which takes discrete values of either 0 and 1 (true and false). These controllers are based on fuzzy set and fuzzy logic theory introduced by Zadeh [42].

The fuzzy set (subset) A on the universe (set) X is defined by a membership function, $\mu_{A,}$ from X to the real interval [0, 1], which associates a number $\mu_A(x) \in [0,1]$ to each element x of universe X. The membership function $\mu_A(x)$ represents the grade of the membership function of x to A, for example the equation $\mu_A(x) = 0.3$ means x has A-ness of about 30%. The block diagram of a typical FLC is shown in Fig.3.2.

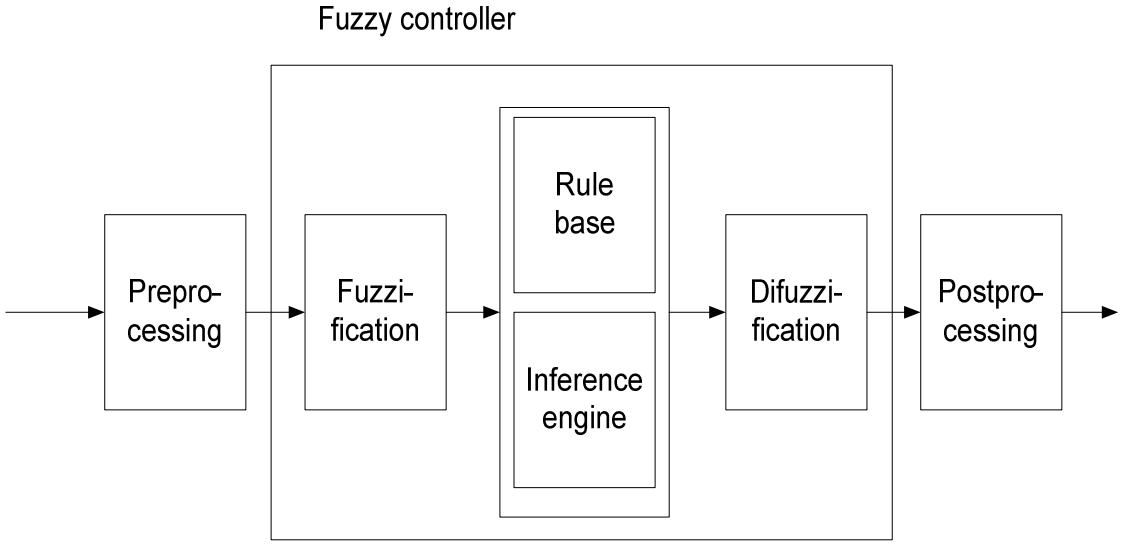

Fig 3.2 Block diagram of a fuzzy logic controller.

The complete process of mapping from a given input to an output using fuzzy logic is known as fuzzy inference. There are two types of fuzzy inference methods namely Mamdani type and Sugeno type. The difference between the two methods is only the way their outputs are defined. In Mamdani type FLC, output is defined by the centroid of a two-dimensional function. But in Sugeno type FLC, the output membership functions are only linear or constant singleton spikes. In Sugeno type inference, implication and aggregation methods are fixed and cannot be edited. The implication method is simply multiplication and the aggregation operator just includes all of the singletons

Regardless of the type, fuzzy inference is mainly based on five components which are: (1) Pre-processing (2) fuzzification, (3) fuzzy inference engine (rule base) (4) defuzzification and (5) Post-processing.

3.2.1 Pre-processing

The inputs are most often hard or crisp measurements from some measuring equipment, rather than linguistic. A pre-processor, the first block in Fig.5.2, conditions the measurements before they enter the controller. Some examples of pre-processing are scaling, filtering, quantization, differentiation, integration etc.

3.2.2 Fuzzification

The first step of fuzzy inference is to take inputs and determine the degree to which they belong to each of the appropriate fuzzy sets via membership functions. The process of converting a numerical variable (real or crisp value) into a linguistic variable (fuzzy value) is called fuzzification. In the FLC, the input is a numerical value limited to

the universe of the input variable and the output is fuzzy degree of membership in the qualifying linguistic set (between 0 and 1 inclusive). Mathematically, the fuzzification of an input can be obtained using a singleton fuzzifier according to the equations of pre-selected membership functions of various fuzzy sets of that input.

3.2.3 Fuzzy inference engine (rule base)

The rules may use several variables both in the condition and the conclusion of the rules. The controllers can therefore be applied to both multi-input-multi-output (MIMO) problems and single-input-single-output (SISO) problems. The typical SISO problem is to regulate a control signal based on an error signal. The controller may actually need both the error and the change in error as inputs. To simplify, this section assumes that the control objective is to regulate some process output around a prescribed reference. Basically a linguistic controller contains rules in if-then format, but they can be presented in different formats. In many systems, the rules are presented to the end-user in a format similar to the one below,

$$\text{Rule } R_k : \text{If } \Delta\omega \text{ is } A_k \text{ and } \Delta e \text{ is } B_k \text{ then i is } C_k \tag{3.2}$$

Where speed error ($\Delta\omega$) and change of speed error (Δe) are the input linguistic variables, current (i) is the output linguistic variable; and A_k, B_k, and C_k are the labels of linguistic variables $\Delta\omega$, $\Delta\omega_e$ and i, respectively. If the antecedent is true to some degree of membership, the consequent is also true to that same degree. The fuzzy operators used for fuzzy rules are AND ($\cap$), OR (U) and NOT ($^-$) which can be defined as follows:

a) AND means classical intersection:

$$\mu_{A\cap B} = \min\{\mu_A(x), \mu_B(x)\} \tag{3.3}$$

b) OR means classical union:

$$\mu_{A\cup B} = \max\{\mu_A(x), \mu_B(x)\} \tag{3.4}$$

c) NOT means classical complement:

$$\bar{\mu}_A = 1 - \mu_A(x) \tag{3.5}$$

Therefore, according to rule R_k, $\mu_{ck}(x) = \min(\mu_{Ak}(x), \mu_{Ak}(x))$, the fuzzy rules can be derived by using the following approaches:

a) from expert experience and control engineering knowledge

b) from the behaviour of human operators

c) from a fuzzy model of a process

d) from a learning process.

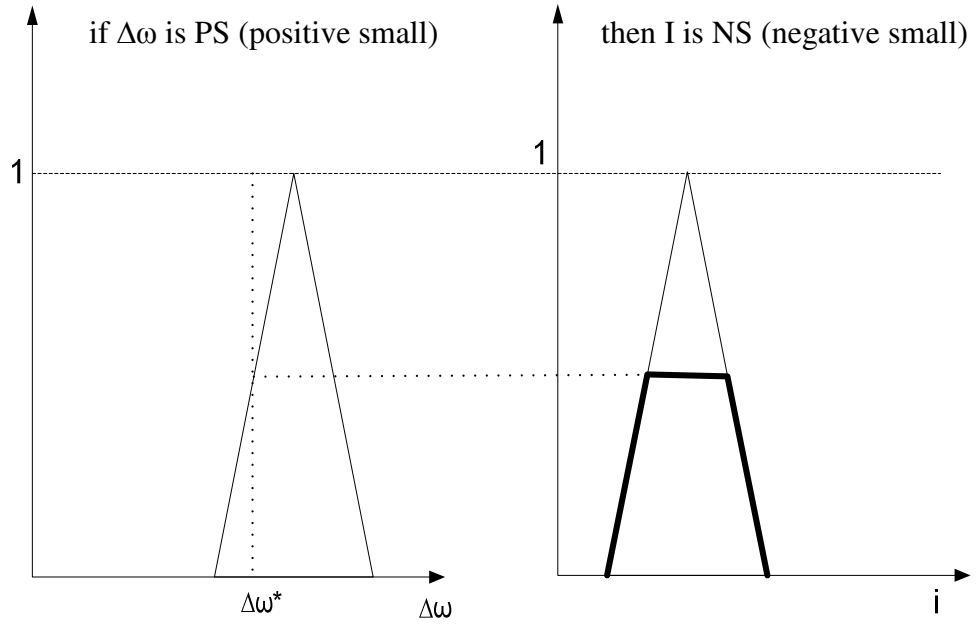

Fig 3.3 The graphical representation of the firing of a rule using Mamdani method.

With respect to fuzzy control, Mamdani implication is the most important implication known in the literature [43].

The graphical representation of Mamdani implication in order to interpret the meaning of a rule is shown in Fig.3.3. This figure shows the firing of a rule "if $\Delta\omega$ is PS (positive small), the output 'i' is NS (negative small)". $\Delta\omega^*$ is the crisp input and the deep solid lines in the output membership function $\mu_{CNS}(i)$ indicates the modified (clipped) membership function $\mu_{CNS}(i)$

Thus according to Mamdani implication,

$$\mu_{CNS}(i) = \min(\mu_{PS}(\Delta\omega^*), \mu_{NS}(i)) \tag{3.6}$$

The process described by this equation is called rule firing. The inference engine or rule firing as described above can be of two basic types such as:

(1) Composition based

(2) Rule based inferences.

The basic differences between them are described below:

(1) Composition based inferences: In this inference, the fuzzy relations representing the meaning of each rule are aggregated into one fuzzy relation describing the meaning of the overall set of rules. Then, inference or firing with this fuzzy relation is performed via the operation composition between the fuzzified crisp input and the fuzzy relation representing the meaning of the overall set of rules. As a result of the composition one obtains the fuzzy set describing the fuzzy value of the overall control output.

(2) Individual rule based inference: In this inference, first each single rule is fired.

This firing can simply be described as: (a) computing the degree of match between

the crisp input and the fuzzy sets describing the meaning of the rule antecedent and (b) clipping the fuzzy set describing the meaning of the rule consequent to which the rule-antecedent has been matched by the crisp input. Finally, the clipped values for the control output of each rule are aggregated, thus forming the value of the overall control output.

Usually, the individual rule based inference is preferred since it is computationally very efficient and saves a lot of memory. In this thesis, the individual rule based inference is used. However, the composition based inference is equivalent to the individual rule based inference in the case of Mamdani-type implication used to represent the meaning of the individual rules. In the case of individual rule based inference, the overall control output which is a combined fuzzy set from a set of rules can be mathematically expressed in [44] as

$$\mu_I(i) = \max(\mu_{CLI(1)}(i),\ldots\ldots..,\mu_{CLI(n)}(i)) \tag{3.7}$$

Where $\mu_{CLI(k)}(i)$ (k=1,2,...,n) is the clipped value of the control output 'i' in the case of individual (kth) rule based inference:

$$\mu_{CLI(k)}(i) = \min(\min(\mu_{A(k)}(\Delta\omega^*),\mu_{B(k)}(\Delta e^*)),\mu_{C(k)}(i)) \tag{3.8}$$

where $\mu_{A(k)}(\Delta\omega^*)$ is the degree of membership of the crisp input $\Delta\omega^*$ in fuzzy set $\mu_{A(k)}$, $\mu_{B(k)}(\Delta e^*)$ is the degree of membership of the crisp input Δe^* in fuzzy set $\mu_{B(k)}$, and $\mu_{C(k)}(i)$ is the degree of membership of the output 'i' in fuzzy set $\mu_{C(k)}$.

3.2.4 Defuzzification

Defuzzification is the final process of fuzzy inference in getting the control output. The input for the defuzzification process is a fuzzy set (combined output of each rule) and the output is a single number, which is non-fuzzy crisp value.

There are several defuzzification methods. The centre of gravity or area is the most popular among all the methods of defuzzification and it is used in this work, in this method, the crisp output value x is the abscissa under the centre of gravity of the fuzzy set,

$$u = \frac{\sum_i \mu(x_i) x_i}{\sum_i \mu(x_i)} \tag{3.9}$$

Here x_i is a operating point in a discrete universe, and $\mu(x_i)$, is its membership value in the membership function. The expression can be interpreted as the weighted average of the elements in the support set.

3.2.5 Post processing

Output scaling is also relevant. In case the output is defined on a standard universe this must be scaled to appropriate unit for instance ampere, volts, meters, or tons per hour. An example is the scaling from the standard universe [-1,1] to the physical units [-20,20] Amperes. The post processing block often contains an output gain that can be tuned, and sometimes also an integrator.

3.3 Implementation of Complete Fuzzy Logic Efficiency and Speed Control Scheme

The proposed efficiency and speed control system includes two fuzzy efficiency controllers FLC (1), FLC (2) and a fuzzy logic based speed controller FLC (3). The fuzzy

efficiency controllers are activated separately for steady and transient states, respectively; to generate the flux component of stator current (d-axis component of stator current).The power processing unit is incorporated to the system to calculate the drive total power loss as the difference between input and output drive power in steady state operations. The value of power loss at each sample is fed to the FLC (1).The fuzzy logic based speed controller generates torque component of stator current (q-axis component of stator current).

In order to solve torque and speed fluctuations caused by continuous step change of (i_d) in the search process, (i_q) is regulated to keep the torque constant by compensation of torque current. The command d-q axis currents are generated using FLCs, these command currents using inverse Park's transformation change from stationary d-q frame into a-b-c. The command phase currents are compared with the actual sensed currents from Hall Effect sensors to generate the six logic signals which act as the gating pulses for the six IGBT switches of the three-phase inverter to feed the IPMSM.

The speed signal detected from an encoder mounted on the rotor is compared to command speed to generate speed error which is the input of two fuzzy logic controllers.

The details and functions of the hardware components of the system will be investigated in depth in Chapter 4 of the thesis. The complete block diagram of IPMSM drive incorporating fuzzy efficiency system is shown in Fig 3.4.

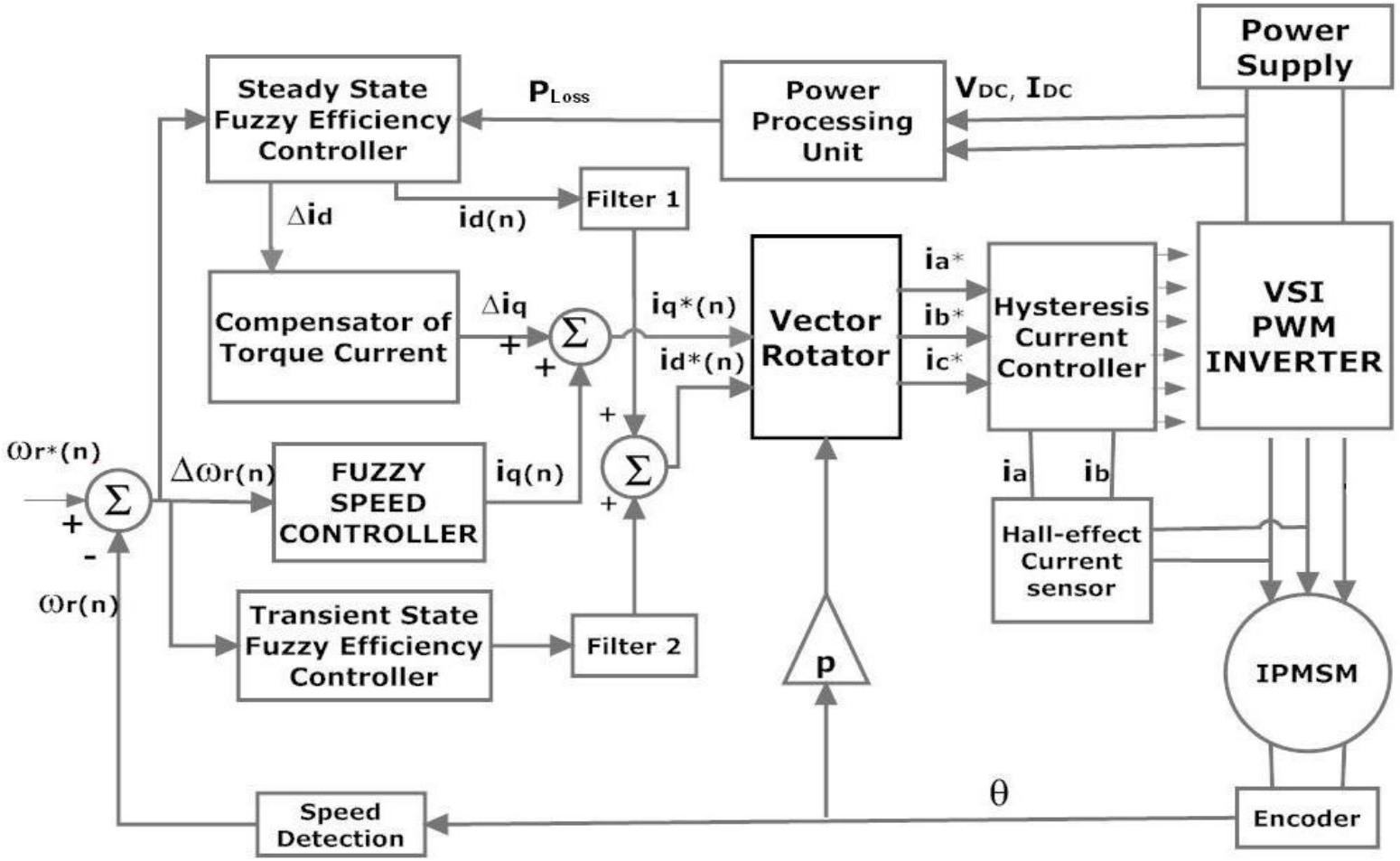

Fig 3.4 Block diagram of IPMSM drive incorporating fuzzy efficiency and speed control system.

3.3.1 Steady State Fuzzy Efficiency Controller

Steady state fuzzy efficiency controller is activated when the system reaches to steady state and it is determined when the speed error maintains a particular value for a predetermined period of time. The contribution of this search controller is online power searching to adjust flux component of stator current (motor's d-axis current) to obtain the minimum power loss. The drive power losses are sampled and calculated by power processing unit and is fed to this controller. The drive power loss value is then compared with the previous value. A change in dc link current value is determined from this comparison, since the dc voltage is essentially constant. A stator flux value is calculated based on the change in dc link current value. Finally, the flux component of the stator current i_d is generated by a search based fuzzy logic controller depending on the stator flux value. Fig 3.5 shows the block diagram of the steady state fuzzy efficiency controller.

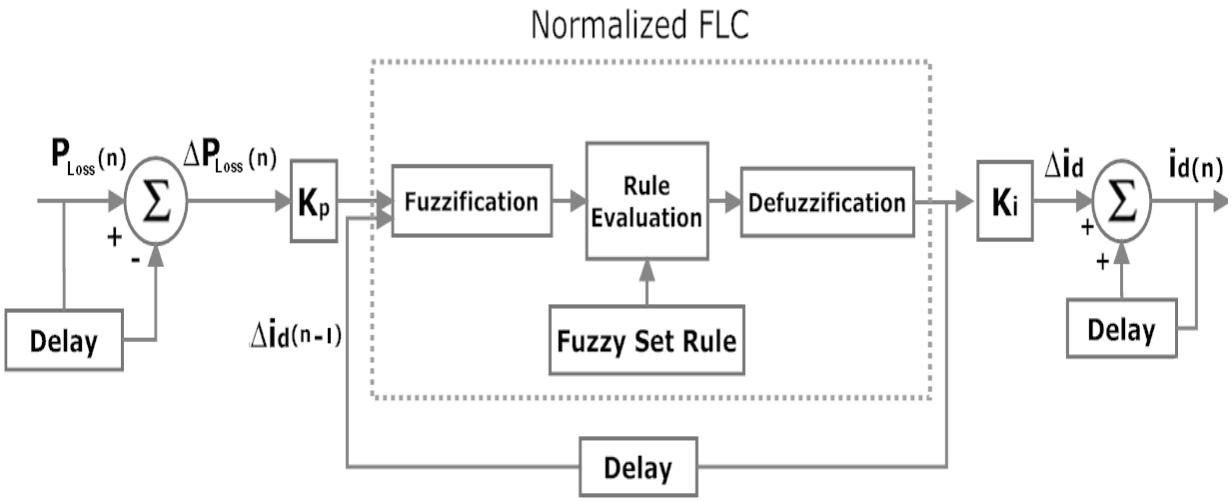

Fig 3.5 Block diagram of steady state fuzzy efficiency controller (FLC 1)

The input variables of (FLC 1) are the current sample for the change in power loss, ΔP_{Loss} (n) and the past sample of the change in d-axis component of the stator current Δi_d (n-1). The output variable of (FLC 1) is the d-axis component of stator current i_d (n). The membership functions for input-output variables of (FLC 1) are shown in Fig 3.6.

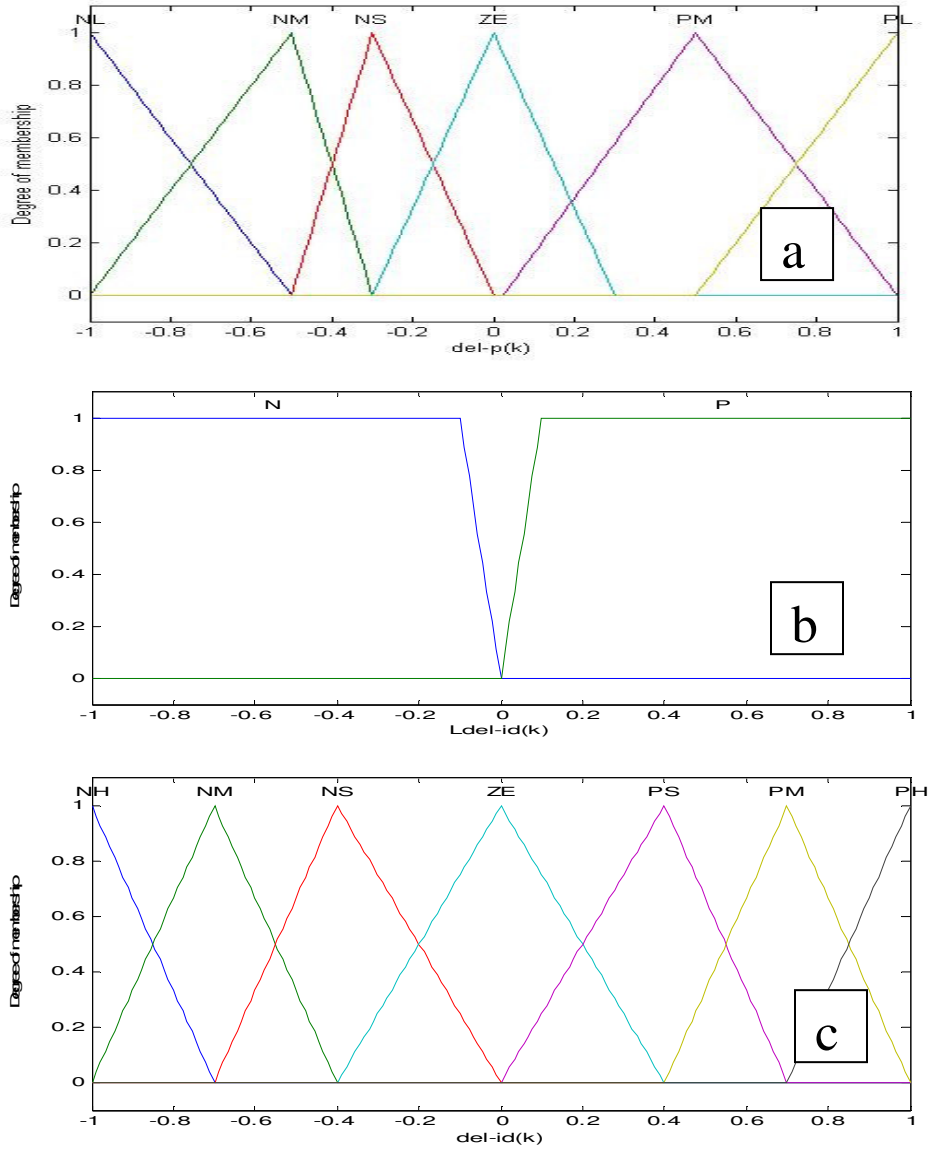

Figure 3.6 Membership functions of the input-output of (FLC 1) (a) change in power loss ΔP_{Loss} (n).(b) past sample of change in d-axis current Δi_d (n-1). (c) d-axis current i_d (n)

The fuzzy rules are selected by trial and error method on experience about efficiency optimization of IPMSM drive. The fuzzy rule based matrix for the (FLC 1) is shown in Table 3.1.

Table 3.1 Fuzzy Rules of FLC (1)

ΔP_{Loss} (n). \ Δi_d (n -1)	N	P
PH	PM	NM
PM	PS	NS
ZE	ZE	ZE
NS	NS	PS
NM	NM	PM
NH	NH	PH

A sample rule from the above rule-based matrix can be written as, if ΔP_{Loss} (n) is positive high (PH) and Δi_d (n -1) is negative (N) then i_d (n) is positive medium (PM)

3.3.2 Transient State Fuzzy Controller

The above fuzzy efficiency controller is only effective with constant speed and torque. When load torque or command speed change takes place, the search process stops. A fuzzy controller actuating as a supervisor is designed for transient state (FLC2).This controller fires up during transient when the absolute value of speed error

exceeds certain value .This controller is used to get fast response, low overshoot/undershoot while maintaining power loss minimal. This controller increases the flux depending on the speed error and its derivative. If the transient is very large or the speed error is very high, the flux is established at rated level in order to let the drive track the command speed. The proposed controller is very simple containing a table of heuristic rules, for reference speed change. The controller only provides positive flux increments, actuating as a supervisor, since it supervises the right command tracking by incrementing the flux if necessary. The block diagram of the proposed fuzzy logic based transient controller is shown in Fig 3.7.

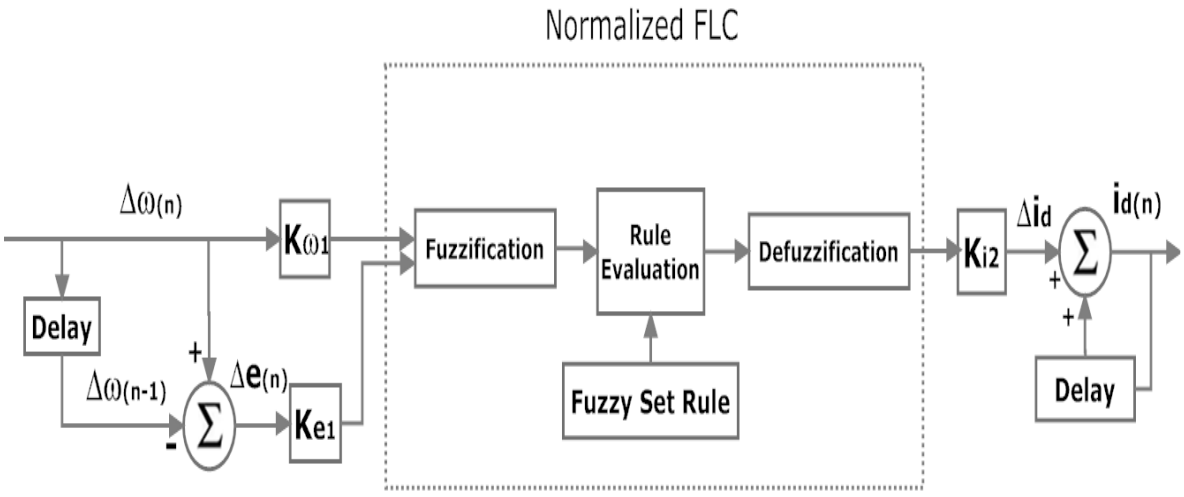

Fig 3.7 Block diagram of transient fuzzy efficiency controller

The membership functions for input-output variables of (FLC 2) are shown in Fig 3.8.

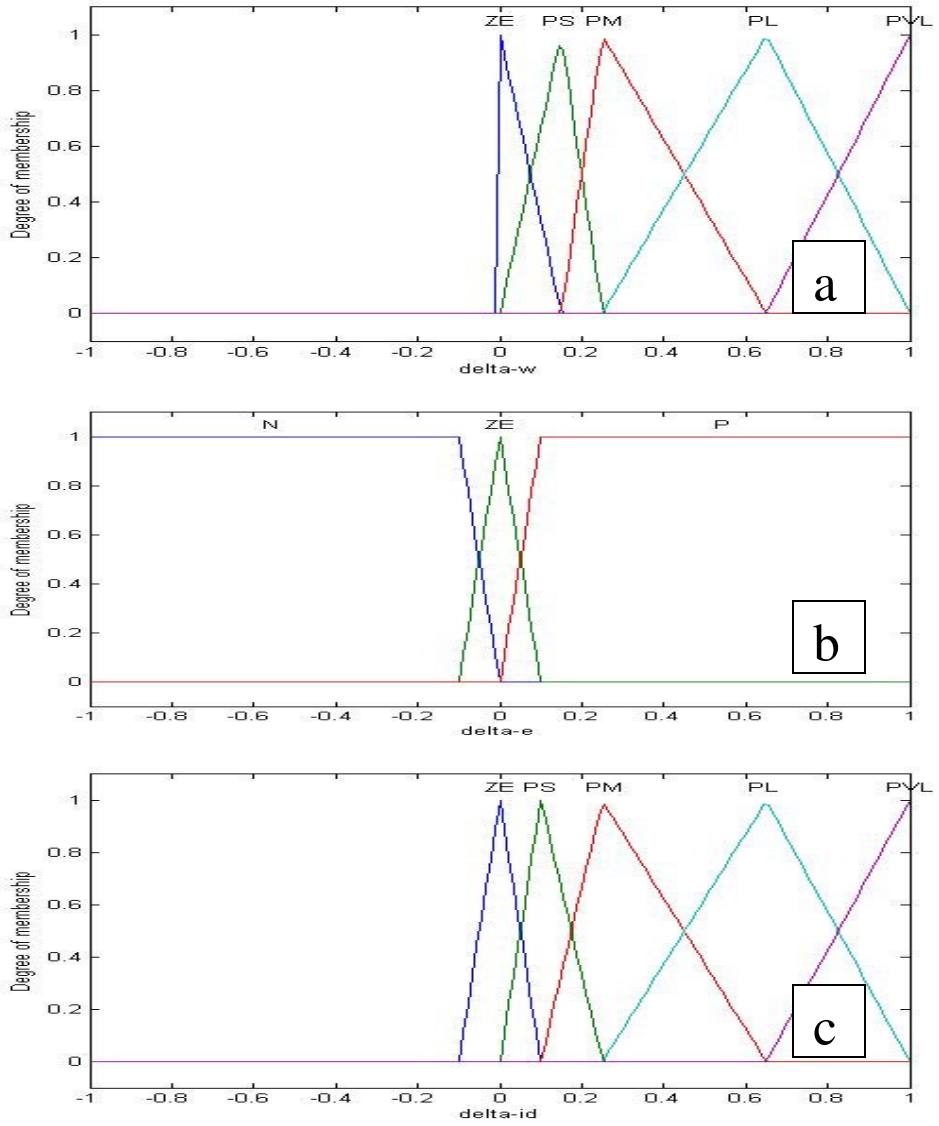

Figure 3.8 Membership functions of the input-output of (FLC 2)
(a) Speed error $\Delta\omega_r$ (n) (b) change of speed error Δe (n).
(c) d-axis current $\Delta i_d(n)$

As it's mentioned earlier since this controller solely increases the flux, it provides only positive flux increments and its rules are suitable for a positive torque transition and for a positive reference speed change.The fuzzy rule based matrix used for (FLC 2) is shown in Table 3.2.

Table 3.2 Fuzzy Rules for FLC (2)

$\Delta\omega_r$ (n) \ Δe (n)	ZE	P	N
ZE	ZE	ZE	ZE
PS	PVL	PS	ZE
PM	PVL	PM	PS
PL	PVL	PL	PM
PVL	PVL	PVL	PL

3.3.3 Fuzzy Speed Controller

In order to follow the command speed without any overshoot and steady state error, q-axis command current, which represents the torque component of stator current is generated by vector control technique using a fuzzy logic controller. Fig 3.9 shows the block diagram of the proposed speed controller.

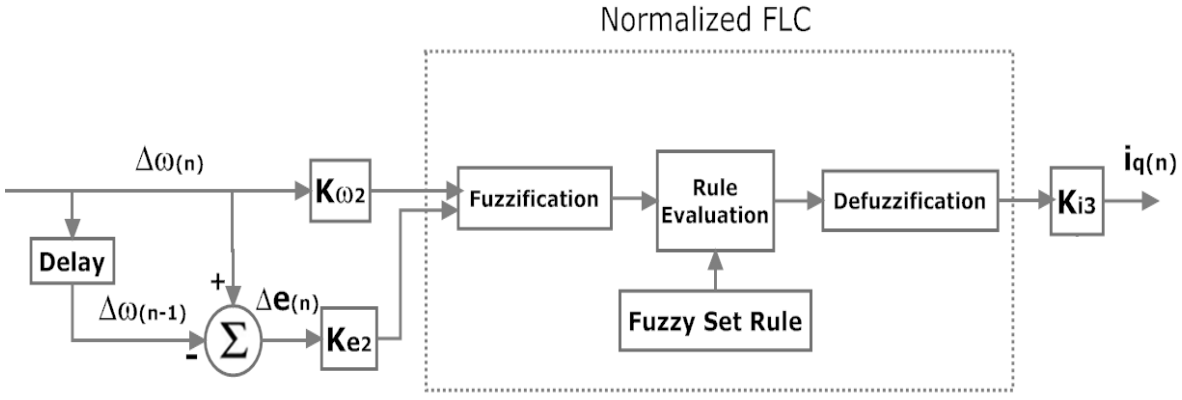

Fig 3.9 Block diagram of fuzzy speed controller

The inputs of the proposed FLC are the present sample of speed error $\Delta\omega_r$ (n) and the change of the speed error Δe (n) and the output vector is the q-axis stator current i_q (n)

[45]. The membership functions for the inputs-output variables are shown in Figure 3.10(a), (b) and (c).

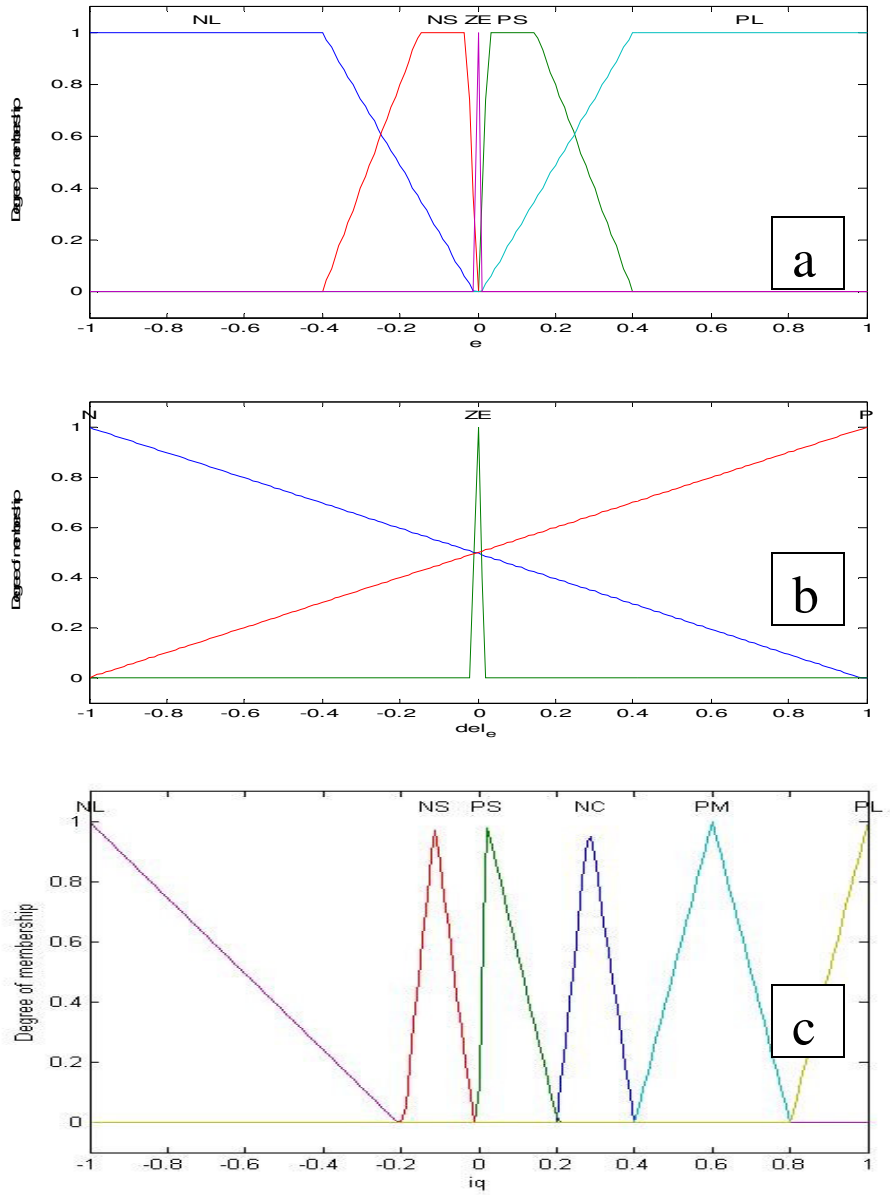

Figure 3.10 Membership functions of the input-output of (FLC 3)
(a) Speed error $\Delta\omega_r$ (n) (b) change of speed error Δe (n).
(c) q-axis current i_q (n).

The fuzzy rule based matrix used for (FLC 3) is shown in Table 3.3.

Table 3.3 Fuzzy Rules for FLC (3)

$\Delta\omega_r$ (n) \ Δe (n)	N	ZE	P
N	NL	NL	NL
NS	NS	NS	NS
ZE	NC	NC	PS
PS	PM	PM	PM
PL	PL	PL	PL

3.3.4 Compensation of Torque Current

In order to solve the torque and speed fluctuations caused by the continuous step change of i_d in the search process the torque will be maintained constant by synchronously regulating the q-axis current i_q. In this way, the IPMSM system will keep in the steady state, the fluctuations will be reduced, and the efficiency optimization will speed up. Before the regulation of the d-axis current, the IPMSM electromagnetic torque T_e is given as:

$$T_e = \frac{3P}{2}\left[\psi_f i_q^r + \left(L_d - L_q\right) i_d^r i_q^r\right] \tag{3.10}$$

The q-axis current value is adjusted accordingly to the d-axis current changes Δi_d to keep the constant torque of IPMSM. The adjusted electromagnetic torque can be expressed as:

$$T_e + \Delta T_e = \frac{3P}{2}\left[\psi_f (i_q^r + \Delta i_q) + \left(L_d - L_q\right)(i_d^r + \Delta i_d)(i_q^r + \Delta i_q)\right] \quad (3.11)$$

Setting $\Delta T_e = 0$ and ignoring the high-order items the q-axis compensation current can be expressed as follows:

$$\Delta i_q(k) = \frac{i_q(k)}{\psi_f + (L_d - L_q) i_d(k)} \Delta i_d(k) \quad (3.12)$$

The compensator of q-axis current is given as the actual q-axis current is expressed as:

$$i_q'(k) = i_q(k) + \Delta i_q(k) \quad (3.13)$$

Therefore, the actual control value is the compensated d-axis current component and the compensated q-axis current component.

3.4 Simulation of the Proposed IPMSM Drive

In order to verify the efficiency optimization, less torque ripple and robustness in different dynamic operation of the proposed drive a computer simulation model is developed in Matlab/Simulink software and Fuzzy Logic toolbox. The performance of the proposed efficiency control system is compared with traditional $i_d = 0$ control technique in different dynamic operation. The model used for simulation is shown in Fig 3.11. The details of the sub-system of this model are shown in Appendix B. From the simulation results it can be observed that the proposed FLC controller can follow the command speed with no overshoot or undershoot. The motor parameter used for this simulation is shown in Table.3.4. Sample results are presented below:

Table 3.4 IPMSM Parameters

Rated Power	5 HP
Number of poles	6
Rated input voltage	183 V
q-axis inductance, L_q	6.42 mH
d-axis inductance, L_d	5.06 mH
Stator resistance per phase	0.242 ohm
Inertia constant J	$0.0133 kg.m^2$
Rotor damping constant B_m	$0.001(Nm)/rad./\sec$
PM flux linkage	$0.24 volts/rad./\sec$
Rated Input Current	14.2 A
Rated speed	183 rad/sec
Rated Load Torque	19 n.m

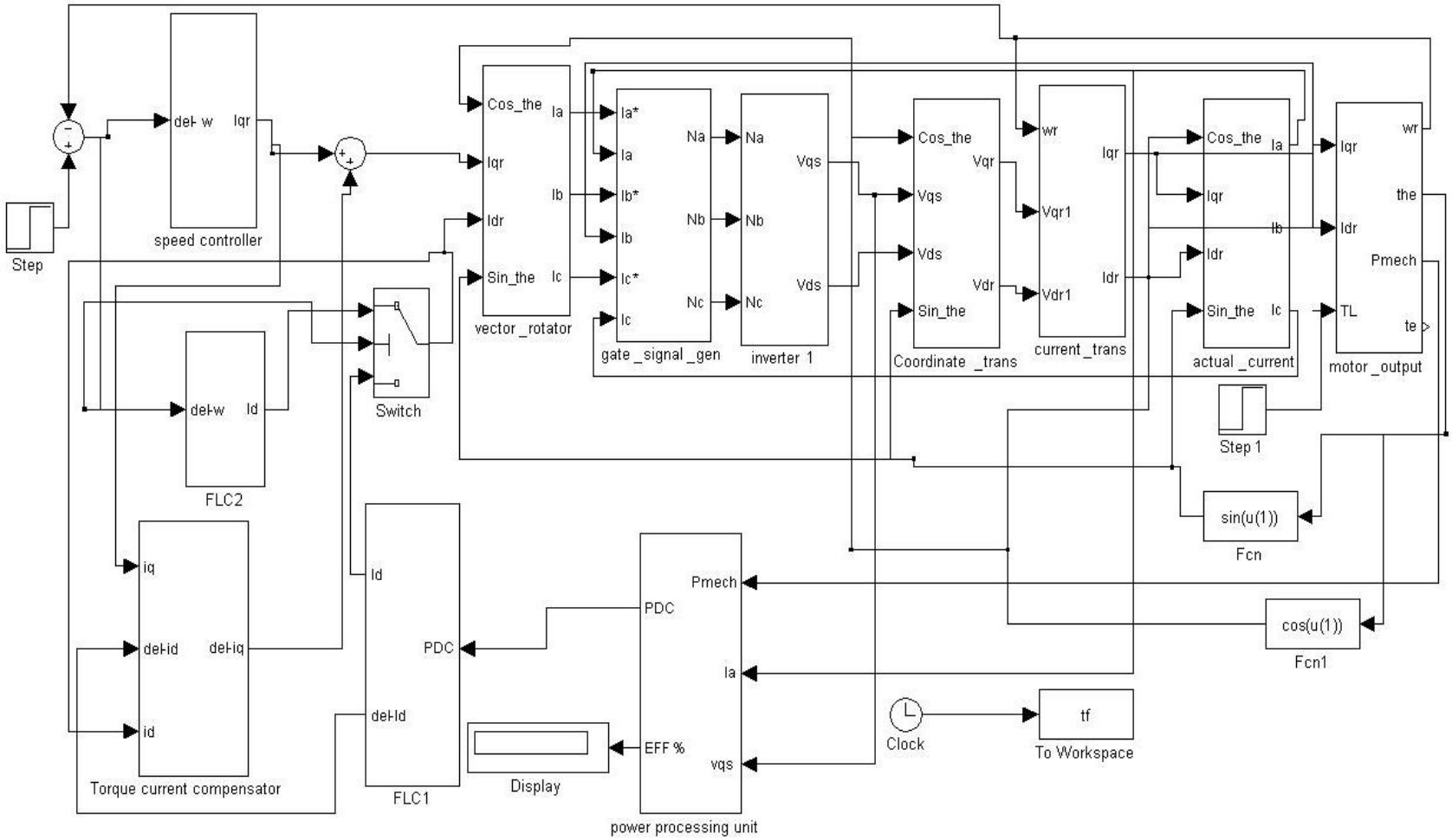

Fig 3.11 Simulink schematic model of complete efficiency and speed control of IPMSM drive

The starting speed response of the IPMSM drive incorporating the proposed FLC based efficiency and speed controller is shown in Fig 3.12. In this case motor was running at rated speed (183 rad/sec) with rated load condition (19 N.m). It is seen that the motor can follow the command speed quickly, smoothly without any overshoot/undershoot and steady-state error.

Fig 3.13 shows the comparison in efficiency between the proposed FLC based drive and the conventional id = 0 controller based IPMSM drive. It is clearly seen from the figure that the efficiency is increased more than 3% by the proposed drive as compared to the conventional control.

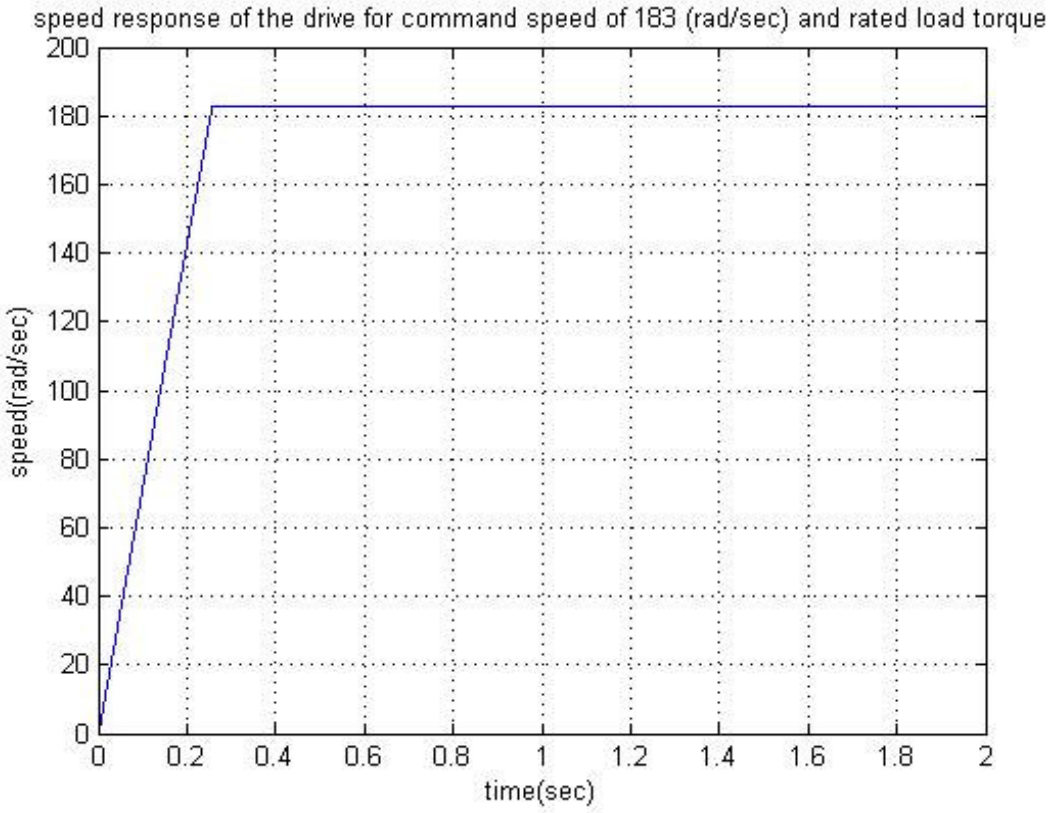

Fig 3.12 Starting speed response of the proposed drive
at rated speed (183 rad/s.) and rated load (19 N.m)

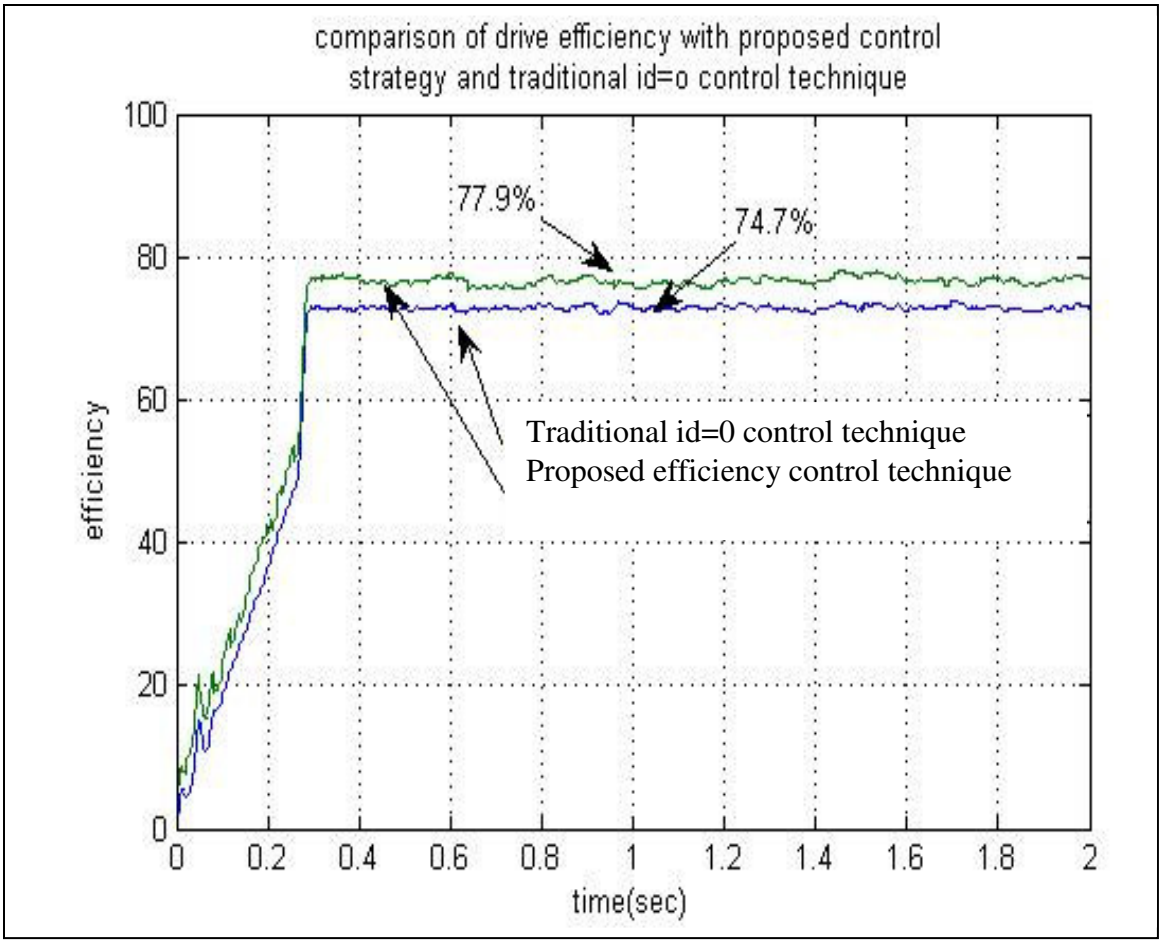

Fig 3.13 Comparison in drive's efficiency between the proposed control strategy and traditional id=0 control strategy at rated speed (183 rad/sec) and rated load (19 N.m)

Developed torque and d-q axis component of stator current are shown in Fig 3.14. As it is seen by compensating the q-axis component of stator current in continuous change of d-axis component of stator current in the search process the developed torque has minimum fluctuations. In this case motor was running at rated speed (183 rad/sec) with rated load condition (19 N.m).

Fig 3.15 shows the phase current response of the drive when the motor starts to run at (183 rad/sec) with rated load (19 N.m)

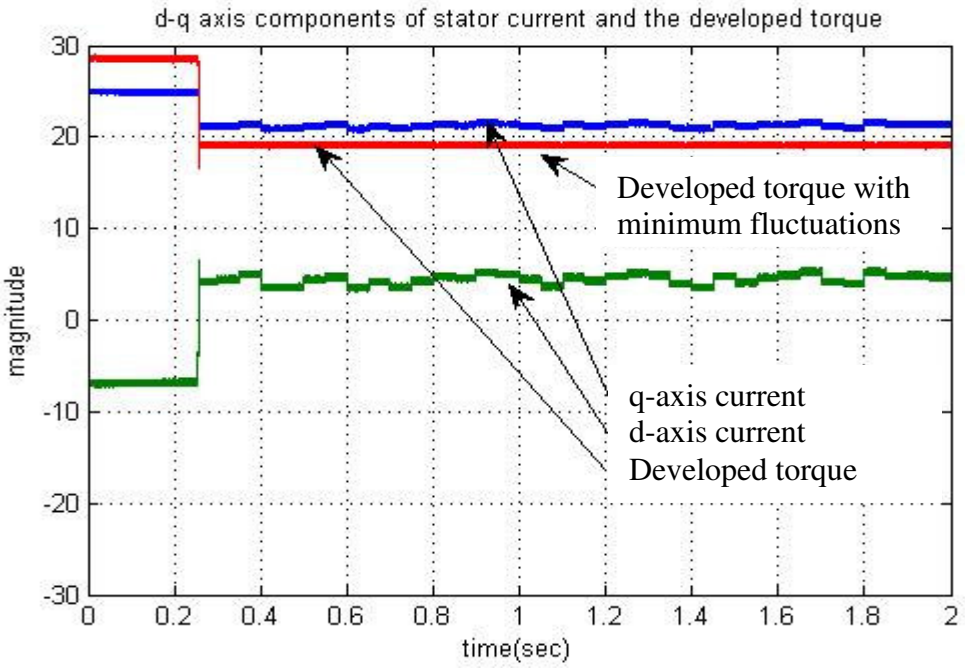

Fig 3.14 Corresponding d-q axis current and the developed torque responses of the proposed FLC based drive

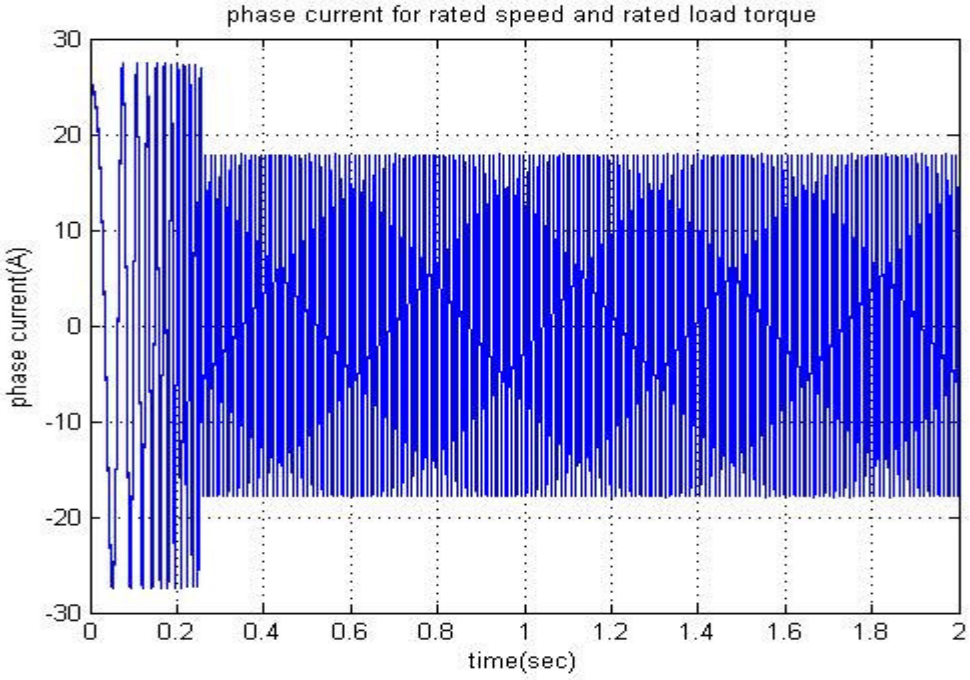

Fig 3.15 Corresponding stator phase current response

of the proposed FLC based drive

Output power response of the 5 hp IPMSM while the motor is running at rated speed of (183 rad/sec) with rated load command of (19 N.m) is shown in Fig 3.16.

A comparison in input power between the proposed FLC based drive and the conventional id = 0 controller based IPMSM drive while the output power remains constant is shown in Fig 3.17. It is clearly seen from the figure that the input power is decreased by the proposed drive as compared to the conventional control hence the efficiency increased. In this case motor was running at rated speed (183 rad/sec) with rated load condition (19 N.m). Corresponding power loss response of the proposed drive is compared to conventional id =0 control in Fig 3.18. The comparison shows that the proposed drive has less power loss as compared to conventional control in constant output power. Fig 3.19 shows a clear comparison of power loss in steady state between the proposed FLC based and conventional id =0 control.

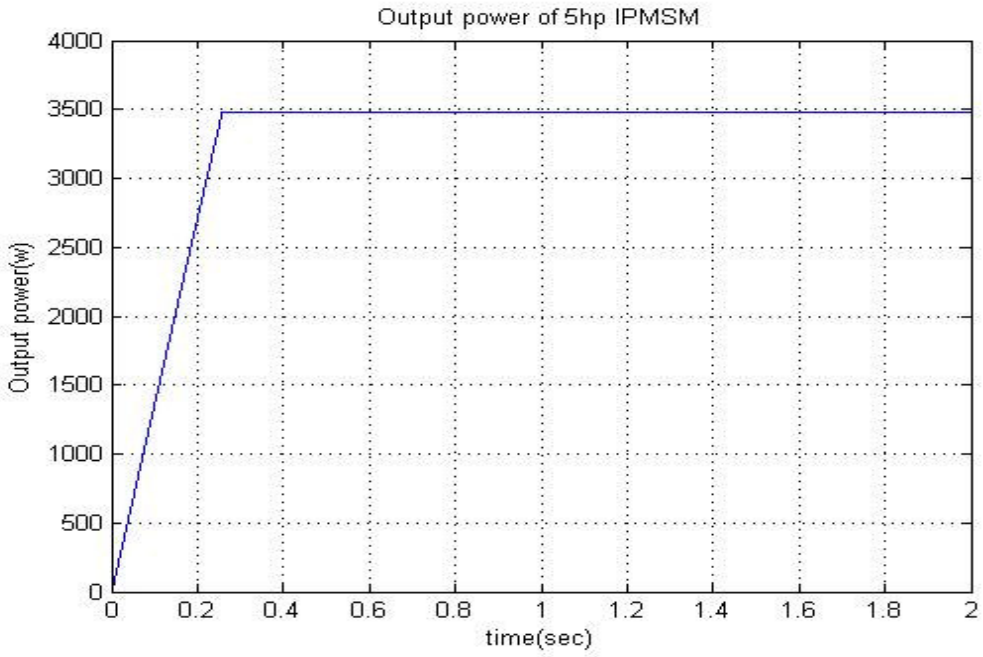

Fig 3.16 Output power response of 5hp IPMSM at

rated speed (183 rad/s.) and rated load (19 n.m.)

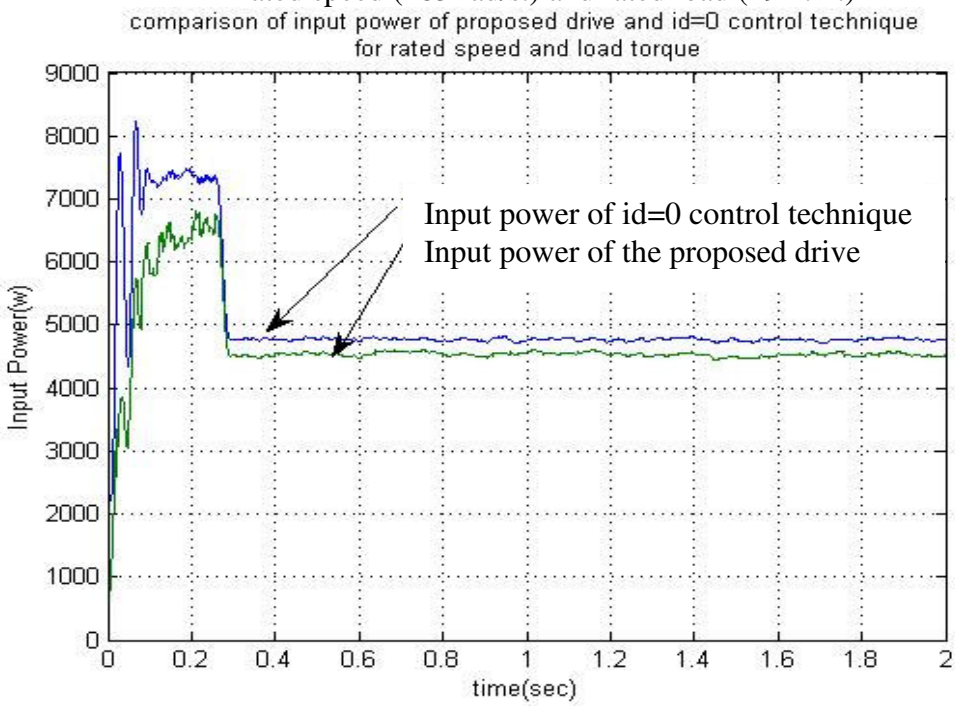

Fig 3.17 Comparison in drive's input power between the proposed control strategy and traditional id=0 control strategy at rated speed (183 rad/sec) and rated load (19 N.m)

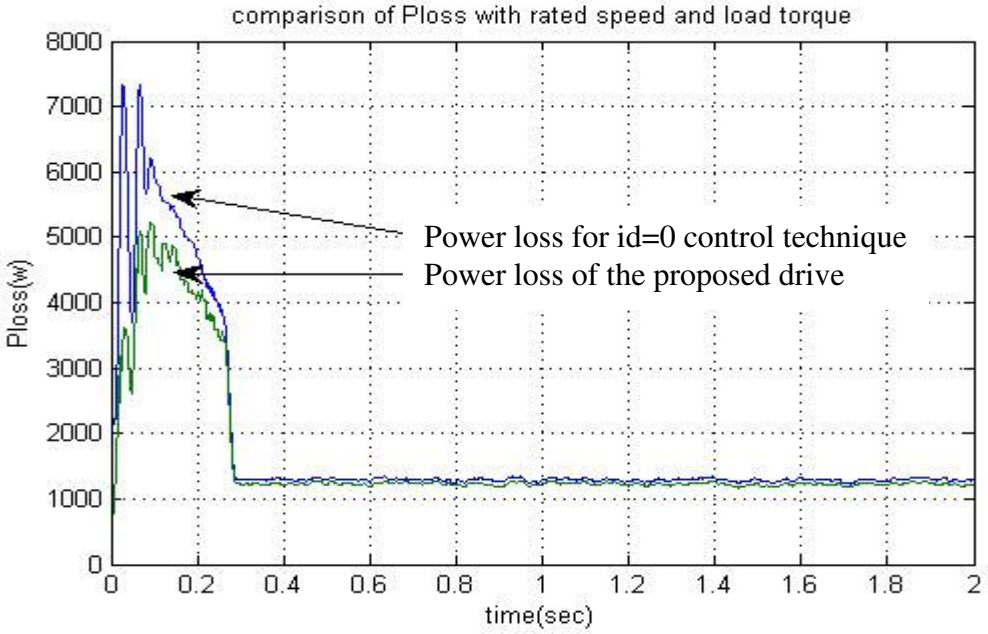

Fig 3.18 Comparison in drive's power loss between the proposed control strategy and traditional id=0 control strategy at rated speed (183 rad/sec) and rated load (19 N.m)

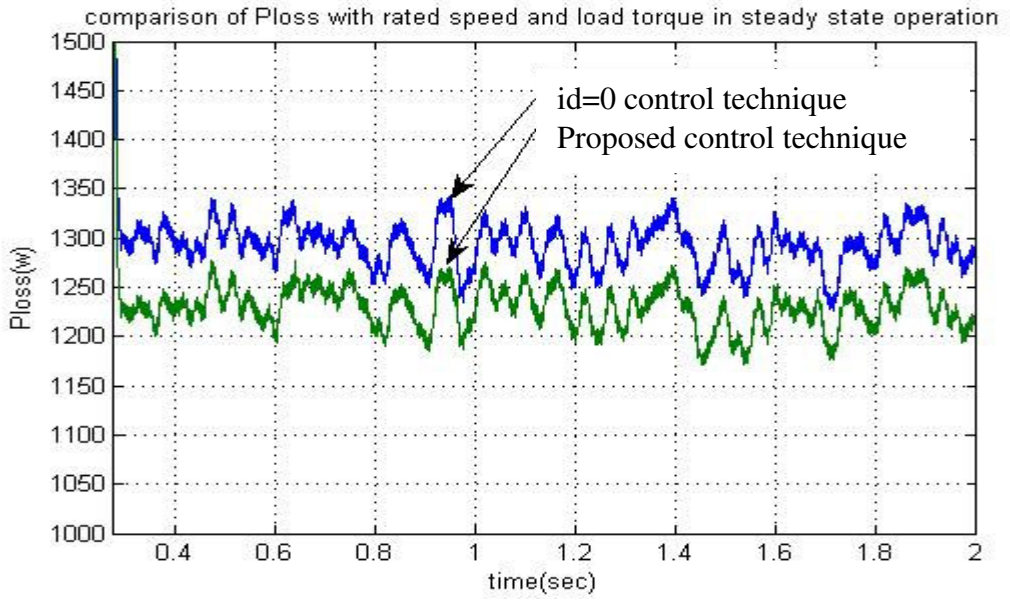

Fig 3.19 Zoom-in view for comparison in drive's power loss between the proposed control strategy and traditional id=0 control strategy at rated speed (183 rad/sec) and rated load (19 N.m)

The effectiveness of the proposed drive is also tested for a step decrease in load from rated value (19 N.m) to 50% of rated value (9.5 N.m). Fig 3.20 shows the speed response of the proposed drive for sudden step change of load from rated value to 50% of rated value at t = 0 . In order to verify the efficiency improvement a comparison in efficiency between the proposed FLC based drive and the conventional id = 0 controller based IPMSM drive has been made for step decrease of load in Fig 3.21. It is clearly seen from the figure that the efficiency is increased more than 3% by the proposed drive as compared to the conventional control. It is also seen that the variation of load torque does not affect the overall efficiency of the drive in steady state operation. Fig 3.22 shows the corresponding response of the d-q axis components of stator current and the developed torque in step decrease of load. It can be seen that the developed torque has minimum

fluctuations by compensating the q-axis component of stator current. In Fig 3.23 the corresponding response of the stator phase current is shown.

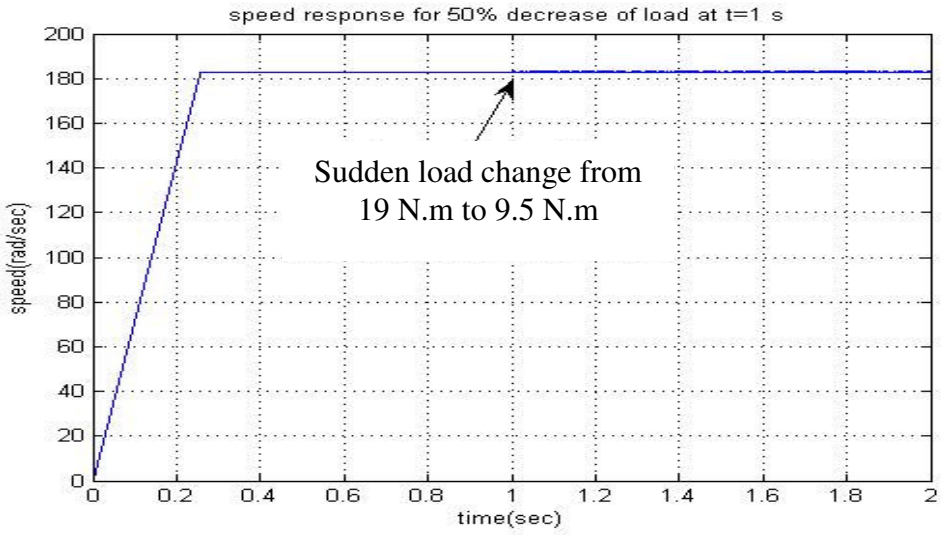

Fig 3.20 speed response of the proposed drive at rated speed (183 rad/sec) and rated load (19 N.m.) and a sudden 50% decrease of load at (t =1 s)

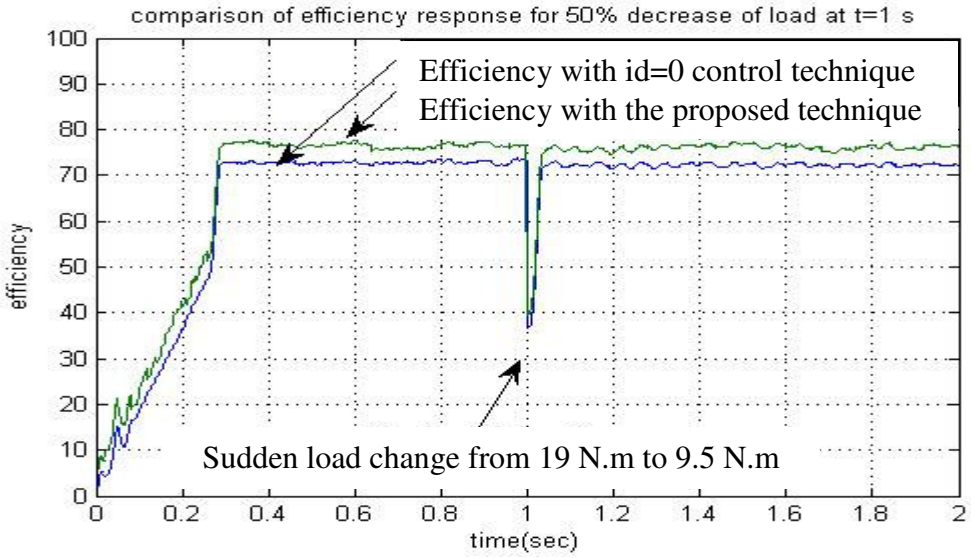

Fig 3.21 Comparison in drive's efficiency between the proposed control strategy and traditional id=0 control strategy at rated speed (183 rad/sec) and rated load (19 N.m) and a sudden 50% decrease of load at (t =1 s)

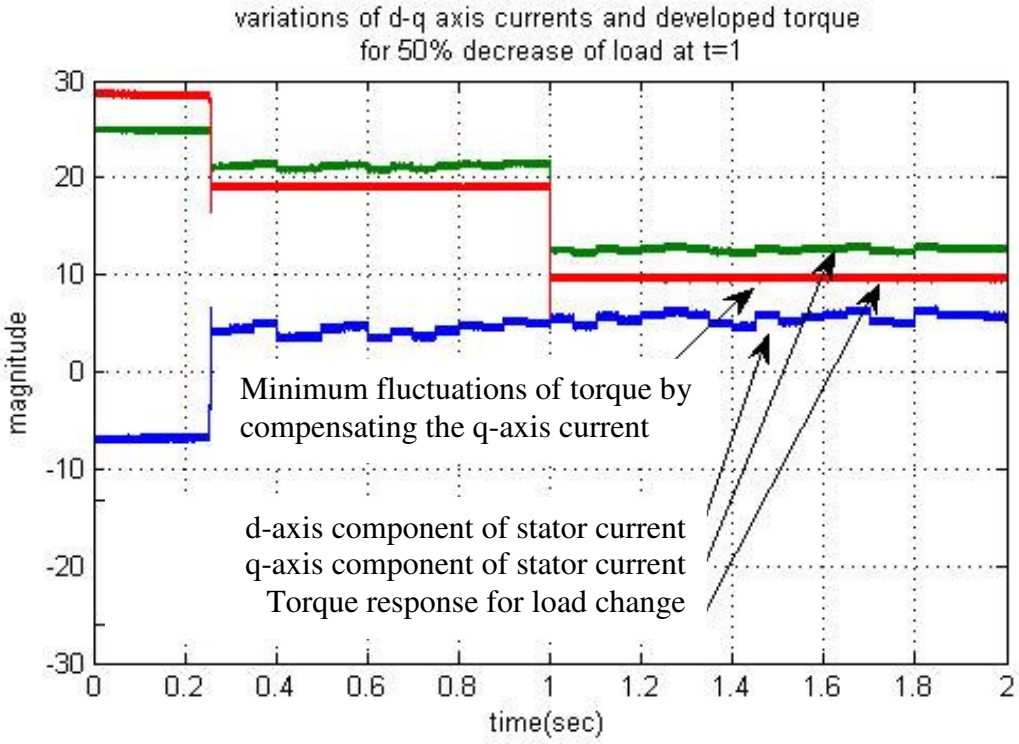

Fig 3.22 Corresponding d-q axis current and the developed torque responses of the proposed FLC based drive

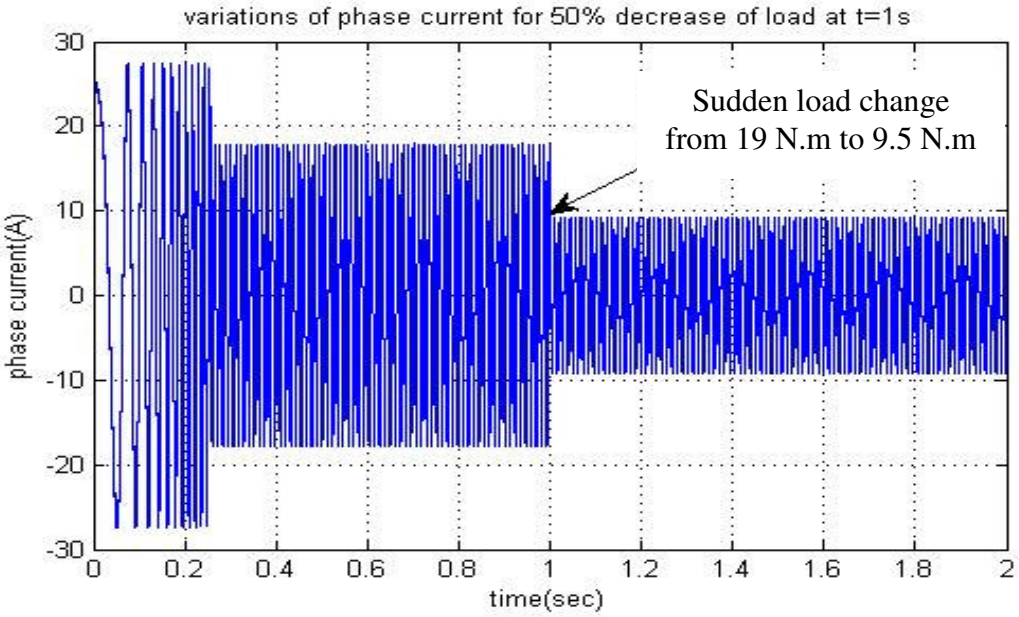

Fig 3.23 Corresponding stator phase current response of the proposed FLC based drive

Output power response of the 5 hp IPMSM while the motor is running at rated speed of (183 rad/sec) with rated load command of (19 N.m) and sudden step decrease of load to 50% of rated amount at t = 1 is shown in Fig 3.24. In this figure a comparison in input power between the proposed FLC based drive and the conventional id = 0 controller based IPMSM drive also has been made. It is clearly seen from the figure that the input power is decreased by the proposed drive as compared to the conventional control hence the efficiency increased. Corresponding power loss response of the proposed drive is compared to conventional id =0 control in Fig 3.25. The comparison shows that the proposed drive has less power loss as compared to conventional control. Fig 3.26 shows a clear comparison of power loss in steady state between the proposed FLC based and conventional id =0 control.

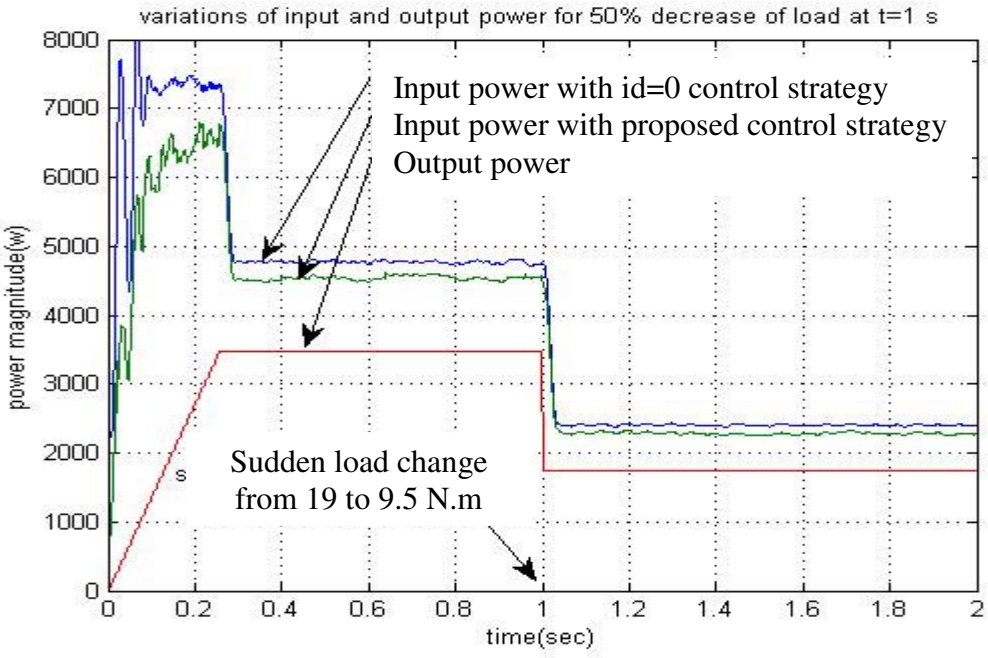

Fig 3.24 Output power response and comparison in drive's input power between the proposed control strategy and traditional id=0 control strategy at rated speed (183 rad/sec) and rated load (19 N.m) and sudden 50% load decrease at t = 1

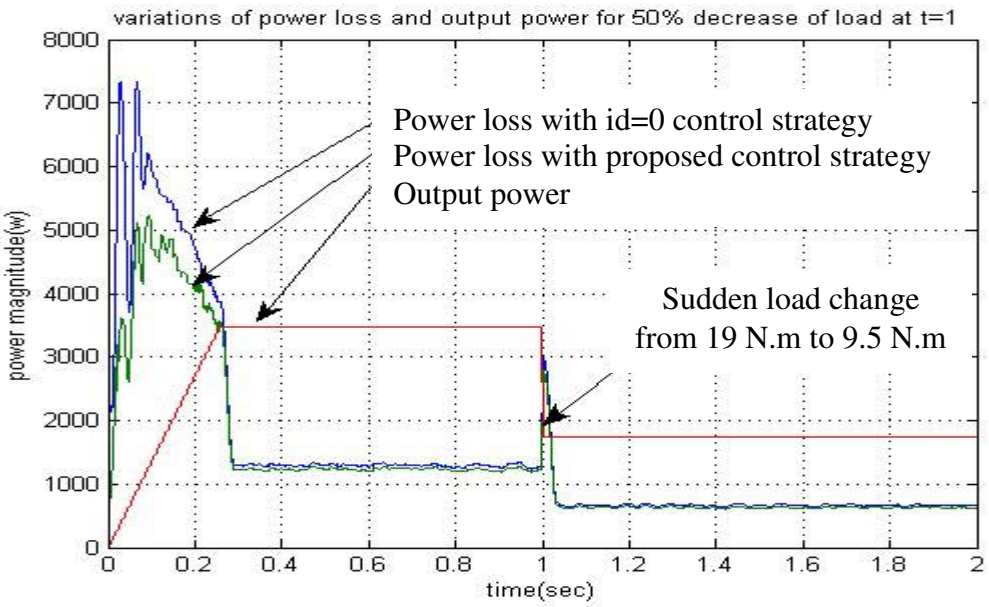

Fig 3.25 Output power response and comparison in drive's power loss between the proposed control strategy and traditional id=0 control strategy at rated speed (183 rad/sec) and rated load (19 N.m) and sudden 50% decrease of load at t = 1

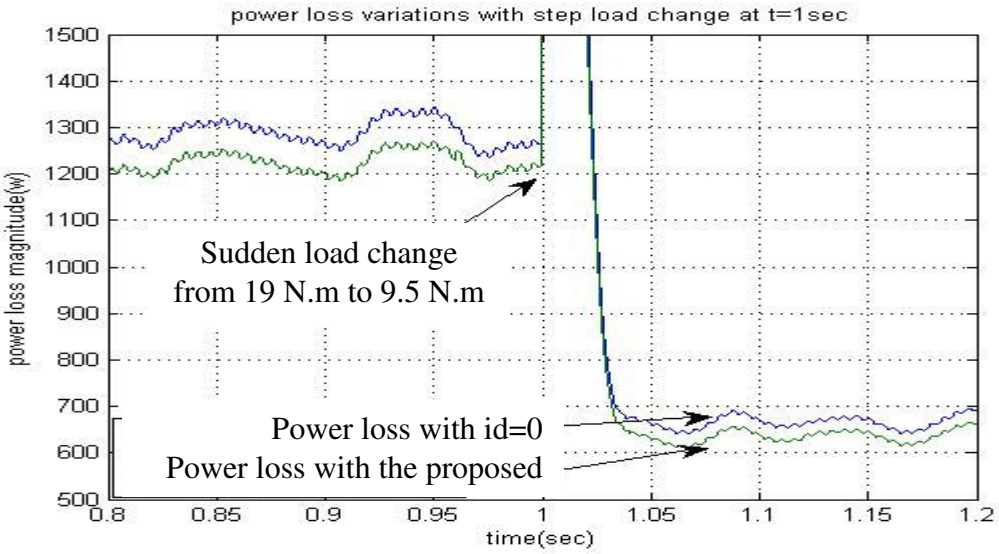

Fig 3.26 Clearer view of comparison in drive's power loss between the Proposed control strategy and traditional id=0 control strategy at Rated speed (183 rad/sec) and rated load (19 N.m) and sudden 50% decrease of load at t = 1

Fig 3.27 shows the speed response of the proposed FLC drive for a step 25% decrease of command speed 183 (rad/sec) to 136 (rad/sec) at rated load (19 N.m). The actual speed converges with the reference speed quickly, smoothly without any overshoot/undershoot and steady-state error. This step change of command speed affects the efficiency of the IPMSM drive. The comparison in efficiency between the proposed FLC based drive and the conventional id = 0 controller based IPMSM drive for step change of command current is shown in Fig 3.28. It is clearly seen from the figure that the efficiency is increased more than 3% by the proposed drive as compared to the conventional control. and the overall efficiency in both cases is decreased by reduction of the command speed.

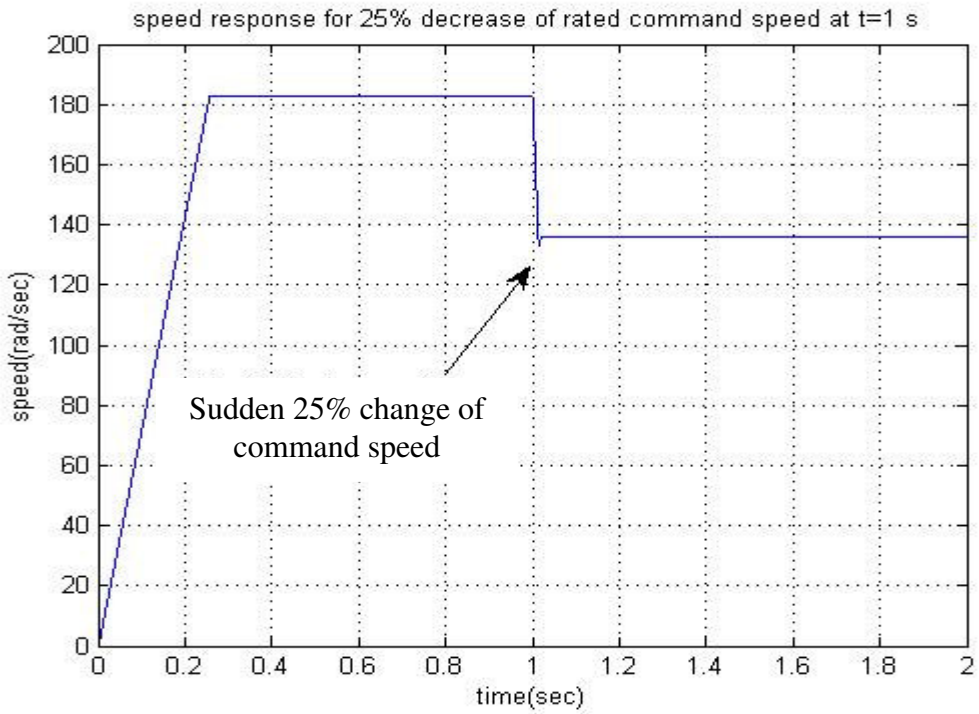

Figure 3.27 speed response of the proposed FLC drive at rated speed (183 rad/s.) and rated load (19 n.m.) and a sudden 25% decrease of command speed at (t =1 s)

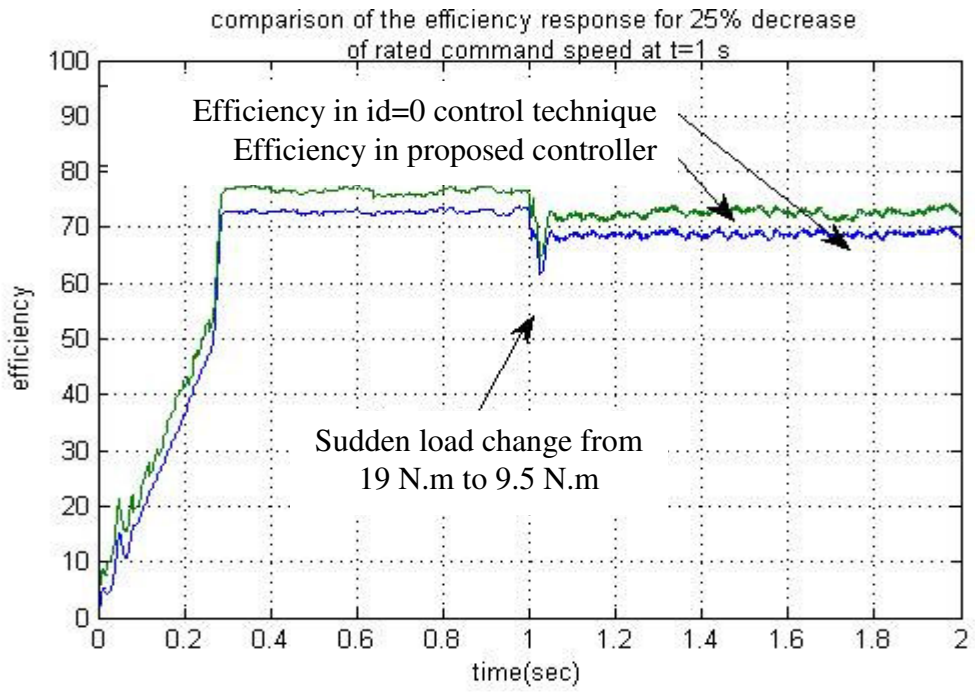

Fig 3.28 Comparison in drive's efficiency between the proposed control strategy and traditional id=0 control strategy at rated speed (183 rad/sec) and rated load (19 N.m) and a sudden 25% decrease of speed at (t =1 s)

The simulation results show the following:

- The proposed drive can follow the speed command smoothly without any overshoot/undershoot and with zero steady-state error even with sudden change of load torque.
- The overall power loss and input power of the drive decreased and efficiency in steady state is improved
- Torque and speed fluctuations caused by continuous step change of i_d in the search process minimized by compensation of q-axis current

- Decreasing the speed from rated amount leads to decreasing the overall efficiency.

3.5 Conclusions

In this chapter IPMSM power loss modeling and proposed loss minimization algorithm using search controller have been presented. Fundamentals of fuzzy logic control to design intelligent controllers have been introduced. A novel IPMSM drive scheme incorporating efficiency and speed control system has been proposed. Simulation model of the proposed drive has been developed using Matlab/Simulink. Finally, simulation results have been presented to investigate and compare the performance of the proposed drive with traditional (id=0) control method. Simulation results demonstrate that the proposed drive yields better performance in efficiency of the drive, robustness and minimization of torque ripples at different dynamic conditions.

Chapter 4

Real-time Implementation

4.1 Introduction

In this chapter the performance of the proposed fuzzy logic based efficiency and speed control system of IPMSM drives is tested in real-time after getting some promising results in simulation. The complete vector control scheme is successfully implemented in real-time using DSP controller board DS 1104 on a laboratory 5 hp motor. The detailed real-time implementation is described in this chapter.

4.2 Experimental Setup

The experimental setup for the real-time implementation of the proposed controller is shown in Fig 4.1 and 4.2. The IPMSM is labelled as 'M'. The rotor position of the test motor is measured by an optical incremental encoder which is labelled as 'E'. The encoder is directly connected to the rotor shaft. The motor is coupled with a DC machine (G) which works as a generator to act as loading machine to the motor. Some resistors (L) are connected to the output voltage terminals of the DC machine as load. The actual motor currents are measured by Hall-effect current transducers. The interface circuit (I) is located between the Hall-effect sensor and the A/D channel of DSP board.

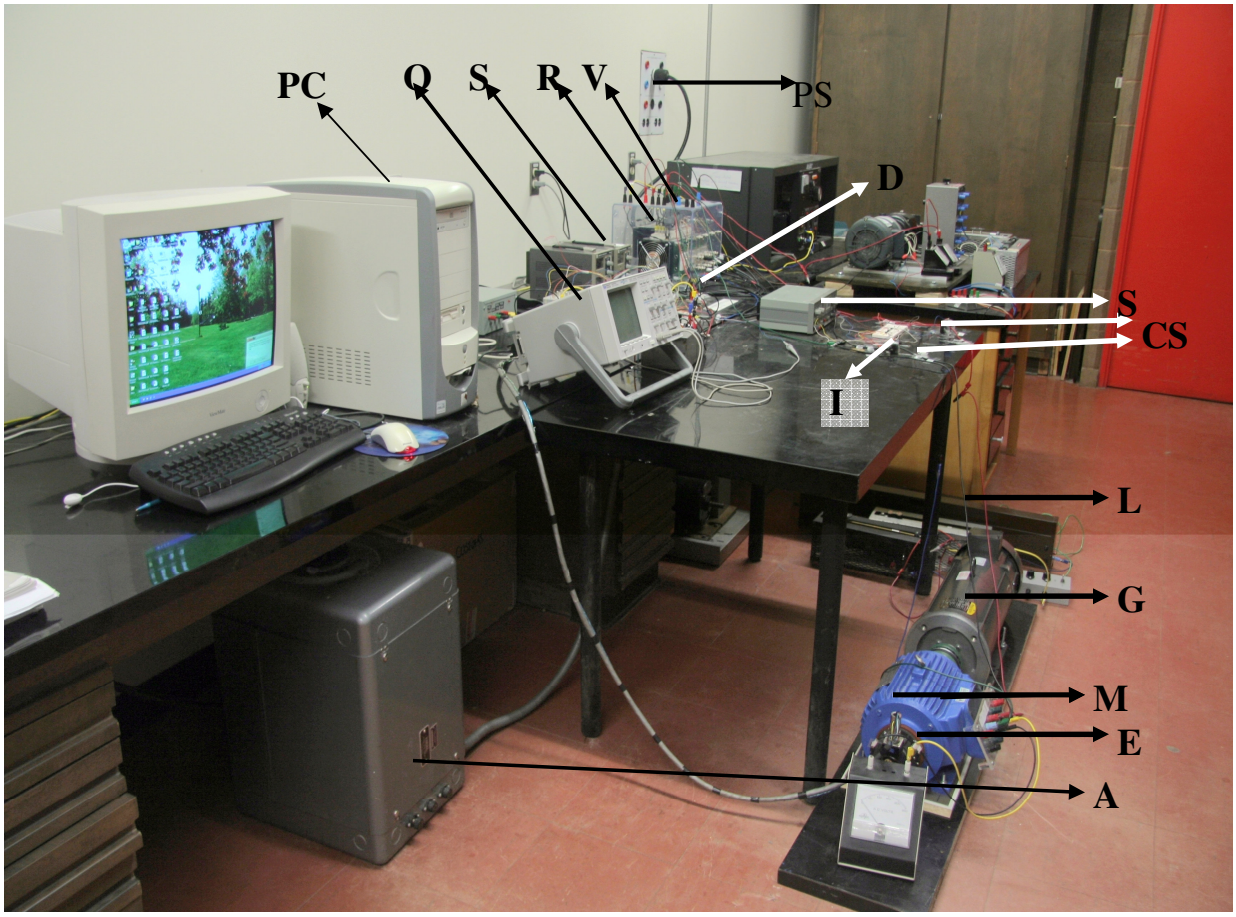

Fig.4.1: Experimental setup of the proposed controller of IPMSM drive

These transducers are labelled as 'CS'. These current sensors (CS) have a linear response over wide range of frequencies (up to 250 kHz). Another gate drive circuit is used to increase the power level of the firing pulses so that these are sufficient to drive the inverter insulated gate bipolar transistor (IGBT) switches. The gate drive circuit also provides isolation between low power control and the high power supply circuits. The gate drive circuit is labelled as 'D'. The power circuits consist of a 3-phase variable ac autotransformer (A), power supply (PS), rectifier (R) and IGBT inverter (V)

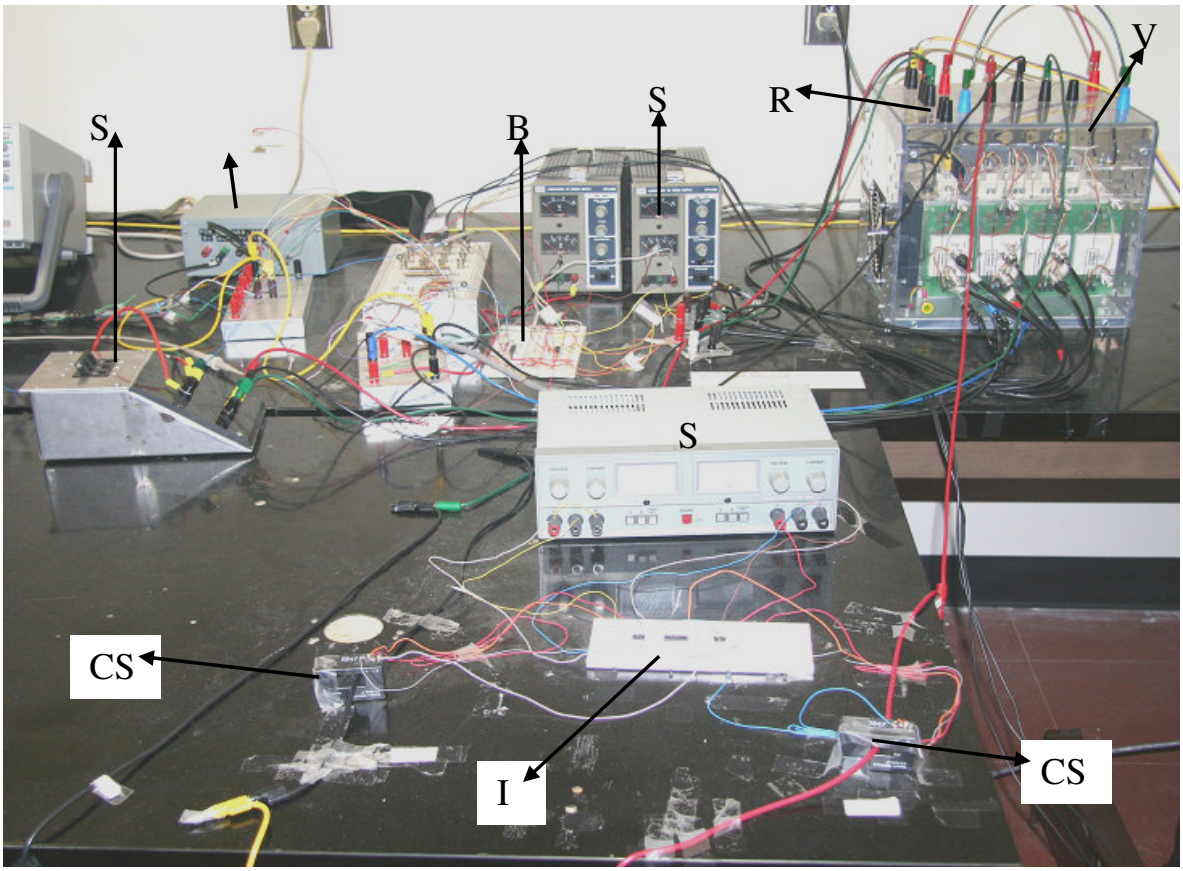

Fig.4.2: Experimental setup of the proposed controller (close-up view).

The DC bus voltage of the voltage source inverter (VSI) is obtained by rectifying ac voltage. The ac voltage is supplied by the power supply through autotransformer. The rectifier enclosed within 3-phase (6 pulses) IGBT inverter is labelled as 'V'. This inverter has active security feature against short circuit, under voltage of power supply as well as built in thermal protection, which prohibits destructive heat sink temperatures. The variable ac power of the rectifier is supplied by autotransformer (A) through a single pole single throw (SPST) switch (SW). The personal computer, in which the DSP board DS1104 is installed, is labelled as 'PC'. A digital storage oscilloscope is used to capture the desired analog signal coming out through D/A port of the DSP board. The

oscilloscope is labelled as 'O'. The complete drive has been implemented through both hardware and software which are discussed below.

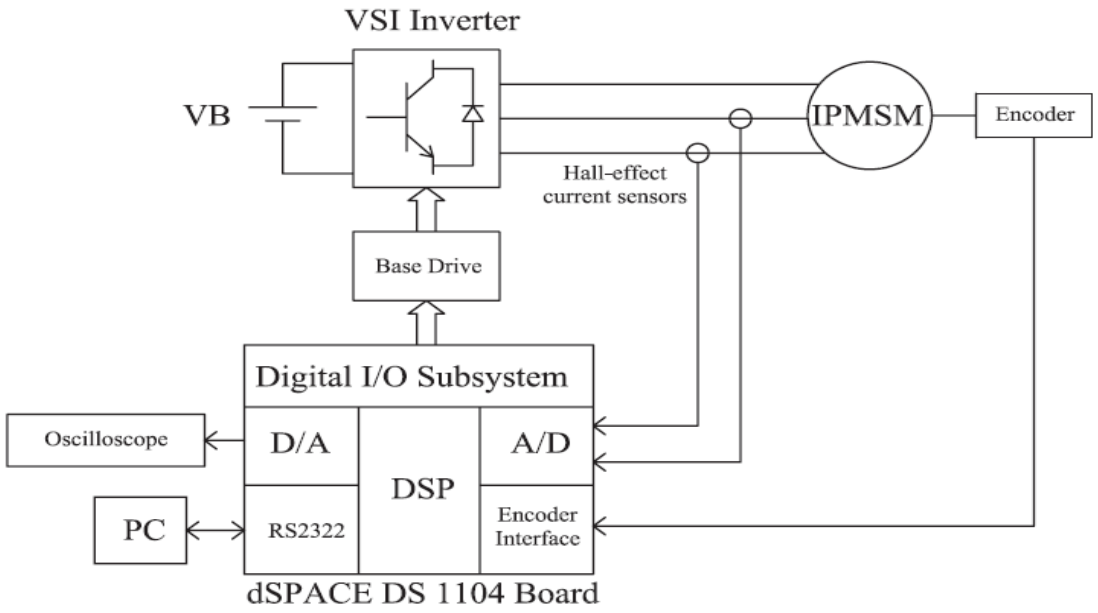

Fig.4.3: Block diagram of hardware schematic of VSI fed IPMSM drive.

4.3 DSP Based Hardware Implementation of the Drive

The block diagram of hardware schematic of VSI fed IPMSM drive is shown in Fig.4.3. The DSP board DS1104 board is installed in an Intel PC with uninterrupted communication through dual port memory to implement the control scheme in real-time. The DS1104 board is mainly based on a Texas Instrument MPC8240 64-bit floating point digital signal processor. The DS1104 board uses a PowerPC type PPC603e processor which operates at the clock of 250 MHz with 32 KB cache. This board has a 32 MB of SDRAM global memory and 8 MB of flash memory. The DSP is supplemented by a set of on-board peripherals used in digital control systems including analog to digital (A/D), digital to analog (D/A) converters and digital incremental encoder interfaces. This board

is also equipped with a TI TMS320F240 16-bit micro controller DSP that acts as a slave processor and provides the necessary digital I/O ports configuration and powerful timer functions such as input capture, output capture and PWM generation. In this work, the slave processor is used for only digital I/O subsystem configuration.. Rotor position is sensed by an optical incremental encoder mounted at the rotor shaft and is fed back to the DSP board through the encoder interface. These pulses are fed to the one of two digital incremental encoder interface channels of the board. A 24-bit position counter is used to count the encoder pulses and is read by a calling function in the software. The counter is reset in each revolution by the index pulse generated from the encoder. The motor speed is computed from the measured rotor position angles using discrete difference equation. The actual motor currents are measured by the Hall-effect sensors, which have current range of 0 ~ ±200A and a frequency range of 0~250 KHz. The current signals are fed back to DSP board through A/D channels. The output current signal of these sensors is converted to a voltage across the resistor connected between the output terminal of the sensor and ground. One can scale the output voltage by selecting the value of the resistors. These resistors can be within the range 0~100Ω. As the output voltages due to these current sensors are low, interface circuit is used to amplify the output of the sensor and it also reduces the noises. The interface circuit consists of non-inverting amplifier with operational amplifier LM741CN as shown in Appendix C. As the motor neutral is not grounded, only two phases current are measured and third phase current is calculated using Kirchoff's Current Law in software. The command voltages are generated from the proposed controller and compared with the triangular carrier wave. This generates the logic signals which act as firing pulses for the inverter switches. Thus, these six logic

signals are the output of the DSP Board and fed to the base drive circuit of the IGBT inverter power module. The outputs of the digital I/O subsystem of the DS 1104 are six pulses with a magnitude of 5 V. This voltage level is not sufficient for the gate drive of IGBTs. Therefore, the voltage level is shifted from +5 V to +15V through the base drive circuit with the chip SN7407N as shown in Appendix C. At the same time it also provides isolation between low power and high power circuits.

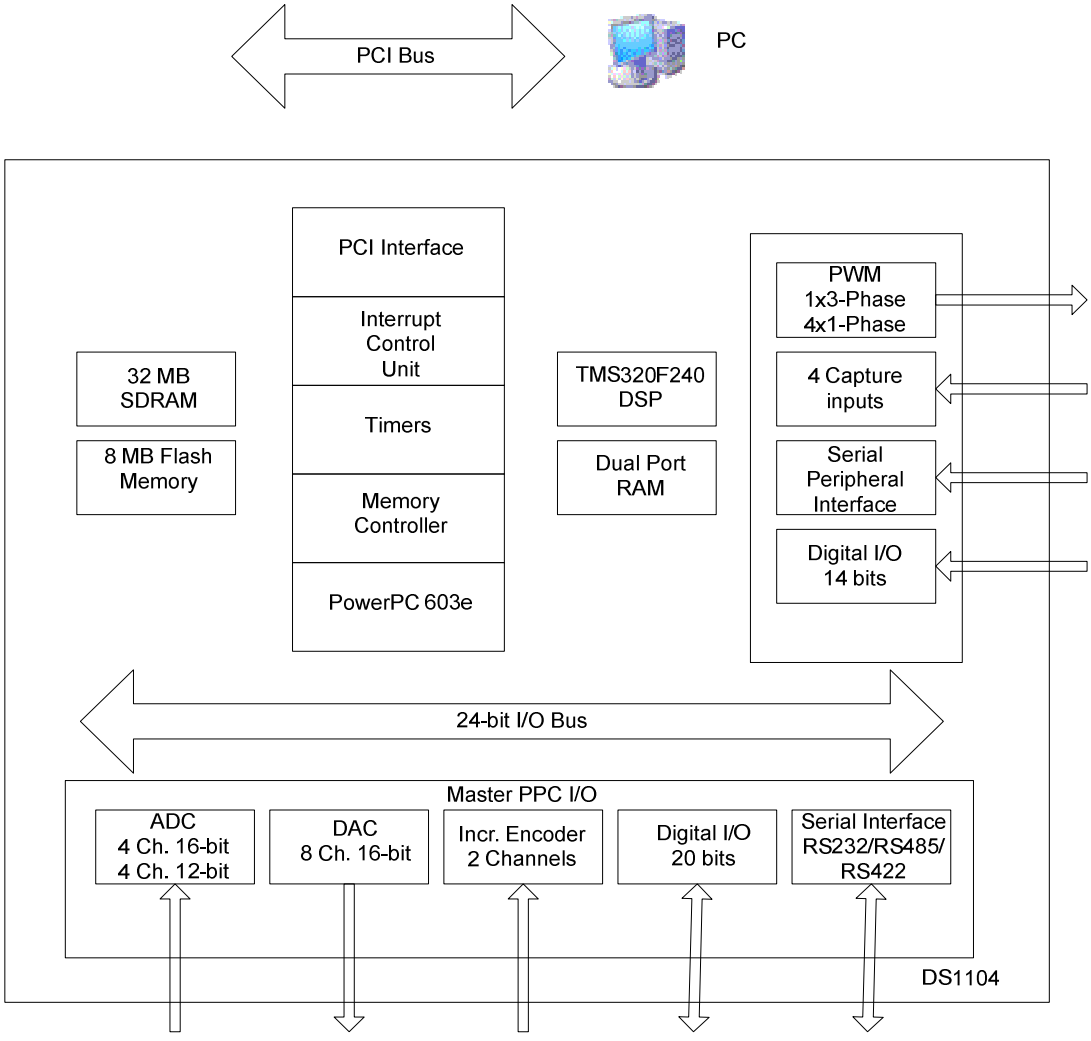

Fig.4.4: Block diagram of DS1104 board.

4.4 Software Implementation of the Drive

In order to implement the control algorithm, a real-time Simulink model is developed according to the complete drive system which is shown in Appendix D.1. Then the model is downloaded to the DSP board using the Control Desk software [46]. The dSPACE DS1104 board is a self-contained system, not an embedded system. This means the board installed in the lab computer through a PCI slot is its own entity and the host PC does none of the processing for a system implemented on the board. As a result, the board requires that software to be created and downloaded to the board for the system to function. The ControlDesk software is used to download software to the DSP board, start and stop the function of the DS1104 as well as create a layout for interfacing with global variables in dSPACE programs. The sampling frequency used in this work is found to be 10 kHz. If the sampling frequency that is higher than 10 kHz is chosen, the 'overrun error' occurs, which indicates too much computational burden for the processor.

The flow chart of the software for real-time implementation is shown in Fig.4.5. After initializing all the required variables, the timer interrupt routine is set up to read the values of the currents and rotor position angle every 100 μS . The motor currents obtained through analog to digital converter (ADC) channels 1 and 2 are multiplied by the gain 18.814 and 16.6667, respectively in order to obtain the actual current values in software. These constants depend on the Hall-effect sensors specifications, the resistors used at the output node of these sensors and the resistors used in the interface circuit. After these digitalized currents in *abc* coordinates are converted into rotating reference frame of *d-q* axes coordinates.

The rotor position angle is measured by encoder, Once the rotor position angle is calculated, the rotor speed is computed from the

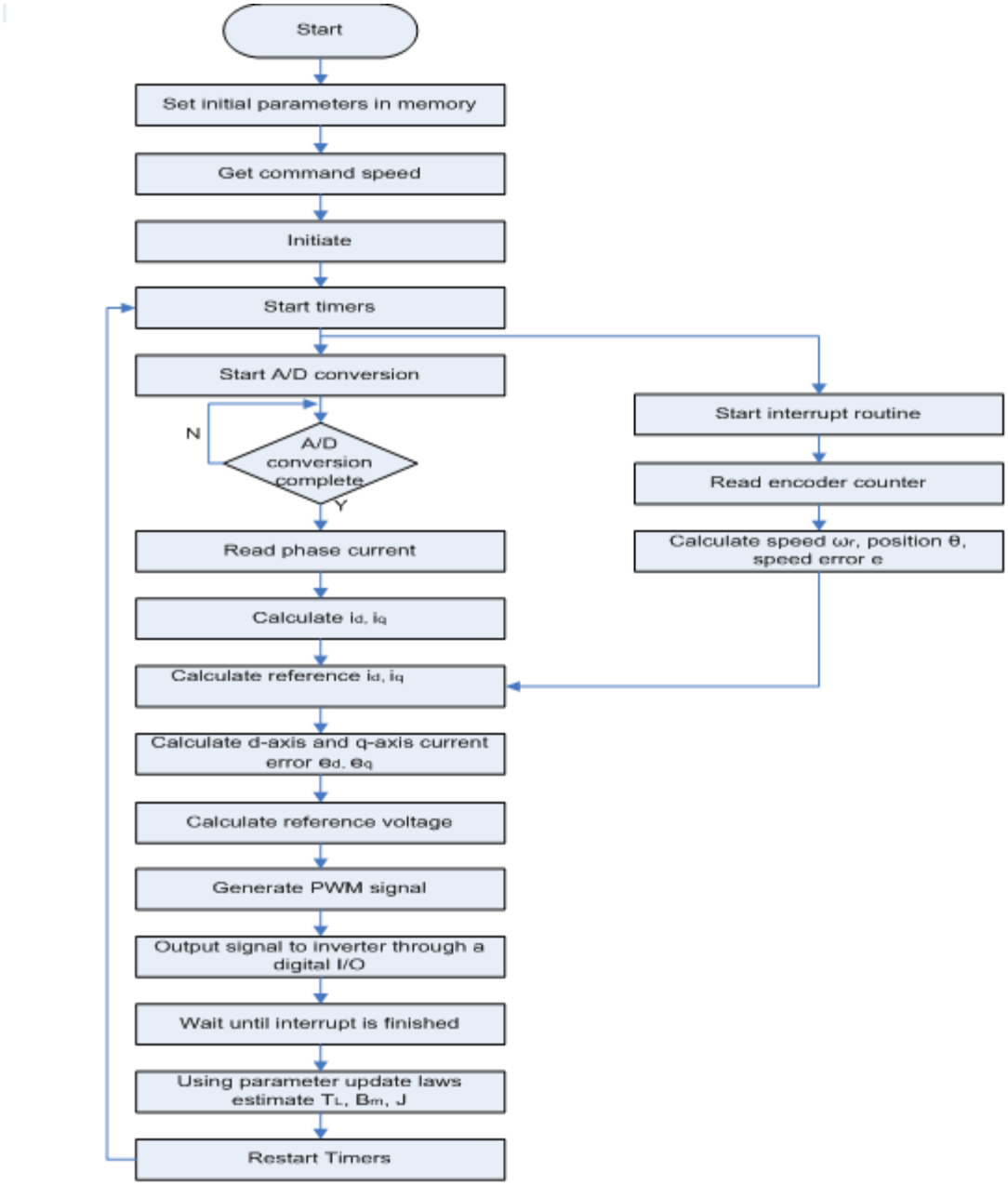

Fig.4.5: Flow chart of the software for real-time implementation of the drive

measured rotor position angles using numerical backward differentiation. Based on the calculated speed, the speed error between actual and reference speed is calculated. Using the speed error and virtual control dynamics error the reference d, q axis voltages are calculated. All the calculated and measured values as explained above such as d, q-axes currents, rotor speed along with initial parameters stored in memory are used to compute the tracking errors. Finally, the reference voltages are compared with the triangular carrier signal (1.2 kHz) to generate the six PWM pulses for the inverter switches. All off-to-on transitions of the PWM pulses are delayed by the dead time of 0.5 milliseconds in order to prevent the shorting of the dc bus voltage to ground. These pulses are sent to the inverter gate drive through a digital I/O subsystem of the board.

4.5 Experimental Result and Discussion

Several experimental tests have been performed to verify the effectiveness of the proposed FLC based IPMSM drive. Its performance is also compared with a conventional id =0 controller based drive. In the following experiments in real-time simulink model the input power of the drive is calculated by the following equation:

$$p_{in} = 3/2(v_q i_q + v_d i_d) \tag{4.1}$$

The real-time speed response of the IPMSM drive incorporating the proposed FLC based efficiency and speed controller is shown in Fig 4.6. In this case motor was running at rated speed (120 rad/sec) with no load and the step 33% increase of command speed applied. It is seen that the motor can follow the command speed quickly, smoothly without any overshoot/undershoot and steady-state error.

Fig 4.7 (a), (b) show the corresponding efficiency response of the proposed FLC based drive. The figure shows that the efficiency of the drive increases by increasing the speed command below the rated speed, in our case the efficiency improves from 66% to 74% by step 33% increase of the command speed.

In Fig 4.8 (a), (b) a comparison in efficiency between the proposed FLC based drive and the conventional id = 0 controller based IPMSM drive for step increase of command speed from 135 (rad/sec) to 175 (rad/sec) is shown. As it is seen this experimental study verifies 2.5-3 % improvement in overall efficiency of the drive in steady state condition with command speed of 175 rad/sec which is just below the rated speed of the motor 183(rad/sec).

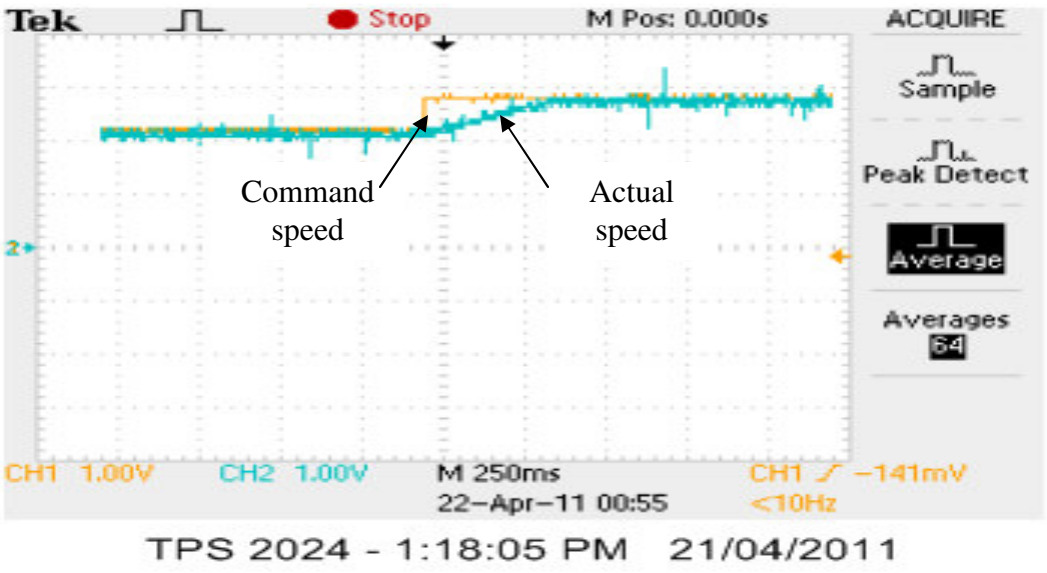

Fig 4.6 Experimental speed response of the proposed IPMSM drive for a step change in speed from 120 (rad/sec) to 160 (rad/sec).

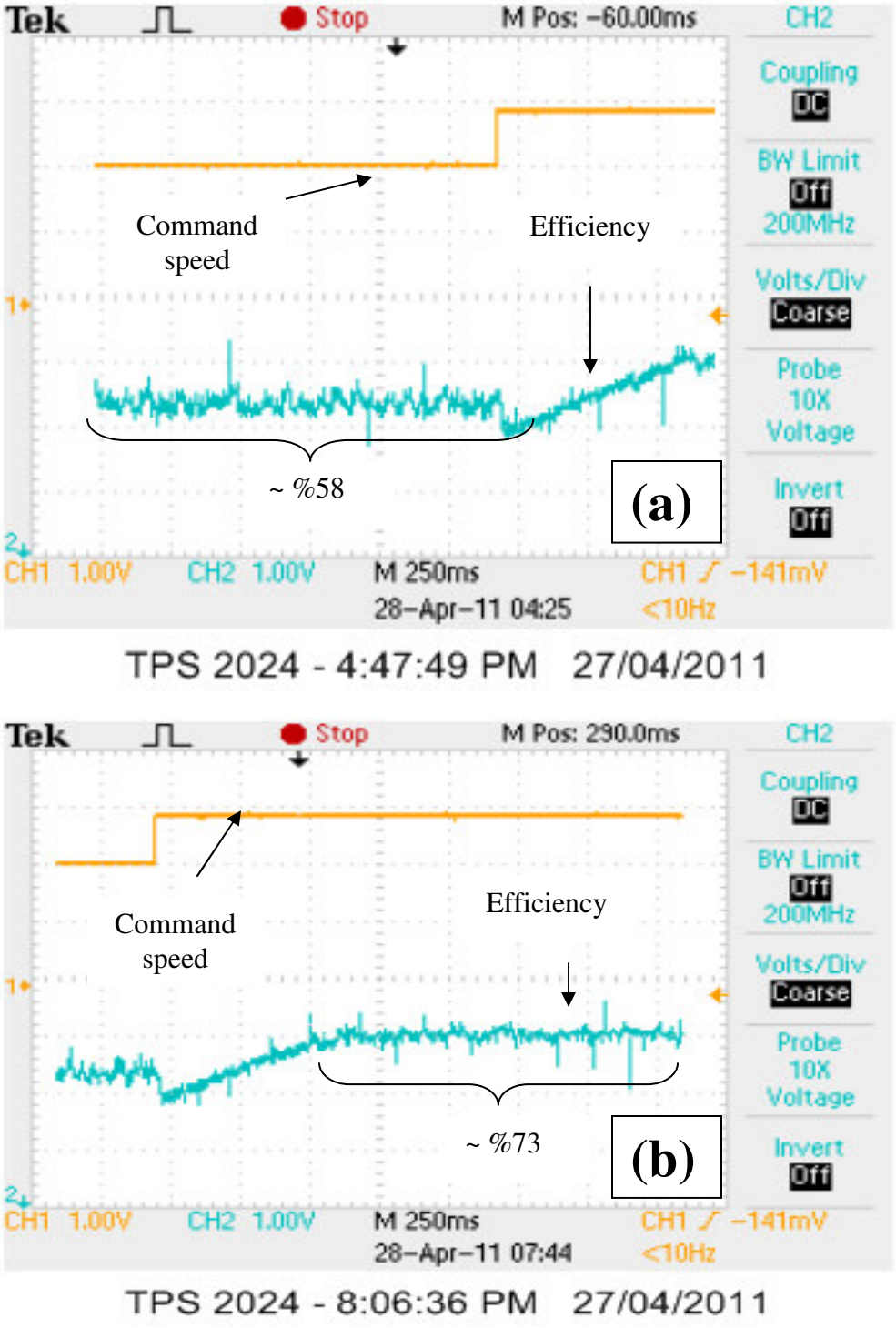

Fig 4.7(a), (b) show the variation of the proposed drive's efficiency by step change of command speed from 120 (rad/sec) to 160 (rad/sec)

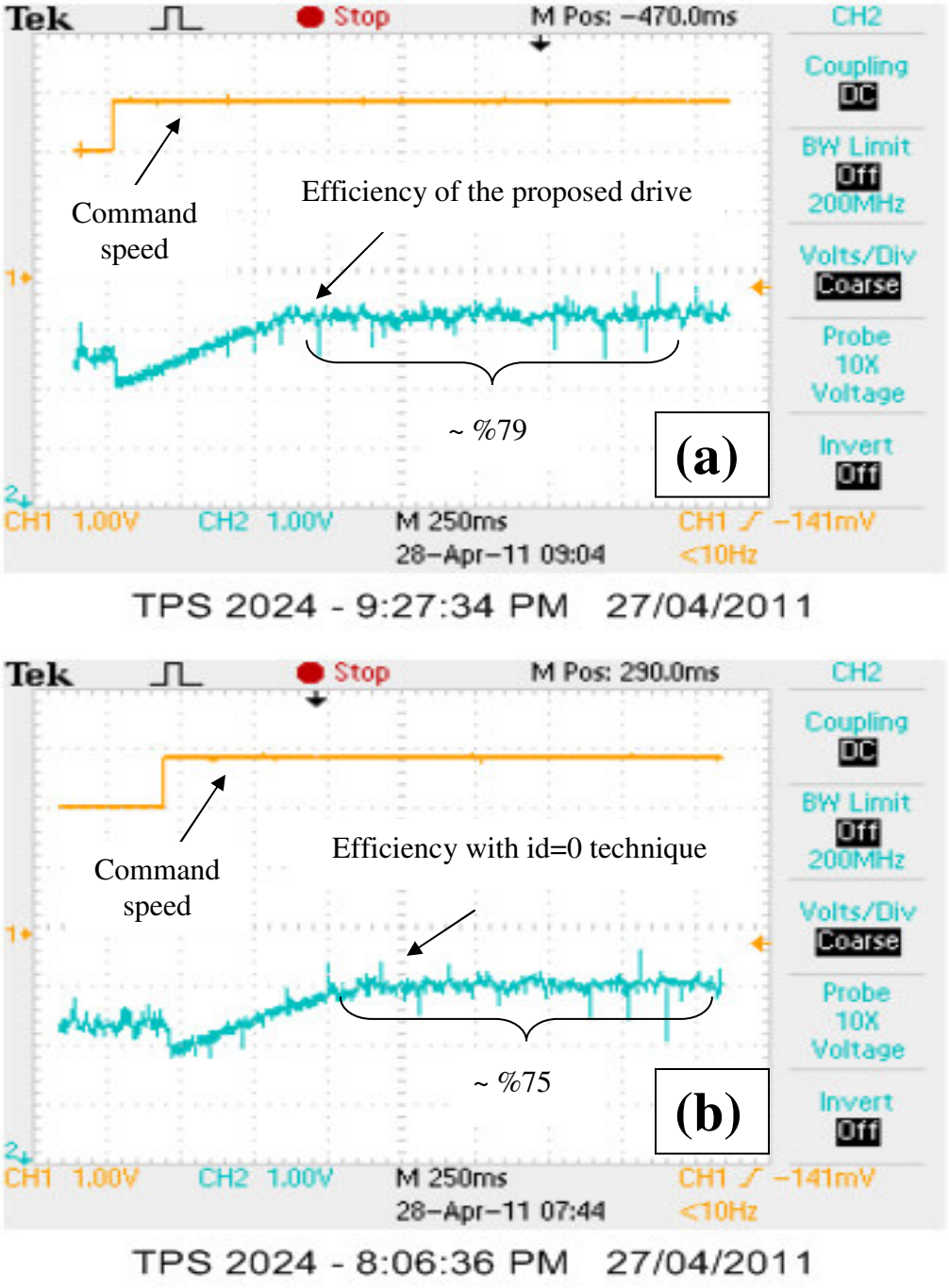

Fig 4.8(a), (b) Experimental efficiency response of the IPMSM drive for a step change in speed from 135 (rad/sec) to 175 (rad/sec); (a) proposed FLC drive, (b) traditional id = 0 control

Fig 4.9 shows the variations of the stator phase current with no load and command speed change from 120(rad/sec) to 160 (rad/sec) This figure implies that the phase current smoothly adjusts to a higher frequency with the step change to higher speed without going through any distortion.

The d-q axis components of stator current and the stator phase current are shown in Fig 4.10 (a), (b). In this case motor was running at steady state condition at (160 rad/sec) with no load

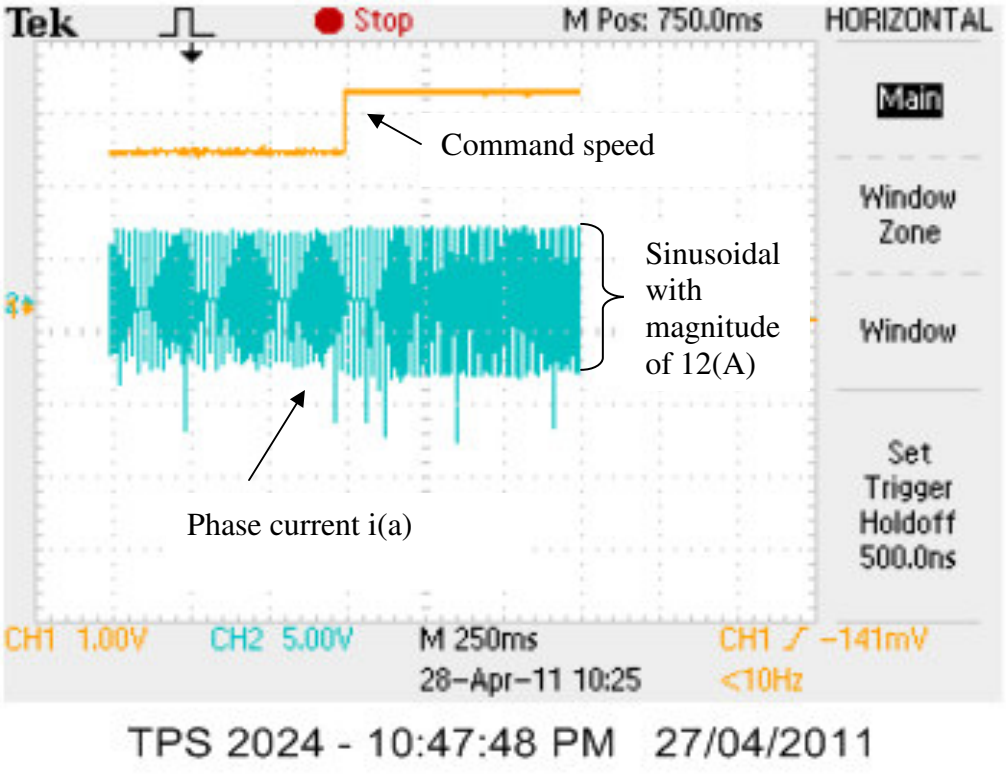

Fig 4.9 shows the variations of the phase current
with no load and command speed change
from 120(rad/sec) to 160 (rad/sec)

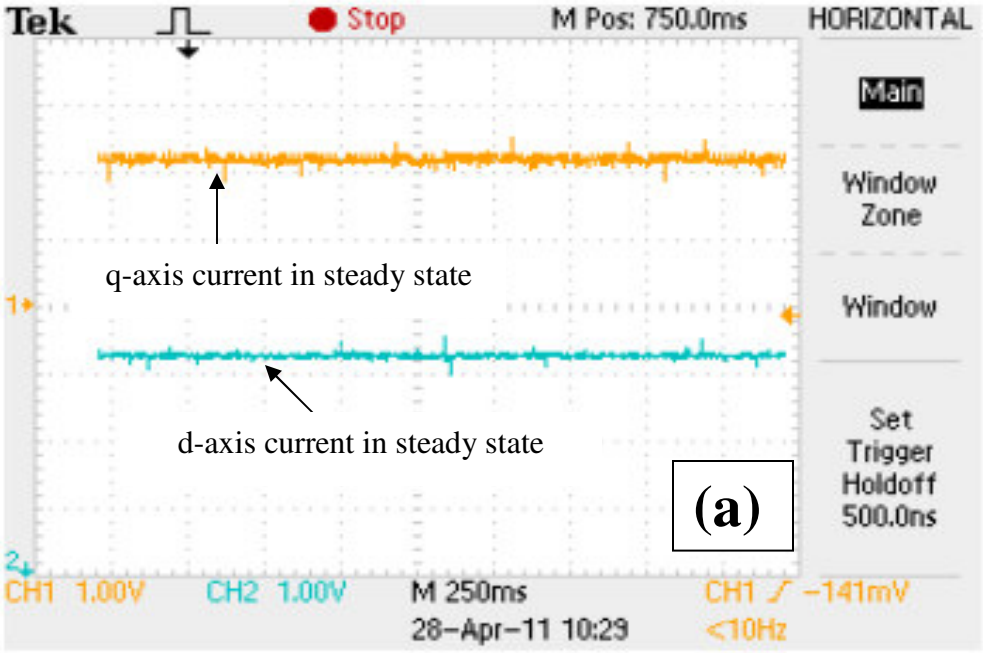

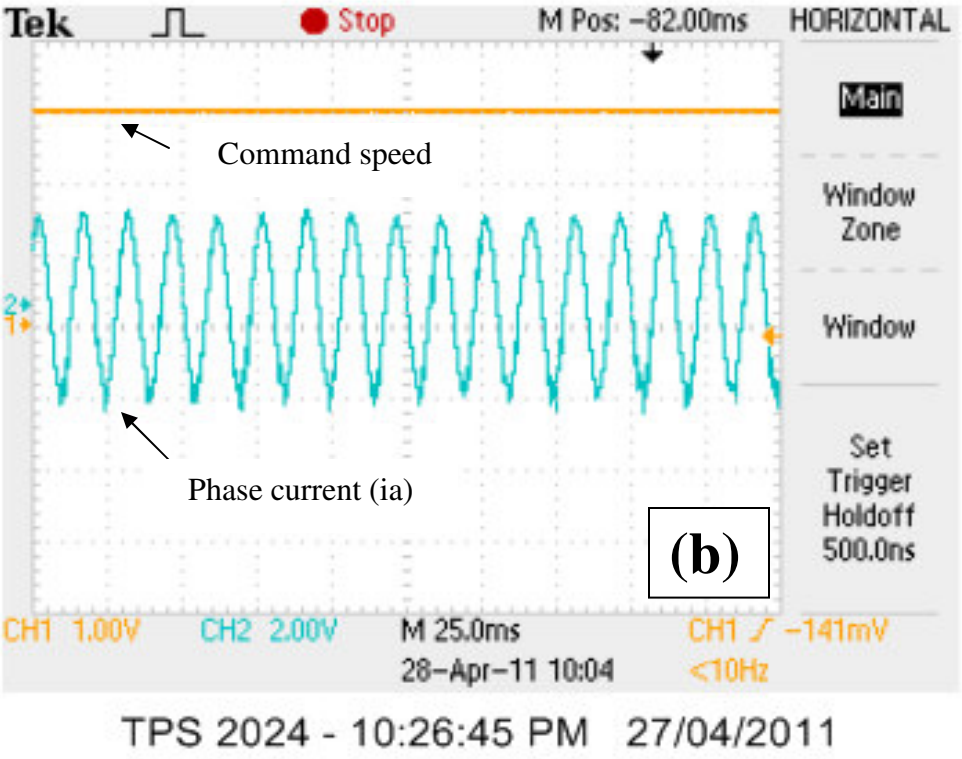

Fig 4.10(a), (b) The d-q axis and phase current in steady state condition with no load and command speed of 160 (rad/sec)

Chapter 5

Conclusions

5.1 Concluding Remarks

In this work, advantages of using fuzzy logic in efficiency optimization and precise speed control of IPMSM drive have been described. The proposed method achieves very satisfactory results in the overall losses minimization of a motor drive system as it considers both cases of operation: transient and steady state. This control system is independent of drive parameters and can be applied to any size or type of speed drive.

In addition to the control of torque component of stator current, the control of flux component of stator current is also important to achieve high efficiency. From the review of previous works as in chapter 1, the IPMSM is a good choice for high performance variable speed drives in industry in view of performance and economy. However, the performance of the drive depends on the type of controllers used. Although using simple controller with the assumption of $i_d=0$, the control of IPMSM becomes easier but the drive wont be efficiently optimized

In Chapter 1, the review of the previous works has been discussed from this review, it is observed that although efficiency improvement is very important in IPMSM drives, only few works have been reported. These previous works includes optimum rotor structure design (IPMSM already benefited from this), power factor control technique which although maximizes the real to apparent power ratio (kW/kVA) of IPMSM but it

wont minimize power losses and finally model based strategy whose application is limited because of dependency on motor parameter and complexity of calculations. So knowing these issues in this thesis, attention was being paid to develop intelligent search based efficiency controllers incorporating flux programming in order to get optimum efficiency.

In Chapter 2, coordinate transformation using Park's transformation method has been introduced and the equivalent circuit model of IPMSM is investigated and the mathematical model of IPMSM for vector control strategy has been derived

Chapter 3 provides details of the power loss modeling of IPMSM and following that the proposed search based loss minimization by programming the flux component of stator current have been presented. In this chapter the fundamental of fuzzy logic control have been investigated. This chapter also covers the development of fuzzy efficiency and speed control scheme of IPMSM to control both torque and flux component such that the motor can be run efficiently. The proposed drive components such as steady state fuzzy controller, transient fuzzy controller, speed controller and compensator of torque current have been explained in detail. In order to verify the efficacy optimization and robustness of the drive in different dynamic operation the vector control scheme of the IPMSM has been simulated.

Chapter 4 provides details of the implementation and experimental result of the proposed efficiency and speed control system. After discussions of the various elements of the experimental set up and DSP controller board, the experimental results have been presented, which verify the simulation results shown in Chapter 3.

5.2 Future work

This thesis develops a novel speed and efficiency control scheme using vector control strategy. Although simulation and experimental results show efficiency improvement and robustness of the controller but there are some possible improvement margins for the system which are as follows:.

- . In simulation part, d and q axis inductances are considered constant with respect to d and q axis current. In practice, that is not true. So in future work, mathematical model of IPMSM can be derived considering the variation of d and q axis inductances in different dynamic operations.
- In the development of fuzzy efficiency controller, the command speed of the motor is considered below the rated speed, by tuning the membership function of i_d, the motor operation above the rated speed can be investigated
- Many research studies have been reported using the speed sensorless approach. This will eliminate the need for a position encoder as well as any difficulties associated with it.

References

[1] Basic training of motors, gears and drives, Leeson Electric Corporation, 1999.

[2] Richard M. Crowder, *Electric Drives And Their Controls*, Clarendon Press, 1995.

[3] "Opportunities for Energy Savings in the Residential and Commercial Sectors with High-Efficiency Electric Motors," *Final Rep*., Arthur D. Little, Inc., pp 1-15, United Kingdom Environmental Protection Agency,1999.

[4] S.Morimoto, Y.Takeda, T.Hirasa and K. Taniguchi, "Expansion of operating limits for permanent magnet motor by current vector control considring inverter capacity," *IEEE Trans. Ind. Applicat, Vol. 26,pp Sep./Oct. 1990. 866-871.*

[5] H.Murakami, Y.Honda, T.Higaki, S.Morimoto,Y.Takeda, "Rotor Design and Control method of Synchronous Reluctance Motor with Multi-flux Barrier",*Proceedings of Power Electronics Drives and Energy Systems for Industrial Growth,* pp.391-396, 1998.

[6] Andrzej M.Trzynadlowski, *The Field Orientation Principle in Control of Induction Motors*, Kluwer Academic, 1994.

[7] A.Abbondati, "Methods of flux control in induction motors driven by variable frequency, variable voltage supplies," *in Conf. Rec. Int. Semiconductor Power Converter, 1997.*

[8] S.J. Chapman, *Electric Machinery Fundamentals*, New York, NY: Mcgraw-Hill, 1999.R. H. Park, "Two-reaction theory of synchoronous machines – generalized method of analysis part 1," *AIEE Transactions,* Vol. 52, June, 1933, pp. 352-355.

[9] Eugene C. Lister and Michael R. Golding, *Electric Circuits and Machines*, Mcgraw-Hill Ryerson Limited, 1987.

[10] T.A. Lipo, "Comparative Analysis of Permanent Magnet AC Machines in Variable Speed Applications." *University of Wisconsin-Madison, ECE Dept.,* WEMPEC Research Report No. 82-12**,** Sept. 1982.

[11] T. M. Jahns, G. B. Kliman, and T. W. Neumann, "Interior permanent magnet synchronous motors for adjustable-speed drives," *IEEE Trans. Ind. Applicat.*, Vol. IA-22 , July/Aug. 1986 pp. 738–747.

[12] W. Shepherd and L. N. Hulley, *Power Electronics and Motor Control,* Cambridge University Press, 1987.

[13] T. M. Jahns, "Flux-Weakening Regime Operation of Interior Permanent Magnet Synchronous Motor Drive," *IEEE Trans. Ind. Appl.*, Vol. IA-23, July /Aug 1987 Pp,681-689.

.[14] H.Lang," Mechanical Design Considerations for Conventionally Laminated, High -speed, Interior PM Synchronous Machine Rotors,"*EC Lovelace, TM Jahns IEEE Trans, Ind Applic, 2004.*

[15] W.L Soong, D.A Staton and Miller, "Design of a new axially laminated Interior permanent magnet rotor," *IEEE Trans. Ind Application., Vol. 31, Mar. /Apr. 1995 pp. 358- 367.*

[16] G.R. SIemon, "On the design of high-performance surface-mounted Permanent Magnet Motors," *IEEE Trans. Ind. Applicat., Vol. 30, Jan/Feb. 1994. pp. 134*

[17] B. I. Kwon *et al.*, "Novel topology of unequal air gap in a single-phase brushless dc motor," *IEEE Trans. Magn.*, Vol.37, No.5 Sep.2001, pp.3723–3726.

[18] Nakamura, Kudou. "Power Factor Control of Permanent Magnet Synchronous Motor", *National Convention IEE of JAPAN, Industry Applications* Society, 44, 1990.

[19] M. Nasir Uddin and Fasil Abera, “Efficiency optimization based speed control of IPMSM drive,” *Int. Journal of Industrial Electronics and Drives*,Vol.1,no 1,2009 pp 34-41.

[20] Mademlis, C. Kioskeridis, I., Margaris, N., "Optimal efficiency control strategy for interior permanent-magnet synchronous motor drives", Energy *Conversion, IEEE Transactions on,* Volume: 19 NO: 4, Dec. 2004, PP 715 - 723.

[21] S. Vaez, V.I. John and M.A. Rahman, "An on-line loss minimization controller for interior permanent magnet motor drives," *IEEE Trans. on energy conversion*, Vol. 14, No. 4, Dec. 1999, pp. 1435-1440.

[22] S. Morimoto, Y. Takeda, and T. Hirasa, "Loss minimization control of permanent Magnet synchronous motor drives," IEEE Trans. Ind. Electronics, Vol. 41, No. 5, Oct. 1994 pp. 511-517.

[23] E. S. Sergaki, G. S. Stavrakakis "Optimal speed trajectory tracking of an AC Motor drive system with simultaneous minimization of its electromagnetic losses and fuzzy logic efficiency optimization in steady and transient states", ICEM 2006, *XVII International Conference on Electrical Machines*, September 2006.

[24] G. D. D. Sousa, B. K. Bose, J. G. Cleland, "Fuzzy logic based on-line efficiency optimization control of an indirect vector-controlled induction motor drive," IEEE Transactions on Industrial Electronics, Vol. 42, pp. 192-198, 1995.

[25] P. Zhou, M. A. Rahman, M. A. Jabbar; "Field circuit analysis of permanent

magnet synchronous motors" *IEEE Transactions on Magnetics*, Vol. 30, No. 4, Part 2, Jul 1994, pp. 1350 – 1359.

[26] Z. Ibrahim and E. Levi. "A Comparative Analysis of Fuzzy Logic and PI Speed Control in High Perfbrmance AC Drives Using Experimental Approach", *IEEE Transactions on Industrial Application,* Vol. 38, No. *5,* Sept./Oct 2002, pp. 1210

[27] C. Butt, M.A. Rahman, "Limitations of Simplified Fuzzy Logic Controller for IPM Motor Drive." *IEEE/IAS Annual Meeting Conf. Record*, 3-7 Oct.2004, Vol. 3, pp.1891 – 1898.

[28] Y. Tang And L. Xu, "Fuzzy Logic Application for Intelligent Control of a Variable Speed Drive," *IEEE Transactions on Power Electron*., Vol.12, Nov. 1997, pp. 1028-1039.

[29] C. C. Lee, " Fuzzy Logic In Control System: Fuzzy Logic Controller – Part I, II*,"* *IEEE Transactions on System, Man And Cybernetics.* Vol.20, No-2, 1990. pp. 404-435.

[30] S. Y. Yi and M. J. Chung, "Robustness of Fuzzy Logic Control for an Uncertain Dynamic System," *IEEE Transactions on Fuzzy Syst.,* Vol. 6, May 1998, pp. 216–224.

[31] M N Uddin and M A Rahman. "Fuzzy Logic Based Speed Control of an IPM Synchronous Motor Drive*". Journal of Advanced Computational Intelligence*, Vol. 4, No. 3, 2000, pp. 212-219.

[32] C. Butt, M.A. Hoque, M.A. Rahman, "Simplified Fuzzy Logic Based MTPA Speed Control of IPMSM Drive." *IEEE Transactions on industry applications,* Vol. 40, No.6, 2004, pp. 1529– 1535.

[33] M. N. Uddin, M. A. Abido and M. A. Rahman, "Real-Time Performance Evaluation of a Genetic Algorithm Based Fuzzy Logic Controller for IPM Motor Drives", *IEEE Transactions on Industry Applications*, Vol. 41, No. 1, Jan./Feb. 2005, pp. 246-252.

[34] K. Zawirski, "Fuzzy Robust Speed Control for Permanent Magnet Synchronous Motor Servo Drive" *Proc. Of 8th Int. Power Electronics & Motion Control Conference, Prague*, 8-10 Sept, 1998.

[35] S Bolognani And M. Zigliono. "Fuzzy Logic Control of a Switched Reluctance Motor Drive''. *IEEE Transactions on Industry Applications*. Vol. 32. No. 5, Sept./Oct. 1996, pp. 1063-1068.

[36] Yen-Shin Lai and Juo-Chiun Lin, "New Hybrid Fuzzy Controller for Direct Torque Control Induction Motor Drives." *IEEE Transactions on Power Electronics,* Vol.18, No. 5, Sept. 2003, pp.1211 – 1219.

[37] P. Stewart, D. A. Stone And P. J. Fleming. "Design of Robust Fuzzy-Logic Control Systems by Multi-Objective Evolutionary Methods with Hardware in the Loop." *Engineering Application of Artificial Intelligence*, Vol. 17, No. 3, April 2004, pp. 275-284

[38] M. N. Uddin, T. S. Radwan, M. A. Rahman, "Performances of fuzzy-logic-based indirect vector control for induction motor drive." *IEEE Transactions on Industry Applications,* Vol. 38, No. 5, Sept.-Oct. 2002, pp. 1219 – 1225.

[39] M A Rahman. M Nasir Uddin. And M. A. Abido. "An Anificial Neural Network for Online Tuning of a Genetic Based PI Controller for Interior Permanent

Magnet Synchronous Motor Drive", *Canadian Journal of Electrical & Computer Engineering,* Vol. 31, No. 3, July 2006, pp. 159-165.

[40] Yang Yi, D.M. Vilathgamuwa, M.A. Rahman, "Implementation of an Artificial-Neural-Network-Based Real-Time Adaptive Controller for an Interior Permanent-Magnet Motor Drive." *IEEE Transactions on Industry Application,* Vol. 39, No. 1, Jan.-Feb. 2003, pp. 96 – 104.

[41] M N Uddin and M A Rahman. "Fuzzy Logic Based Speed Control of an IPM Synchronous Motor Drive*". Journal of Advanced Computational Intelligence*, Vol. 4, No. 3, 2000, pp. 212-219.

[42] L. A. Zadeh, "Outline of a new approach to analysis of a complex system and decision process", *IEEE Transactions on System, Man and Cyber*, vol. SMC-3, 1973, pp.28-44.

[43] M. N. Uddin, T. S. Radwan, M. A. Rahman, "Performances of fuzzy-logic-based indirect vector control for induction motor drive." *IEEE Transactions on Industry Applications,* Vol. 38, No. 5, Sept.-Oct. 2002, pp. 1219 – 1225.

[44] T. Takagi and M. Sugeno, "Fuzzy identification of systems and its applications to modeling and control," *IEEE Transactions on System, Man and Cyber*, Vol 15 No 1, 1885, pp. 116–132.

[45] Md. M. I. Chy. and M. N. Uddin "A Novel Fuzzy Logic Controller Based Torque and Flux Controls of IPM Synchronous Motor." accepted for *IEEE/IAS Annual Meeting*, New Orleans, Louisiana, USA, 2007.

[46] *dSPACE*, "Digital Signal Processing and Control Engineering", Implementation Guide, Paderborn, Germany, 2003.

Appendix – A

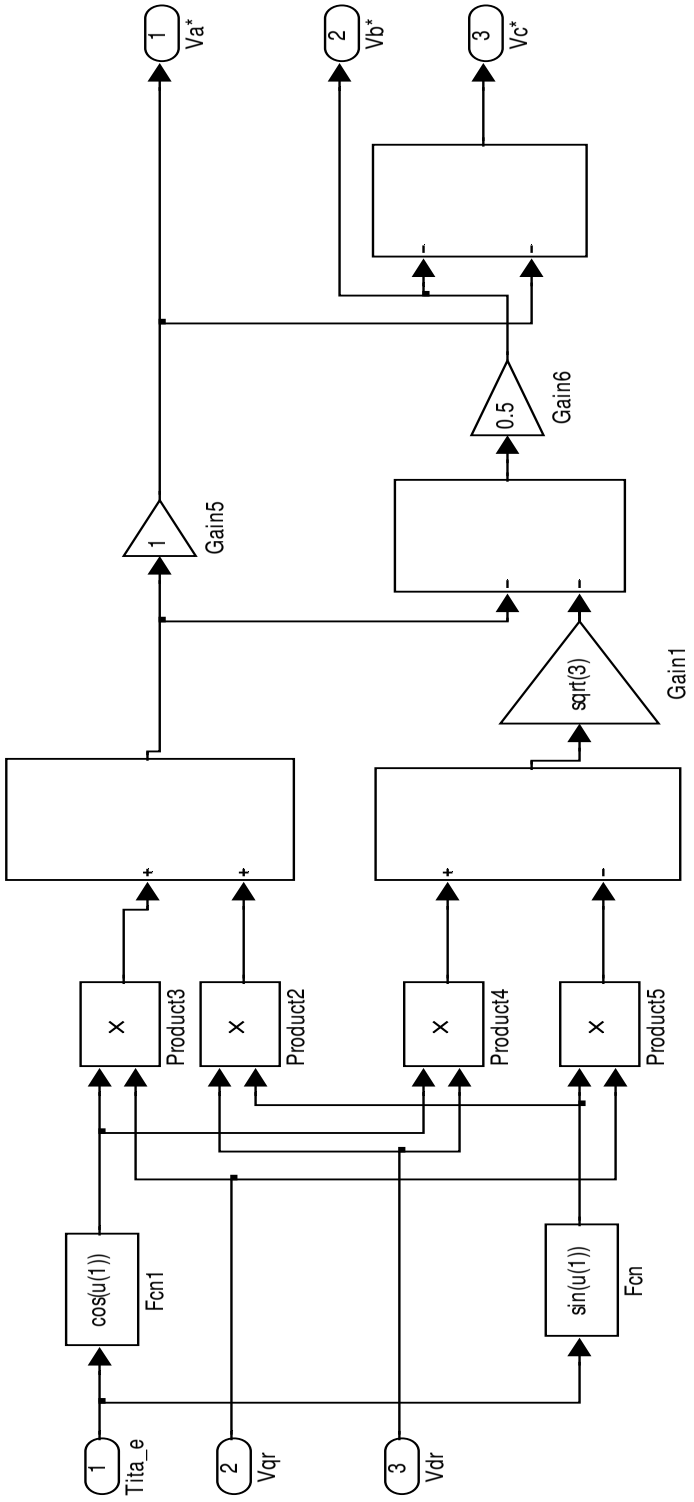

A1. DQ/ABC Vector Rotator

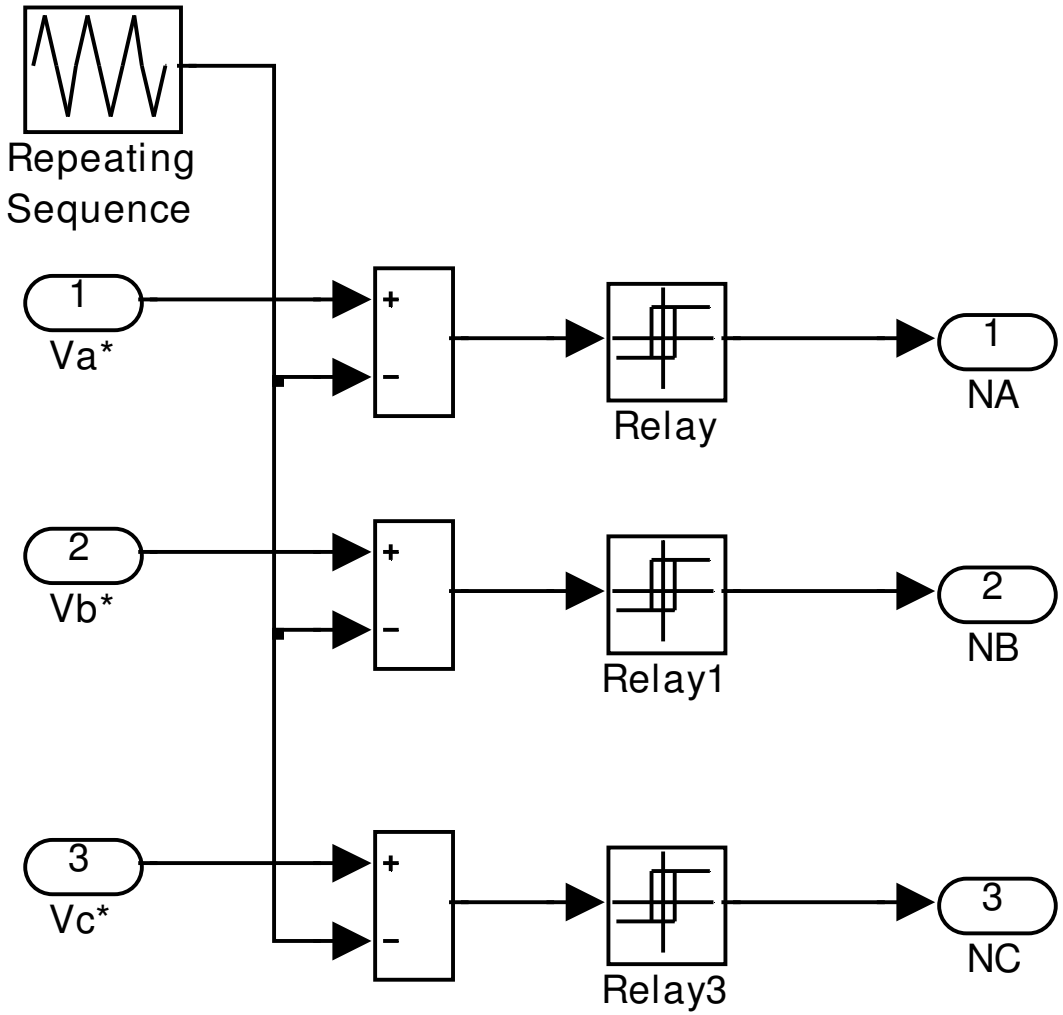

A2. PWM Signal Generator

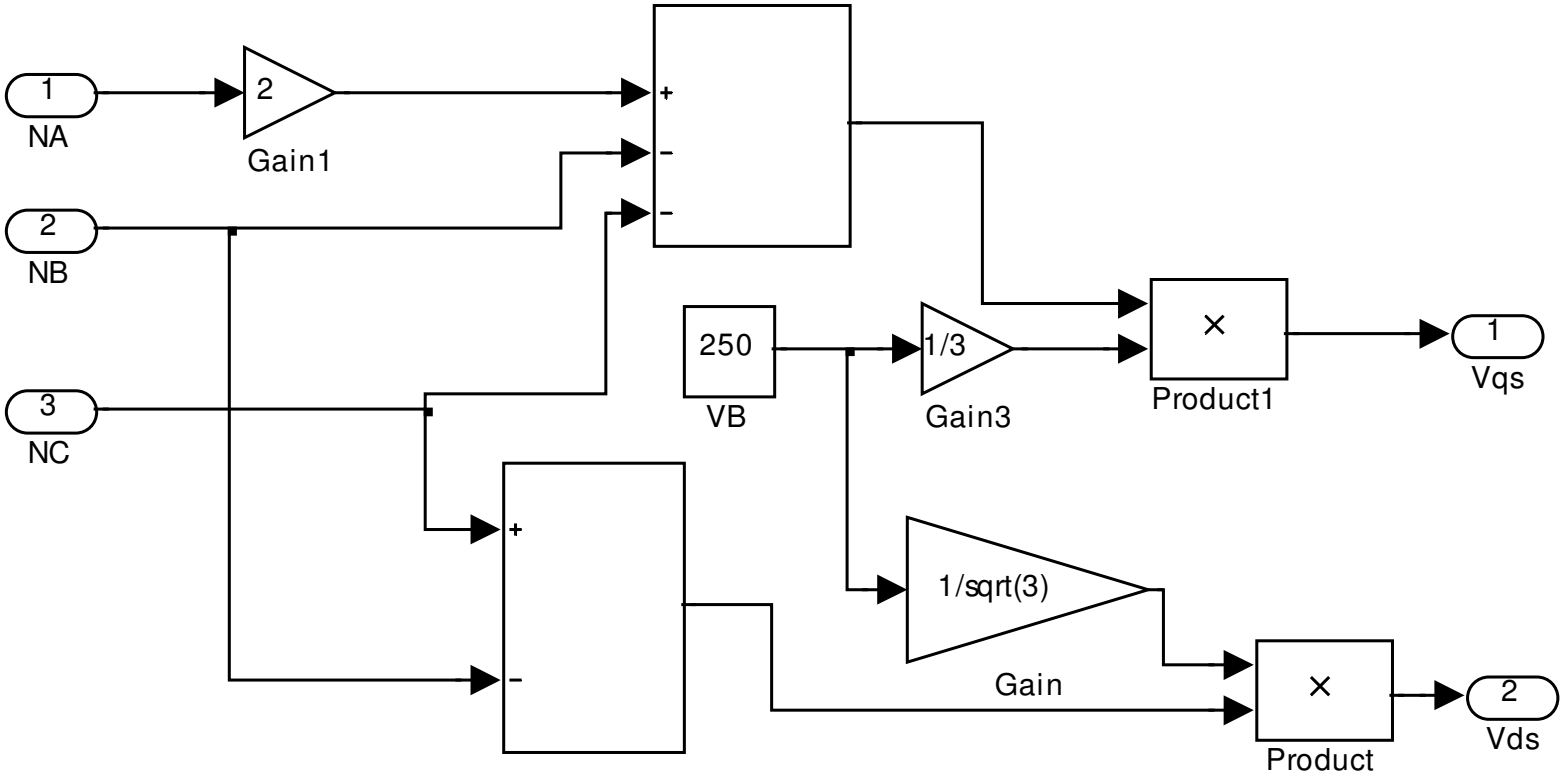

A3. 3-Phase Inverter

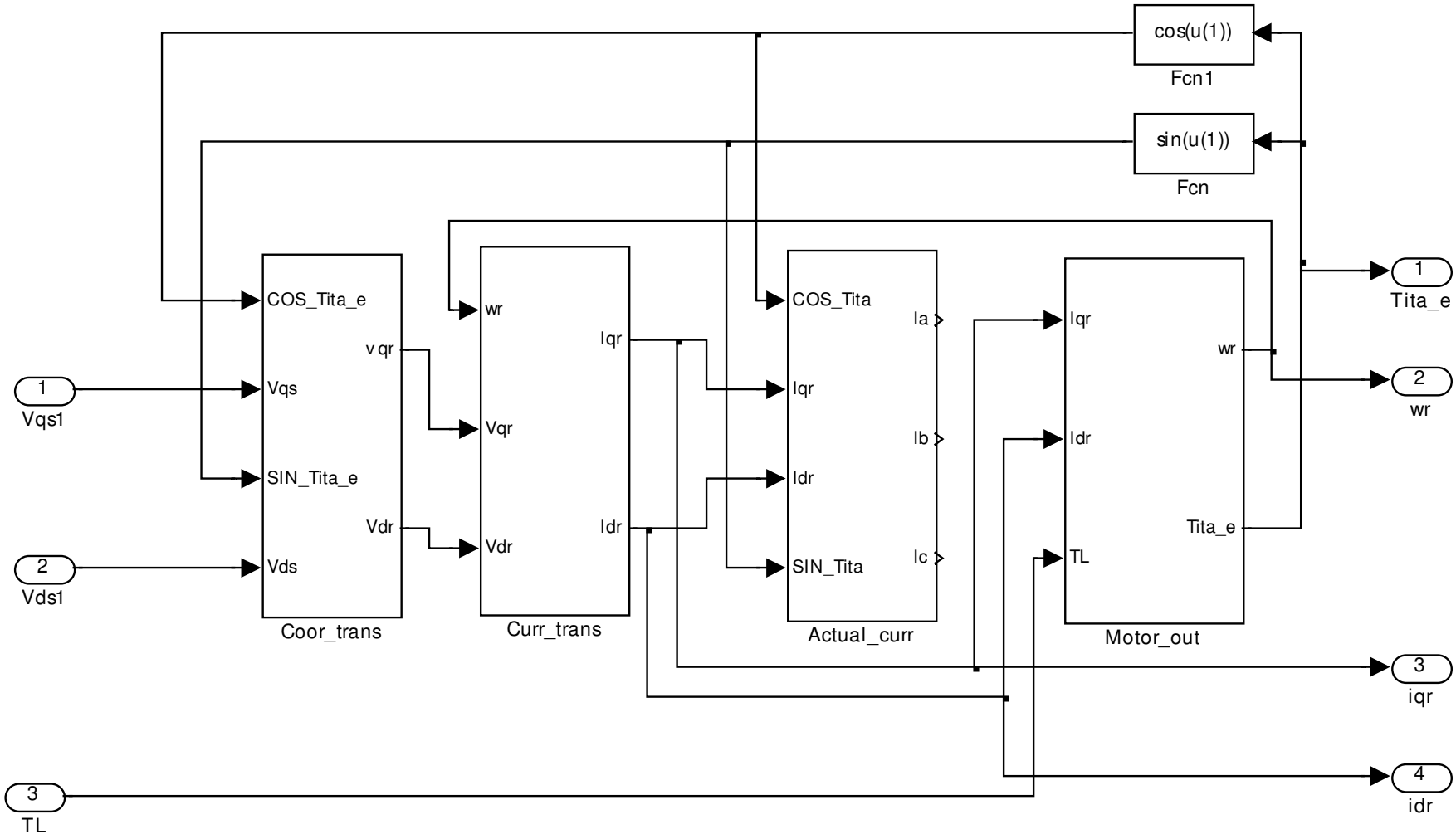

A4. Motor Subsystem

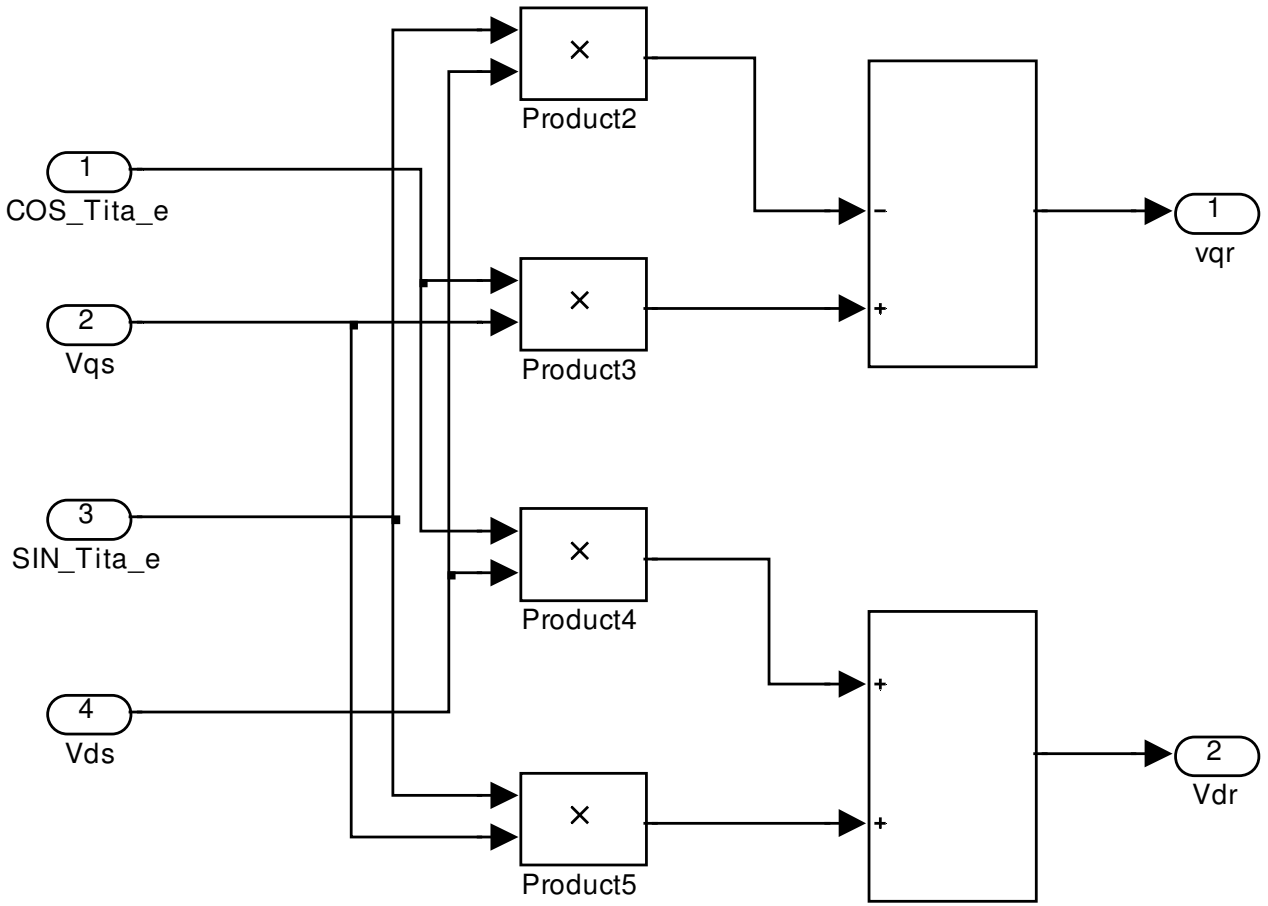

A4.1. Co-ordinate Transformer Subsystem (Coor_trans)

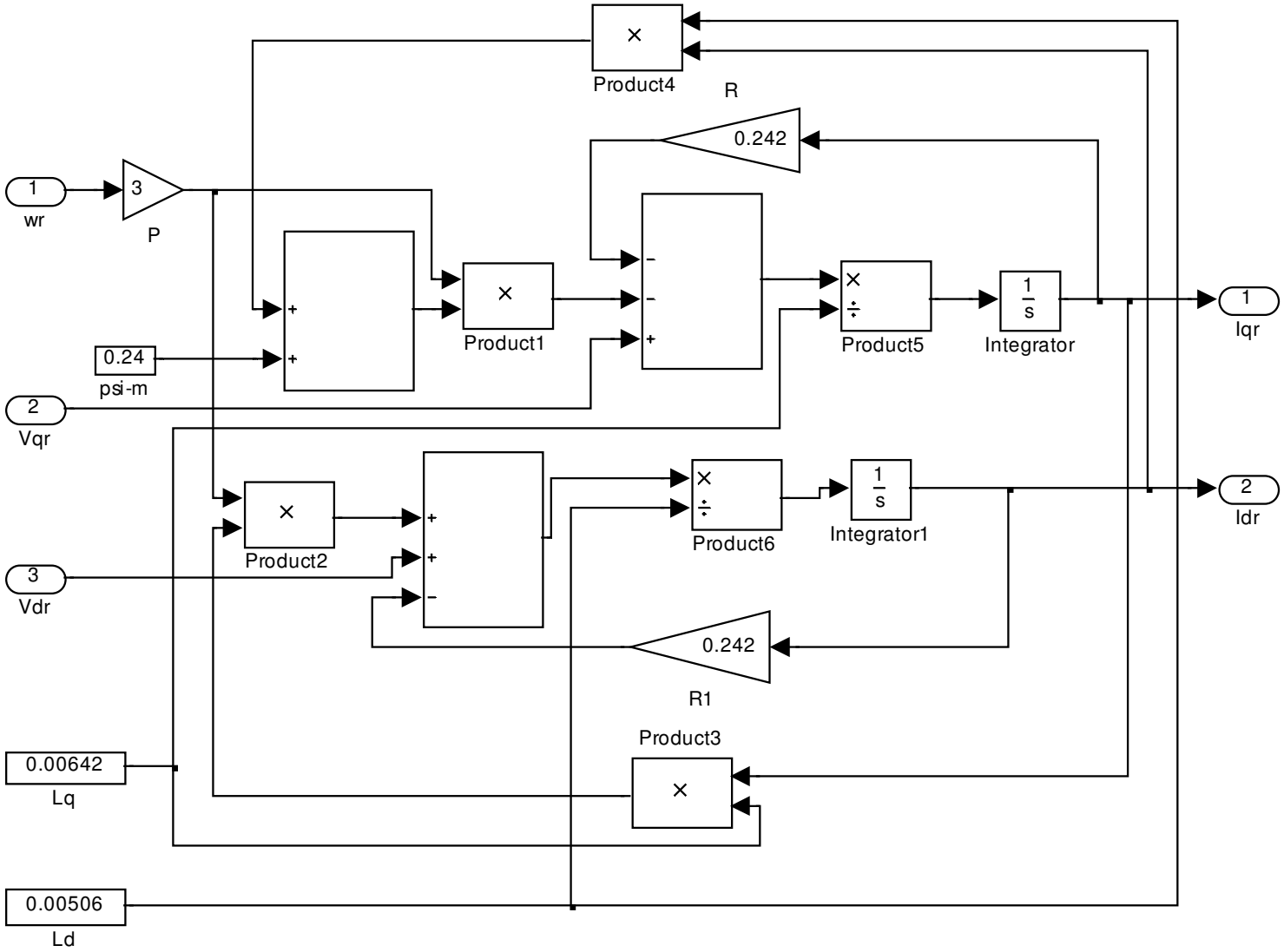

A4.2. Current Transformer Subsystem (Curr_trans)

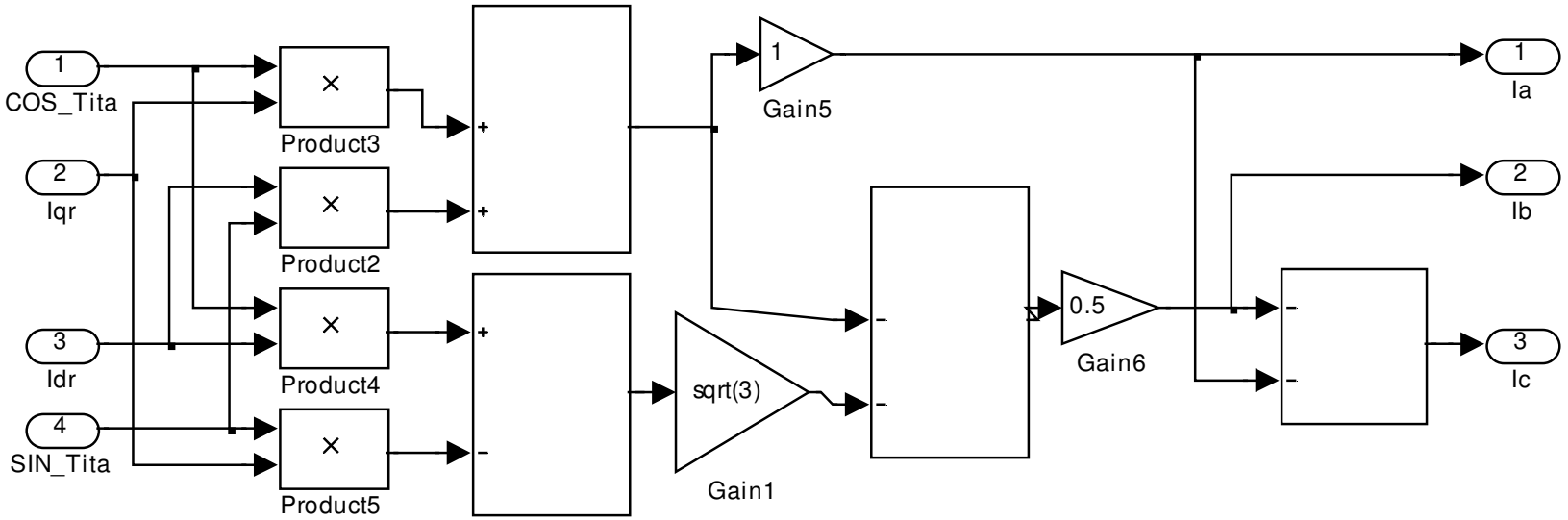

A4.3. Vector Rotator Subsystem (Actual_curr)

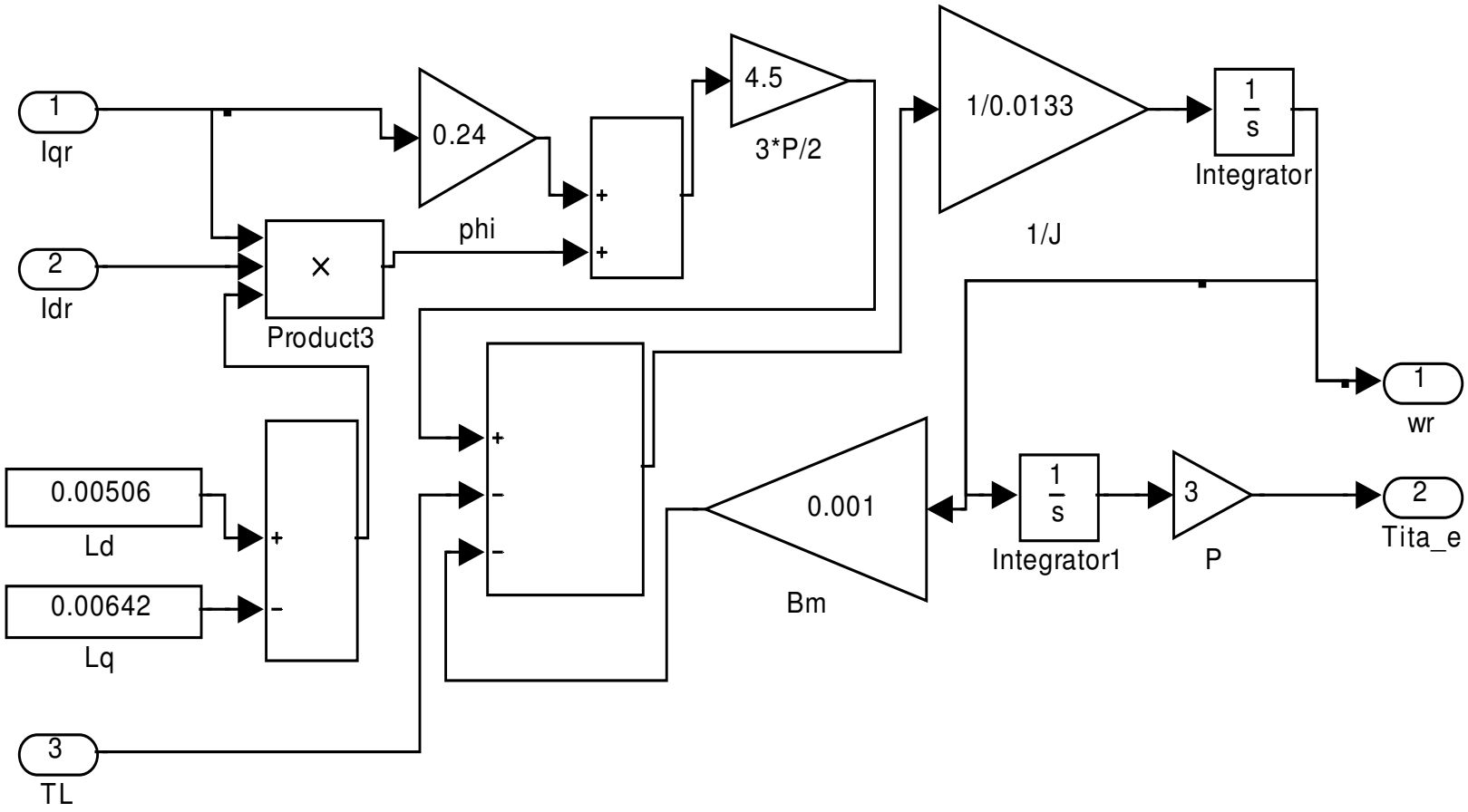

A4.4. Motor Output Subsystem (Motor_out)

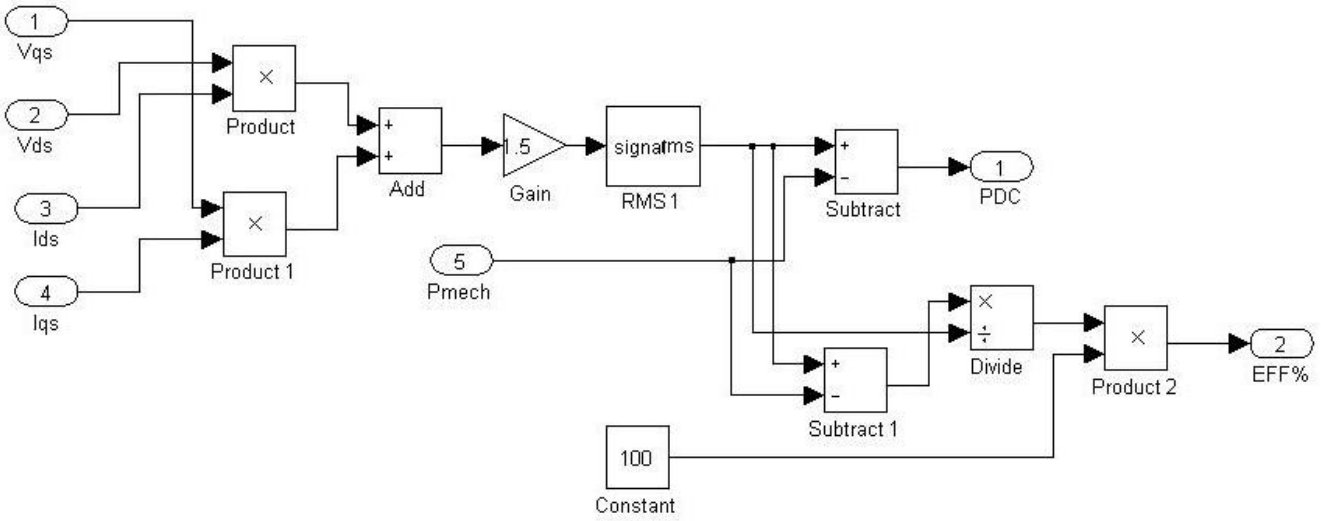

A.5. Power Processing Unit

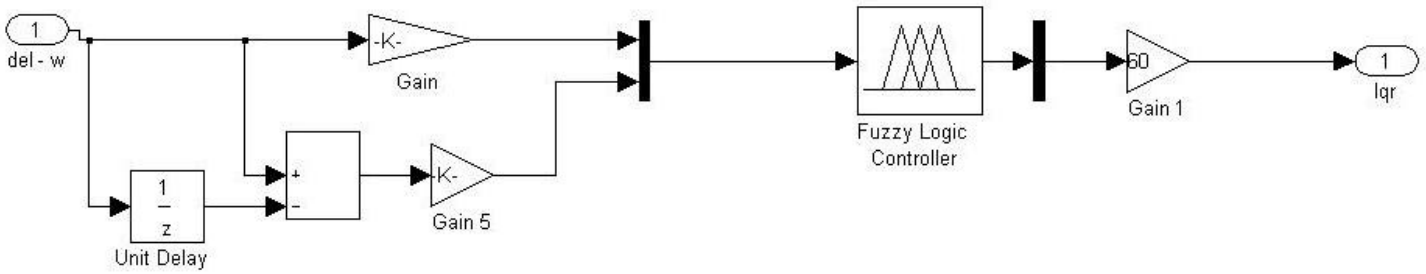

A.6. Fuzzy Logic Speed Controller

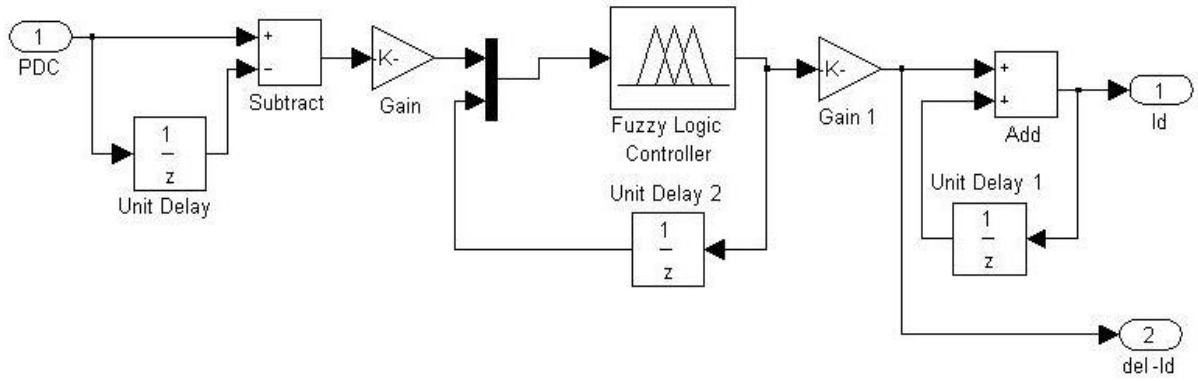

A.7.Steady State Fuzzy Logic Efficiency Controller (FLC 1)

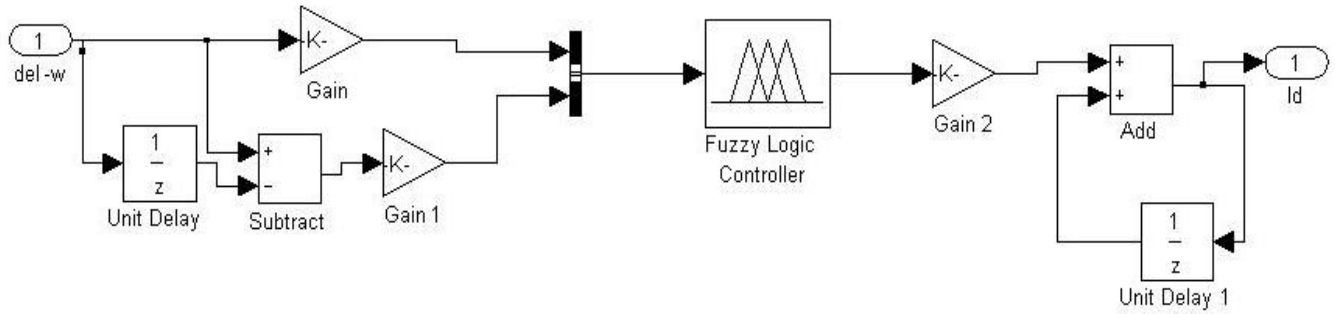

A.8. Transient State Fuzzy Logic Controller (FLC 2)

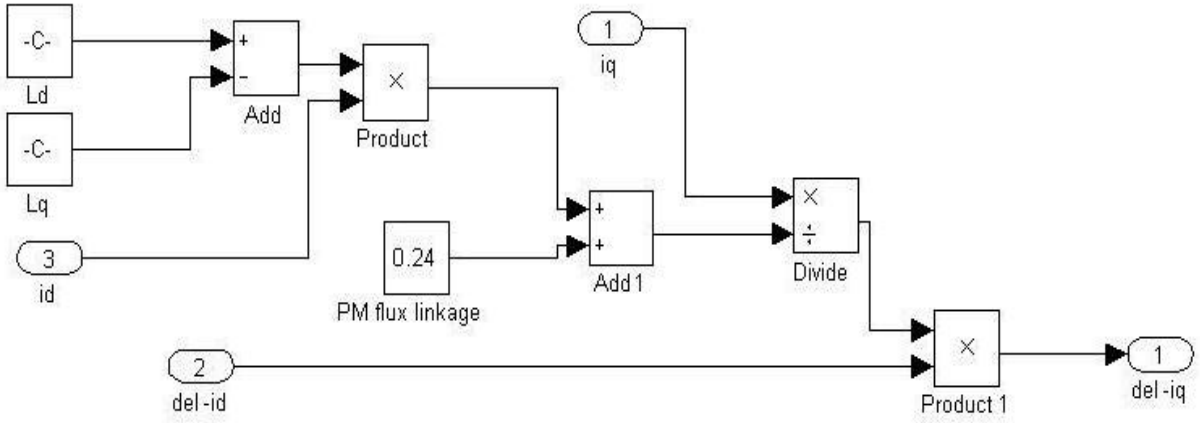

A.9. Compensator of Torque Current

Appendix B

Base drive circuit for the inverter and interface circuit for the current sensor

R1= R2 = R3 = R4 = R5 = R6 = 1.5k

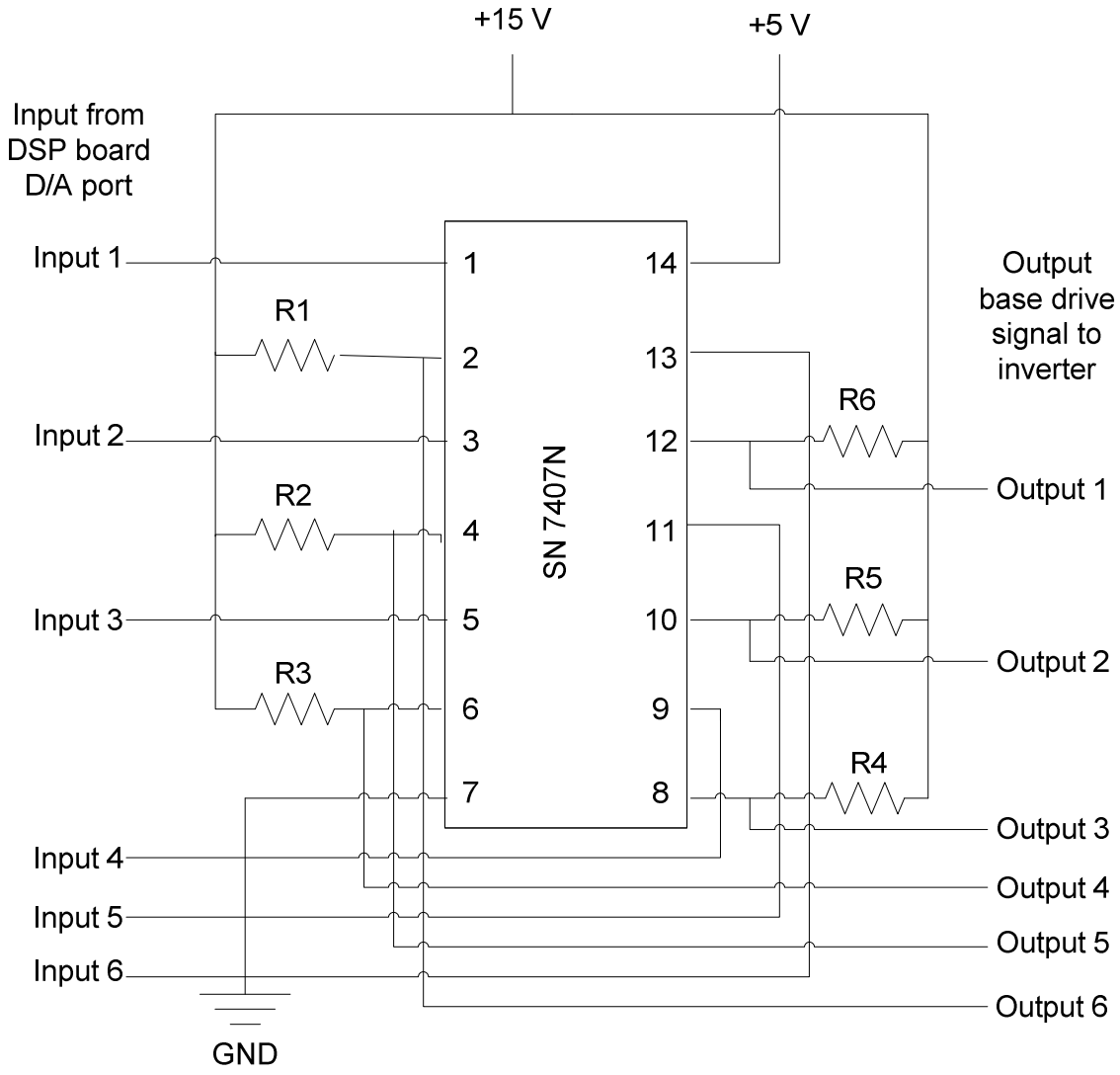

B.1. Base drive circuit for the inverter

Gain of Op-Amp (741CN) = 1+R3/R2

Magnitude of resistors:

	Current sensor for phase 'a'	Current sensor for phase 'b'
R1	98.7 ohm	99 ohm
R2	1.8 k	2 k
R3	5.5 k	5.1 k

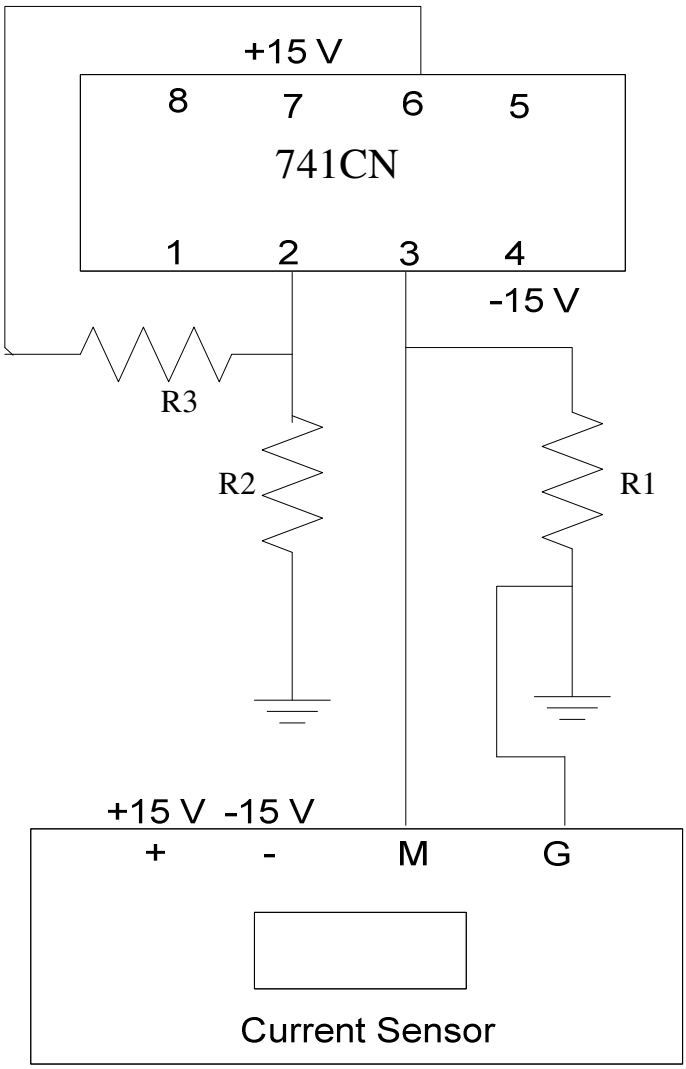

B.2. interface circuit for the current sensor

Appendix C
Real-Time Simulink Model

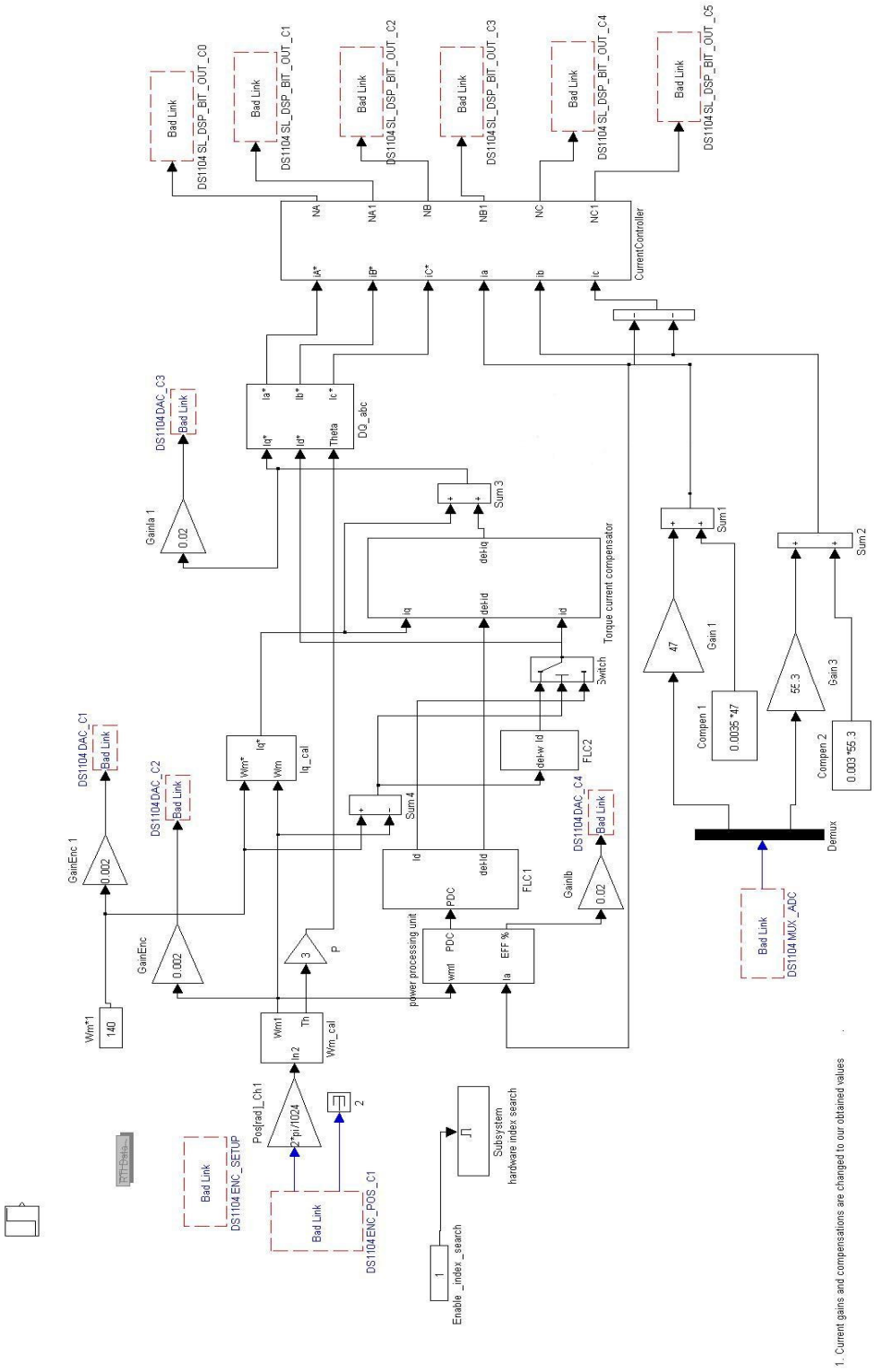

C. Real-Time Simulink Model